DEPOSITIONAL HISTORY AND STRATIGRAPHY OF THE APHEBIAN TAMARACK RIVER FORMATION AND THE PALEOHELIKIAN SIMS FORMATION, WESTERN LABRADOR

MICHAEL JAMES WARE

DEPOSITIONAL HISTORY AND STRATIGRAPHY OF THE APHEBIAN TAMARACK RIVER FORMATION AND THE PALEOHELIKIAN SIMS FORMATION, WESTERN LABRADOR

© Michael James Ware B.Sc.

A thesis submitted in partial fulfillment of
the requirements for the degree of
Master of Science

Department of Earth Sciences
Memorial University of Newfoundland

St. John's, Newfoundland January, 1983

This thesis is dedicated to the memory of Rick Sheppard, a fellow Memorial University of Newfoundland Geology student who died in February, 1982, when the semi-submersible drilling rig, the Ocean Ranger, capsized on the Grand Banks.

ABSTRACT

Alphebian sedimentary rocks of the Tamarack River Formation rest unconformably on the Knob Lake Group in the south-central portion of the Labrador Trough. The formation appears to consist of two transgressive-regressive cycles. The first cycle, present in Member A, consists of subtidal siltstone, which grades upward into a mixed siliciclastic-carbonate unit of shallow subtidal and intertidal origin. The second cycle, recorded by members B and C, is composed of subtidal siltstone which passes upward into the intertidal and fluvial sandstone. Detritus of member A was derived from the north, whereas the provenance of member C was the Superior Province to the west. The formation may be part of the third Aphebian miogeoclinal sequence which developed in the Labrador Trough. The first and second sequences are recorded by the Knob Lake Group. The northern Labrador Trough may contain third sequence strata correlative to the Tamarack River Formation.

The Paleohelikian Sims Formation rests unconformably on deformed Aphebian strata and consists of a lower unit of terrestrial redbeds and an upper unit of fluvial to shallow-marine quartzarenite. The relatively thin terrestrial redbed unit is composed of three facies, a talus-slope breccia, a pebbly braided-river conglomerate and a sandy braided-river deposit. These facies grade upward into a thick, tabular quartzarenite unit composed of fluvial sandstone, beach conglomerate, and nearshore to shallow-marine sandstone. Throughout its deposition the formation progressively onlapped from west to east and derived its detritus from an uplifted area to the east. The formation may represent post-Hudsonian molasse, and is possibly correlative with the lithologically similar but undated Sakami Formation of northern Quebec.

Both the Tamarack River and Sims Formations were intruded by tholeiitic dikes and sills of the Elsonian (1.4Ga) Shabogamo Intrusive Suite. Paleomagnetic samples from the suite yield a virtual paleopole position at 3.97°E, 3.4°S with dp = 5.8° and dm = 11.0°, which is similar to the antipole of the nearby Elsonian Michikamau Intrusion.

ACKNOWLEDGEMENTS

The field work for this thesis was supported by the Newfoundland Department of Mines and Energy and was under the able direction of Dr. Richard Wardle. My thesis supervisor, Dr. Richard Hiscott, is thanked for making many valuable suggestions and for substantially improving the quality of the manuscript.

I would also like to thank Dr. Richard Hyde of the Newfoundland Department of Mines and Energy, Drs. Brian Fryer, Joseph Hodych, Noel James, and L. Toby Rivers of Memorial University, and my fellow graduate students for their constructive comments on various aspects of the thesis. Mr. X.Y. Zhang helped with the processing of the paleomagnetic results.

Brian Burt and Denis Fitzpatrick provided excellent field assistance, and Dr. Henry Longerich, Jaan Vahra, and David Press aided in the laboratory investigations. Wilf Marsh helped prepare the photographs. The manuscript was typed by Ann McEwen and Anita McKearney. A Natural Sciences and Engineering Research Council Operating Grant to Dr. R.N. Hiscott provided part of my stipend at Memorial University and supported various aspects of the research.

CONTENTS

LIST OF TABLES

LIST OF FIGURES (SHORT TITLES)

CHAPTER 1 - INTRODUCTION

SETTING AND PHYSIOGRAPHY

Sedimentary rocks of the Aphebian Tamarack River Formation and the Paleohelkian Sims Formation are located on the Canadian Shield, in the Churchill and Grenville Provinces of western Labrador (Fig. 1.1). This region is readily accessible either by float plane or by railway from Labrador City and Schefferville, and by road from Churchill Falls (Figs. 1.2, 1.3).

The physiography of the area is closely related to the lithology and structure of the bedrock. The landscape is dominated by monadnocks which rise up to 500 m above the surrounding flat lowlands (Fig. 1.2). These highlands are formed by the erosionally resistant quartzarenite of the Sims Formation (Fig. 1.2) whereas the lowlands are underlain by less resistant Aphebian rocks of the Knob Lake Group and Tamarack River Formation.

Pleistocene glaciers scraped the hills formed by the Sims Formation bare and deposited a thick mantle of moraine on the surrounding lowlands. Striations, grooves, chatter marks and crescent marks on the surfaces of outcrops indicate that the ice moved towards the southeast (Fig. 1.3). Other prominent glacial features in the area include southeasterly-trending eskers, outwash moraines, drumlinoid ridges and patches of kettle terrain (Fig. 1.3).

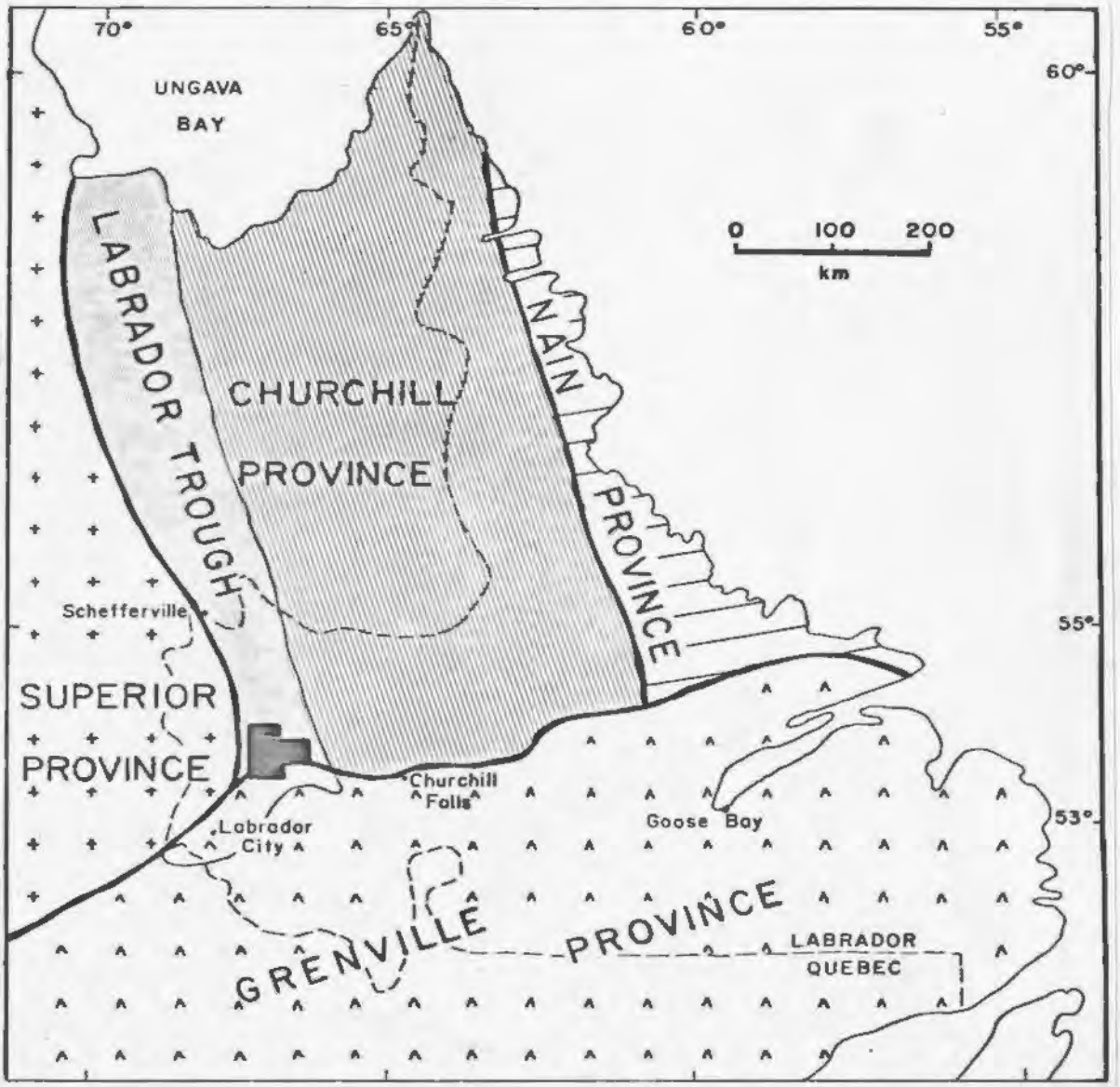

Fig. 1.1: Regional geological subdivisions of Labrador and eastern Quebec. Location of study area shown in black.

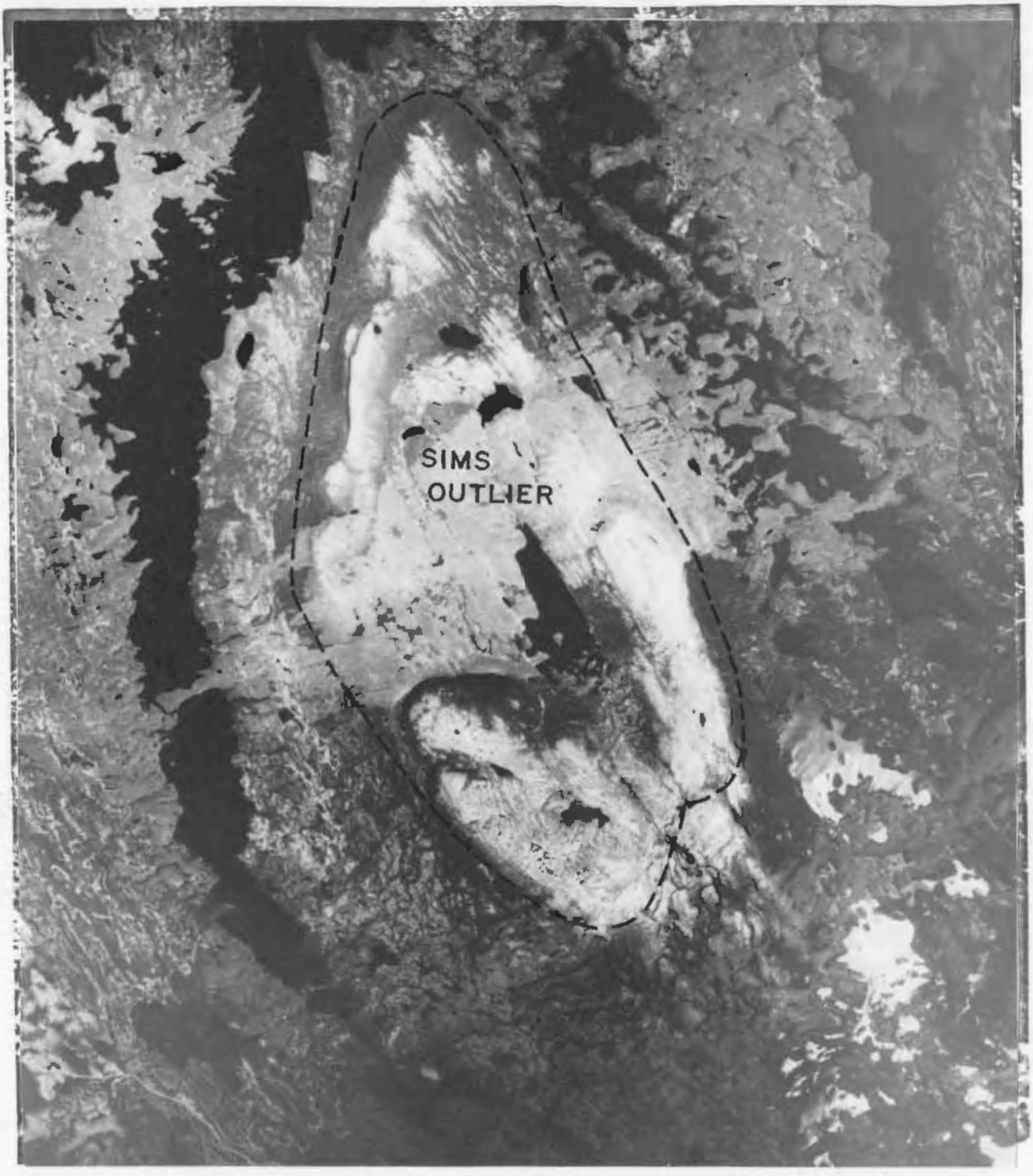

Fig. 1.2: An aerial view of Sims outlier illustrating the prominent hilly topography formed by the white quartzarenite of the Sims Formation. Scale is 1:110,000. Road to Churchill Falls appears in lower left.

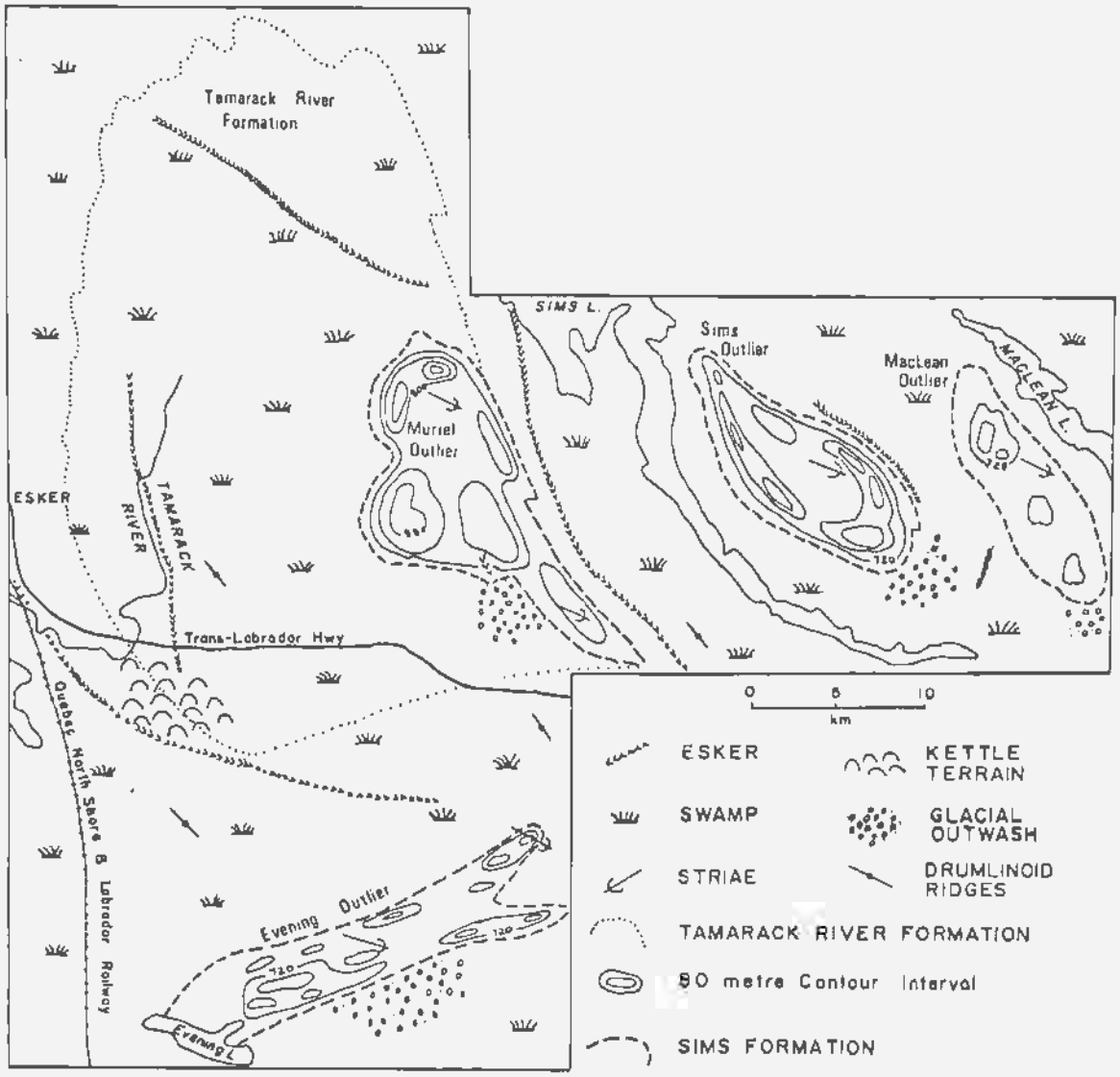

Fig. 1.3: Physiographic and glacial features associated with the Tamarack River and Sims Formations.

PREVIOUS WORK

In the late 1800's, A.P. Low, of the Geological Survey of Canada, explored western Labrador and named the prominent hills surrounding Sims Lake, the "Icy Mountains" (Low, 1896).

During the late 1940's and early 1950's, geologists of the Labrador Mining and Exploration Company and the Iron Ore Company of Canada, while assessing iron ore potential of the Labrador Trough, mapped the strata now belonging to the Tamarack River and Sims Formations. Eade (1949) and Tiphane (1951) described the northern portions of the Sims Formation and rocks now included in the Tamarack River Formation. Beland (1949), Baird (1950), Fraser (1952) and Goodwin (1951), mapped the southern exposures of the Sims Formation near Evening Lake (Fig. 1.2). Geological Survey of Canada 1:250,000 maps by Wynne-Edwards (1959, Michikamau Lake; 1961, Ossokmanuan Lake), Frarey (1961, Menihek Lakes) and Fahrig (1967, Shabogamo Lake) cover the study area.

In the 1970's, geologists employed by B.P. Minerals (MacDonell and Walker, 1975) and British Newfoundland Exploration Company, or Brinex (Busch, 1979), carried out uranium exploration programs, concentrating on the Tamarack River and Sims Formations. This increased exploration activity prompted the Newfoundland and Labrador Department of Mines and Energy to initiate 1:100,000 mapping of both formations (Ware, 1979; Ware and Wardle, 1979; Ware, 1980).

PRESENT STUDY

This thesis contains the results of the author's work on the Sims Formation mapping project which was sponsored by the Newfoundland and Labrador Department of Mines and Energy. The bulk of the field work was performed during the summer of 1978 by a two-man field party with float-plane and helicopter support. A three-week visit was made the following summer.

CHAPTER 2 - GENERAL GEOLOGY

INTRODUCTION

The Labroador Trough is an Aphebian fold belt (Dimroth et al., 1970) which extends from southwestern Labrador northward to Ungava Bay (Fig. 1.1). On its western margin the Trough strata rest unconformably on Archean gneiss and granite of the Superior Province. In the east, the Trough rocks are in fault contact with the Eastern Basement Complex of the Churchill Province (Dimroth, 1978: Wardle, 1979a).

The south-central portion of the Labrador Trough (between latitudes 53^{o} 30' and 55^{o} 00' north, Fig. 1.1) contains three distinct miogeoclinal sequences, each of which is bounded by unconformities, and composed of clastic and chemical sediments. The two lower sequences or cycles are recorded by Knob Lake Group and the uppermost is represented by the Tamarack River Formation.

During the Hudsonian Orogeny, the Eastern Basement Complex, Knob Lake Group, and Tamarack River Formation were slightly to moderately deformed into northwesterly-trending structures (Fig. 2.1) Dimroth, 1978; Wardle, 1979). This deformation was followed by deposition of the Paleohelikian Sims Formation (Ware and Wardle, 1979). At approximately 1.4 Ga, during Elsonian magmatism, mafic intrusions of the Shabogamo Intrusive Suite were injected into the Labrador Trough rocks and Sims Formation (Brooks et al., 1981).

The Grenvillian Orogeny moderately to strongly deformed the southern portions of the Knob Lake Group and Sims Formation into easterly-trending structures (Fig. 2.1) (Fahrig, 1967; Rivers, 1980a).

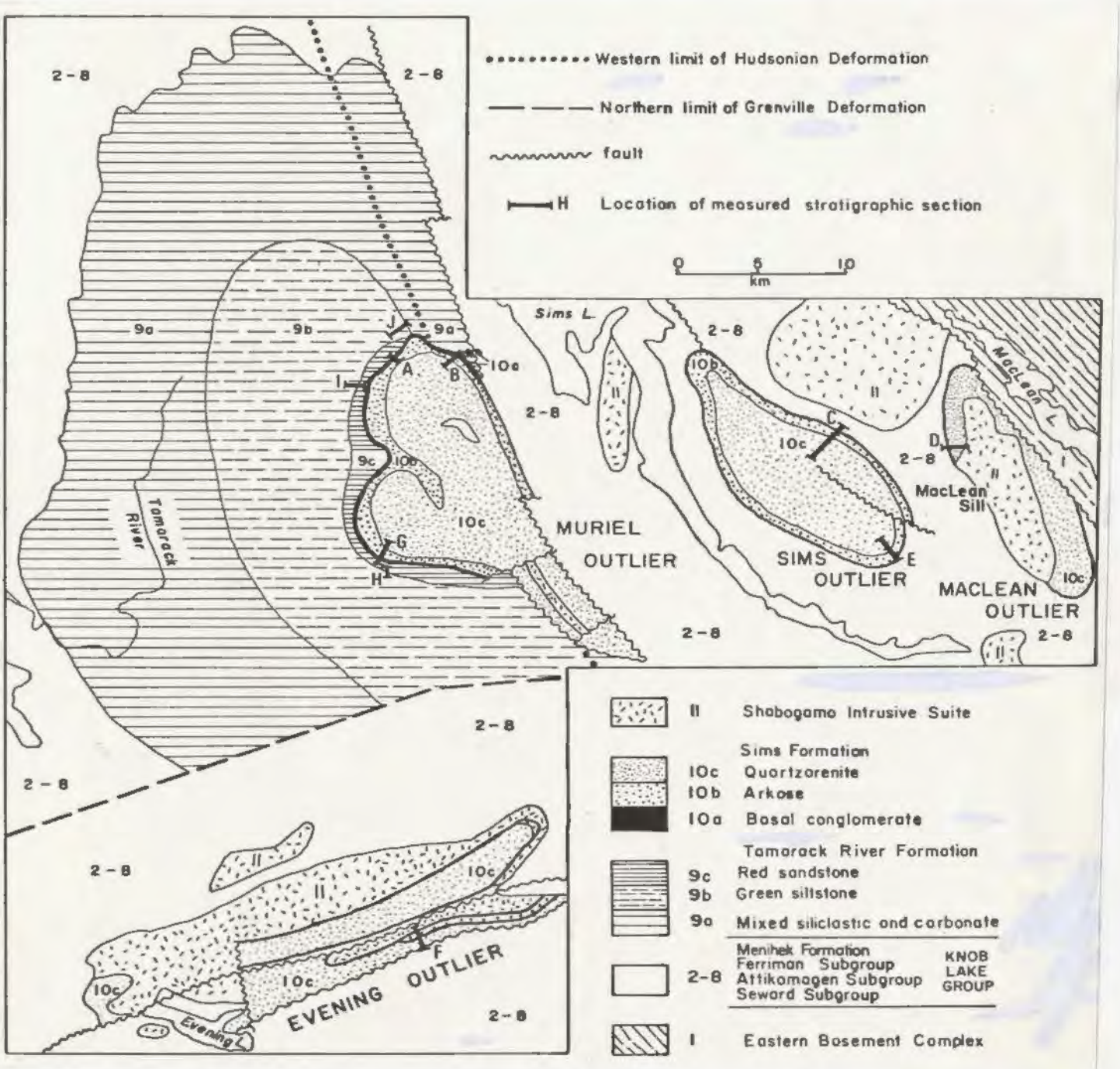

Fig. 2.1: Generalized geologic map of the Tamarack River and Sims Formations.

EASTERN BASEMENT COMPLEX

The Eastern Basement Complex is composed of granite-gneiss, amphibolite, and granite (Ware and Wardle, 1979) and is separated from the MacLean outlier of the Sims Formation by the Wade Lake Fault (Fig. 2.2). The age of the complex is uncertain. Both Dimroth (1978) and Wardle (1979a) suggest an Archean age, whereas Taylor (1979) interprets the terrane to be Aphebian.

KNOB LAKE GROUP

Stratigraphic nomenclature used for the Knob Lake Group (Table 2.1) follows Dimroth's (1978) usage. Ware and Wardle (1979) have previously described the lithologic units of the Knob Lake Group in the area surrounding the Tamarack River and Sims Formations (Fig. 2.3 in back pocket). Appendix A lists modal analyses for some of the sandstones of the group.

The Knob Lake Group in the south-central part of the Labrador Trough is divided into two distinct sedimentary sequences, the lower and upper Knob Lake Group (Wardle and Bailey, 1982).

The lower Knob Lake Group is about 2 km thick, and is composed of the Seward and Attikamagen Subgroups (Wardle, 1979). The fluvial to shallow-marine conglomerates and sandstones of the Seward Subgroup were deposited in a northwest-trending rift valley (Dimroth, 1978; Wardle, 1979). The Seward Subgroup fines upward into the dark-coloured, fine-grained, turbiditic clastic rocks of the Le Fer Formation and stromatolitic carbonates of the Denault Formation (Wardle, 1979).

Eon	Era	Rock Unit			Unit	Lithology
Proterzoic	Paleohelikian	Shabogamo Intrusive Suite			11	Gabbro and diabase.
		Intrusive Contact				
		Sims Formation			10	c. Quartzarenite. b. Arkose. a. Conglomerate.
		Angular Unconformity				
	Aphebian	Tamarack River Formation			9	c. Red sandstone. b. Green siltstone. a. Mixed siliclastic and carbonate.
		Disconformity				
		Knob Lake Group	Menihek Formation		8	Shale, slate, phyllite, schist minor greywacke and conglomerate.
			Ferriman Subgroup	Sokoman Formation	7	Silicate-oxide facies iron formation.
				Nimish Formation	6	Mafic porphyritic lava.
				Wishart Formation	5	Feldspathic sandstone and quartzite.
			Disconformity			
			Attikamagen Subgroup	Denault Formation	4	Dolostone and chert.
				Le Fer Formation	3	Black shale, argillite, phyllite, schist, minor greywacke and conglomerate.
			Seward Subgroup		2	Greywacke, conglomerate and argillite.
Fault Contact						
Aphebian or Archean		Eastern Basement Complex			1	migmatitic granodiorite, tonalite gneiss, amphibolite, and granite.

Table 2.1: Stratigraphic units of the south-central portion of the Labrador Trough.

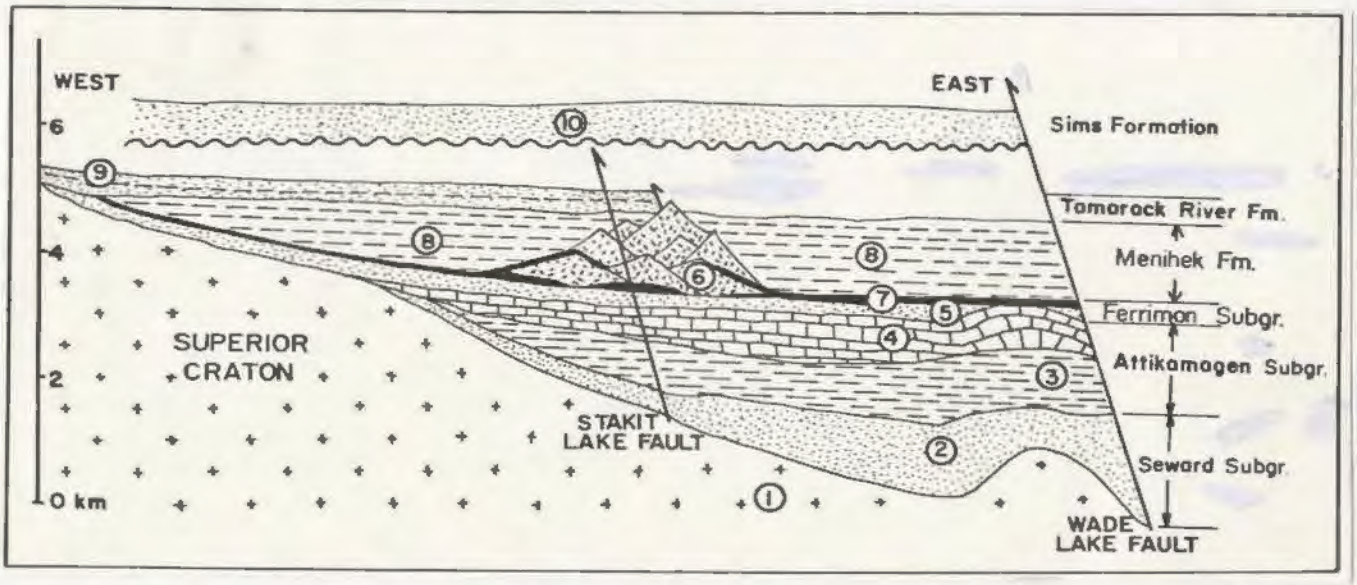

Fig. 2.2: Basinal development model for the south-central portion of the Labrador Trough, adapted from Wardle and Bailey (1982). Circled numbers refer to rock units found in Table 2.1.

Together both the Le Fer and Denault Formations form the Attikagamen Subgroup (Table 2.1).

The upper Knob Lake Group is made up of the Ferriman Subgroup (Wishart, Nimish, and Sokoman Formations) and the Menihek Formation. A widespread transgression deposited about 100 m of shallow-marine sandstone belonging to the Wishart Formation unconformably on the Superior Province and disconformably on the Lower Knob Lake Group (Fig. 2.2) (Wardle, 1979). Sedimentation was interrupted by the eruption of submarine and subaerial alkaline lavas of the Nimish Formation (Evan, 1978). This differentiated suite is up to 2 km thick and exhibits a pervasive potassium metasomatic alteration. The volcanics are believed to be of continental rift origin (Evans, 1978) and are extensively developed in the more northern sections of the Trough.

Only one outcrop of the formation occurs in the map-area (Fig. 2.3 in back pocket) and a chemical analysis of a sample from this outcrop is similar in composition to Evans'(1979) analyses (Appendix B). The 200 m-thick shallow-marine iron formation of the Sokoman Formation rests conformably upon the Wishart Formation or is interbedded with the Nimish Formation (Fig. 2.2) (Wardle, 1979). The Sokoman Formation is overlain by the Menihek Formation, a 1 km-thick unit of dark-coloured turbidites and shales, which has yielded a Rb/Sr isochron age of 1.84 ± 0.5 Ga (Fryer, 1972) (decay constant = $1.42 \times 10^{-11} yr^{-1}$).

TAMARACK RIVER FORMATION

Strata of the Tamarack River Formation represent the development of a third sequence in the south central portion of the Labrador Trough.

The formation is poorly exposed and was previously mapped as either part of the Menihek Formation (Tiphane, 1951; Fahrig, 1967) or as part of the Sims Formation (MacDonell and Walker, 1967). Recent work by Ware (1980) indicates that the Tamarack River Formation rests unconformably on upper Knob Lake Group and was deformed during the Hudsonian Orogeny. The formation is about 300 m thick and can be subdivided into three members (Table 2.1): member A, subtidal to intertidal mixed siliciclastic and carbonate; member B, subtidal green siltstone; and member C, intertidal to terrestrial red sandstone.

SIMS FORMATION

The Paleohelikian Sims Formation rests unconformably on deformed Knob Lake Group and Tamarack River Formation. It is exposed on four topographically defined outliers (Fig. 2.1). The three northern outliers, Muriel, Sims and MacLean, lie in the Churchill Province and are essentially flat lying. Evening outlier, to the south, lies in the Grenville Province and was deformed during the Grenvillian Orogeny. The formation is over 700 m thick and can be subdivided into three members: member A, talus-slope and fluvial conglomerate; member B, fluvial arkose; and member C, coastal and shallow marine quartzarenite.

SHABOGAMO INTRUSIVE SUITE

Mafic sheets, sills, and dikes of the Shabogamo Intrusive Suite intruded the Knob Lake Group and the Sims Formation at 1.37 Ga (Brooks

et al., 1981). The suite is synchronous with the widespread Elsonian magmatic event which affected much of central Labrador. Appendix D outlines the petrochemistry and paleomagnetism of the MacLean Sill which intrudes the MacLean outlier of the Sims Formation (Fig. 2.1).

STRUCTURE AND METAMORPHISM

Structural features in the Tamarack River Formation were generated by the Hudsonian Orogeny (Ware, 1980), whereas those of the Sims Formation were produced in the Grenvillian Orogeny (Ware and Wardle, 1979) (Table 2.2).

During the Hudsonian Orogeny (ca. 1.7 Ga, Stockwell, 1970), the Tamarack River Formation and the Knob Lake Group strata were deformed into northwesterly-trending structures of variable complexity and were metamorphosed to subgreenschist or lower greenschist facies (Ware and Wardle, 1979; Ware, 1980). West of Muriel outlier and extending to the boundary between the Churchill and Superior Provinces (Section A-A', Fig. 2.3) deformation is slight and characterized by gently-dipping strata with broad folds, minor faults, and a locally-developed fracture cleavage. East of the Stakit Lake Fault (Harrison et al., 1972) Hudsonian deformation increases and the Aphebian rocks lie in the Hudsonian foreland zone which is characterized by tight, periclinal folds, reverse faults and an extensively-developed fracture cleavage (Section A-A', Fig. 2.3). Further east, this foreland zone is separated from the Eastern Basement Complex, a high grade metamorphic zone (Wardle and Bailey, 1982), by the Wade Lake Fault (Fig. 2.3).

	HUDSONIAN (1.7Ga)	GRENVILLIAN (1.0Ga)
CHURCHILL PROVINCE: includes Tamarack River Fm. and northern outliers of Sims Fm.	Northwest trending structures with deformation intensity increasing eastward. Tamarack River Fm is flat-lying in the west but is tightly folded and highly faulted in the east. Metamorphism at lower greenschist facies.	Slight reactivation of the northwest trending Hudsonian structures. Sims Fm. is gently folded and is cut by faults.
GRENVILLE PROVINCE: includes Evening outlier of Sims Fm.	Absent or slight folding.	Easterly trending structures with deformation intensity increasing southward. Sims Fm. is tightly folded and cut by major faults. Metamorphism at greenschist facies.

Table 2.2: Summary of the deformational effects produced by the Hudsonian and Grenvillian Orogenies in the Tamarack River and Sims Formations.

The northern limit of widespread Grenvillian deformation (Fig. 2.3) separates the northern outliers of the Sims Formation which lie in the Churchill Province from the southern outlier, Evening outlier, which lies in the Grenville Front Zone (Wynne-Edwards, 1972; Gover et al., 1980). During the Grenvillian Orogeny (ca. 1.0 Ga, Stockwell, 1970), Evening outlier was moderately deformed into northeasterly-trending folds and faults (Section B-B', Fig. 2-3). The effects of the Grenvillian event extend northward into the Churchill Province, resulting in reactivation of pre-existing Hudsonian structures, northwest-trending gentle folds, and normal faults in the northern outliers of the Sims Formation (Section A-A', Fig. 2-3).

ECONOMIC POTENTIAL

A promising exploration target is possible uranium mineralization in the sandstones of the Tamarack River and Sims Formations. During field work, several small anomalies (3 to 4 times background) were encountered in both formations. Other Canadian Middle Proterozoic sandstones, notably those of northern Saskatchewan and the Northwest Territories, contain significant concentrations of epigenetic uranium (McMillian, 1978). A possible mineralization model entails the leaching of uranium from basement gneisses, or from shales of the Knob Lake Group, by circulating ground water or hydrothermal fluids and its subsequent precipitation at redox traps at the basal contacts of the formations or within roll fronts (Gabelman, 1977).

CHAPTER 3 - TAMARACK RIVER FORMATION

INTRODUCTION

The Tamarack River Formation is an Aphebian, mixed siliciclastic and carbonate sequence, which rests unconformably on the Knob Lake Group. The formation is poorly exposed and underlies approximately 900 sq. km. of flat, swampy ground between Menihek and Sims Lakes (Fig. 2.3). Previously these rocks were mapped either as part of the Menihek Formation (Frarey, 1961; Fahrig, 1967), or as part of the Sims Formation (MacDonell and Walker, 1975). Ware and Wardle (1979) demonstrated that this sequence deserves formational status and proposed the name Tamarack River Formation, after the largest river in the area. Subsequently, the northern limits of the formation were mapped by Wardle (personal communication, 1980) and an Aphebian age assigned to the formation by Ware (1980).

Strata of western and central portions of the formation appear to be disposed in a gentle, eastward-dipping homocline (cross-section A-A', Fig. 2.3). Along its western margin, this homocline is truncated by numerous northwest-trending folds and high-angle faults which were produced during the Hudsonian Orogeny (Ware, 1980). The southern boundary of the formation is interpreted to be a major northeasterly-trending fault (Fig. 3.1) which represents the northern limit of Grenvillian deformation (Ware, 1980).

Three stratigraphic sections (H, I, J, Fig. 3.1 and Fig. 3.2) were measured and, taken together, they represent a composite type section (Ware, 1980). Three informally-defined members are recognized with a total thickness of about 320 m (Fig. 3.2). Member A, the lowermost unit, is best exposed at the base of section J (Fig. 3.2) and outcrops

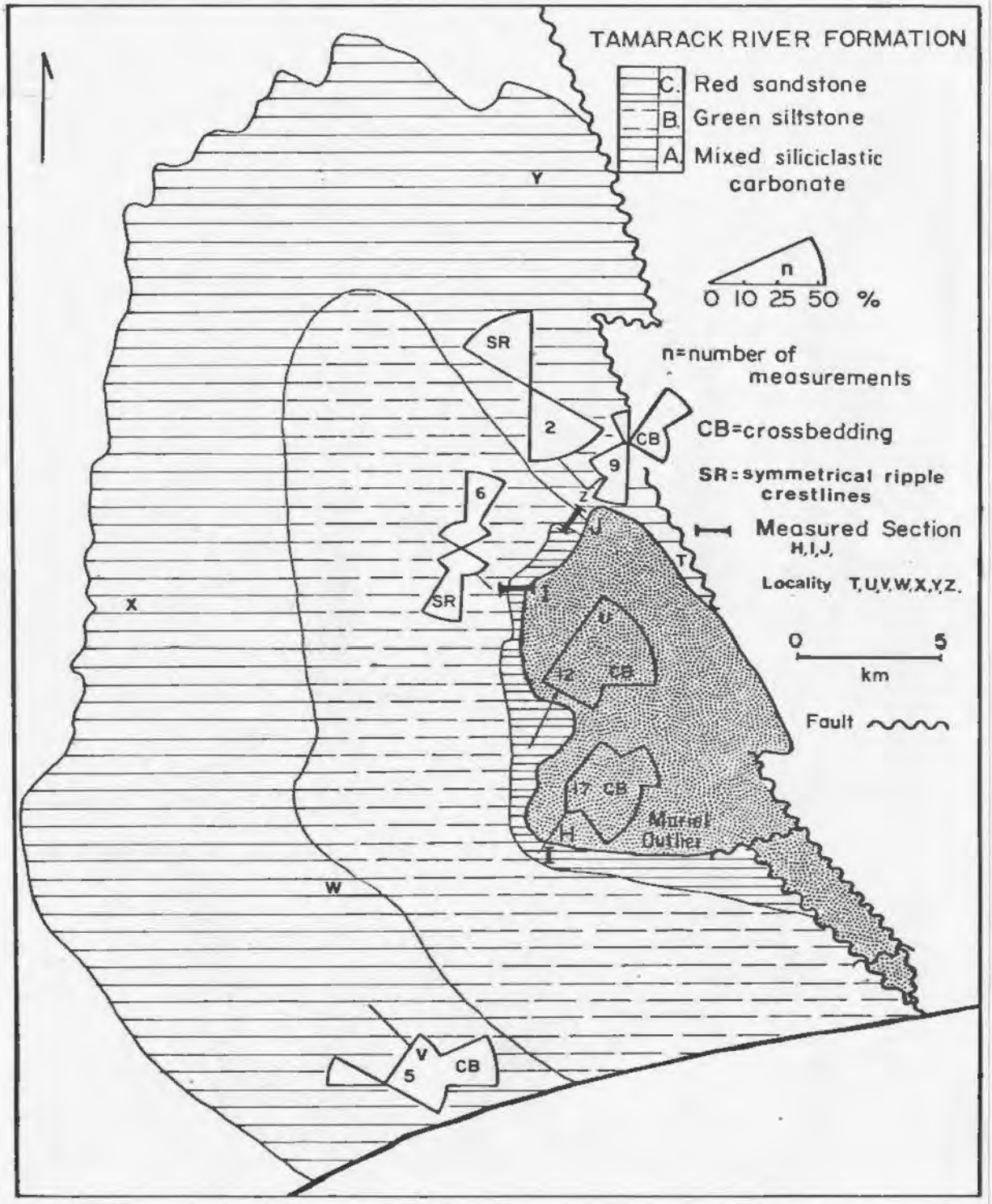

Fig. 3.1: Generalized geologic map of the Tamarack River Formation with paleocurrent data and outcrop localities mentioned in the text.

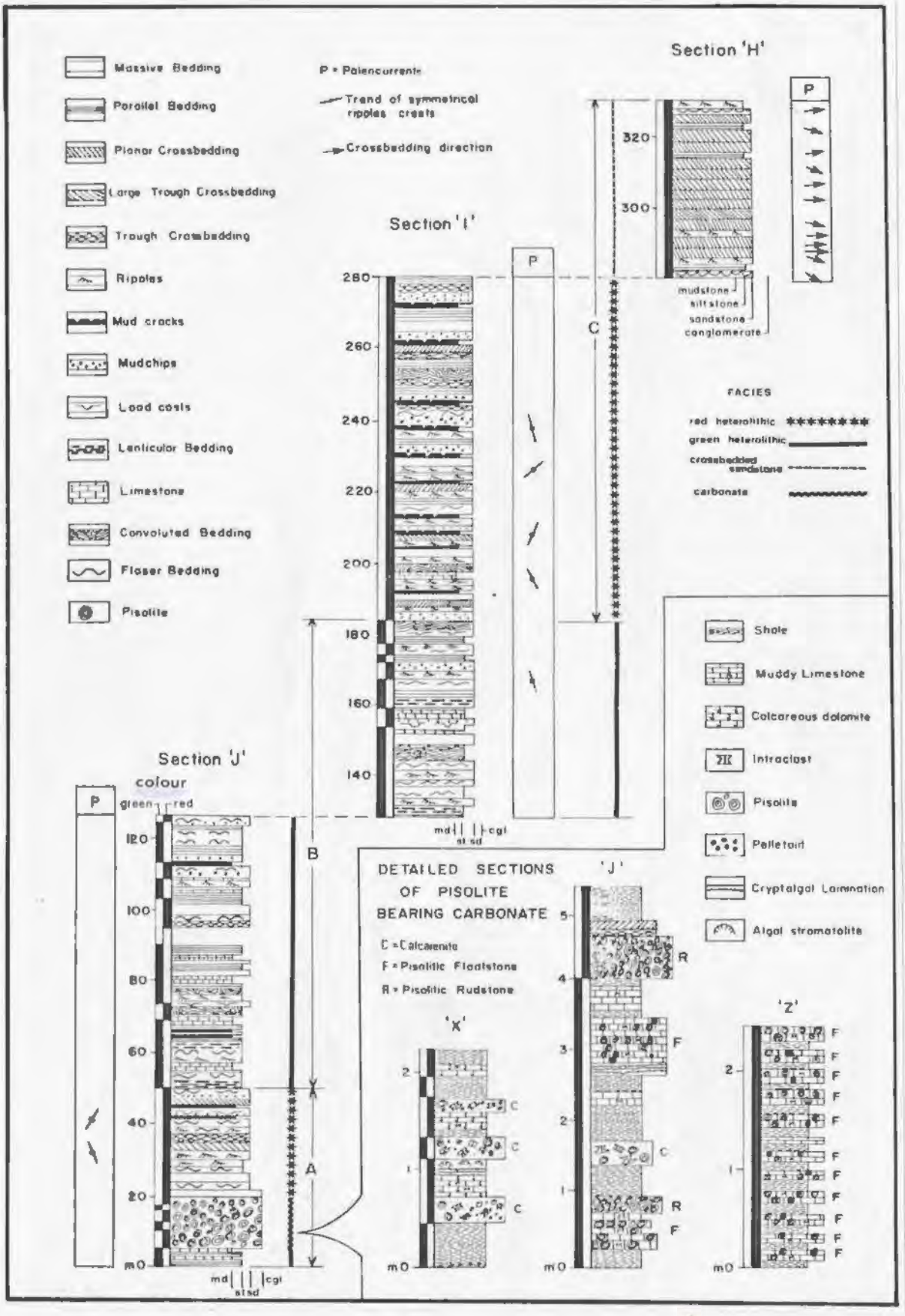

Fig. 3.2: Generalized stratigraphic sections (J, I, H). See Fig. 3.1 for location of sections.

along the formation's northern and western boundaries. It is 50 m thick and composed of coarse- to fine-grained, varicoloured siliciclastic and carbonate lithologies. Member A fines upward into the 120 m thickness of green-coloured, fine-grained, siliciclastics and minor carbonates of member B. This unit is best exposed in sections J and I and underlies the central portion of the formation (Fig. 3.1). Member C outcrops along the western flank of Muriel outlier (sections I and H, Fig. 3.1) and consists of 150 m of red sandstone with minor red siltstone and mudstone.

The Tamarack River Formation is considered to be Late Aphebian in age, because it rests unconformably on the 1.8 Ga Knob Lake Group (Fryer, 1972) and was deformed at approximately 1.7 Ga by the Hudsonian Orogeny (Stockwell, 1970).

FACIES

Based on lithologies and sedimentary structures, the formation has been divided into four facies:
(1) green heterolithic facies, (2) red heterolithic facies, (3) carbonate facies, and (4) crossbedded sandstone facies (Table 3.1).

Green Heterolithic Facies

Description

This facies forms the basal strata of member A and the bulk of member B (Fig. 3.2). It consists of predominantly green siltstone, mixed with varying proportions of sandstone and mudstone. In the

TABLE 3.1

Facies of the Tamarack River Formation

facies abundance (%)	distribution	lithology abundance (%) (T=Trace)	sedimentary structures	diagenetic structures	depositional environment
Red Heterolithic (50)	member A lower member C	sandstone (80), mudchip cgl. (10), mudstone and siltstone (5), granule and pebble cgl (5).	trough, planar and herringbone crossbedding, reactivation surfaces, flaser and wavy bedding, mudcracks.	red colouration with buff colored reduction spots.	intertidal
Green Heterolithic (25)	member B basal member A	siltstone (70), mudstone (20), sandstone (10), mudchip cgl. (T), dolomicrite (T).	flaser, wavy, and lenticular bedding, parallel lamination, graded beds, ripple marks, soft sediment deformation.	green colour locally changed to red, pyrite nodules calcareous concretions.	subtidal shallow marine
Crossbedded sandstone (20)	upper member C	sandstone (95), siltstone (5).	large scale cross - bedding, ripple marks.	red colouration with buff reduction spots.	fluvial
Carbonate (5)	member A	pisolitic floatstone (40), pisolitic rudstone (30), micrite (20), cryptalgal laminite (5) calcarenite (5), chert (T).	crossbedding, flatpebble cgl., stromatolites, fenestral porosity.	widespread dolomitization isopachous calcite cement, silica cement, stylolites	subtidal to intertidal

siltstone-dominated beds, parallel to rippled lamination defined by graded couplets of silt and mud are the most common structures. These laminations range in thickness from 0.5 to 1 cm, form beds up to 1 m thick (Fig. 3.3A), and are occasionally interbedded with lenses of graded sandstone (Fig. 3.3B). Beds with equal proportions of sandstone and siltstone contain wavy bedding, parallel lamination, low-angle crossbedding, and climbing ripple-lamination. Within sandstone-dominated zones, beds range in thickness from 10 cm to 2 m and average 0.5 m. The sandstones are fine to medium grained, poorly to moderately sorted, and contain subangular to subrounded grains. Most sandstones are structureless, but occasionally small-scale crossbedding, flaser bedding and green mudchip clasts up to 10 cm in diameter were recognized (Fig. 3.3C). Bedding planes display symmetrical ripples with wavelengths generally between 7 and 12 cm and amplitudes ranging from 1 to 3 cm. A few sets of large- symmetrical ripples are present with wavelengths over 70 cm and amplitudes greater than 30 cm (Fig. 3.3D). In some cases these large ripples contain smaller internal symmetrical ladder-back ripples. The average trend of the crests of large symmetrical ripples is northeast-southwest (Fig. 3.1).

This facies contains abundant examples of soft-sediment deformation features, which include pseudo-nodules (Fig. 3.3E), load casts, flame structure, and 'ball and pillow' structure. Also noted were diagenetic features, such as calcareous concretions, pyrite nodules and local zones where the normal green tint of siltstones has been changed to a reddish colour (Fig. 3.3F).

FIGURE 3.3

Green Heterolithic Facies

A. Thinly laminated bedding composed of alternating siltstone and mudstone.

B. Lenses of graded sandstone interbedded with mudstone and siltstone.

C. The base of a massive sandstone bed containing green mudchips eroded from the underlying strata.

D. Large symmetrical ripples at the top of a thick sandstone bed.

E. A load cast composed of lenticular to rippled sandstone and siltstone which sank into massive siltstone.

F. Green laminated siltstone with a red colouration zone (top and right) of replacement origin.

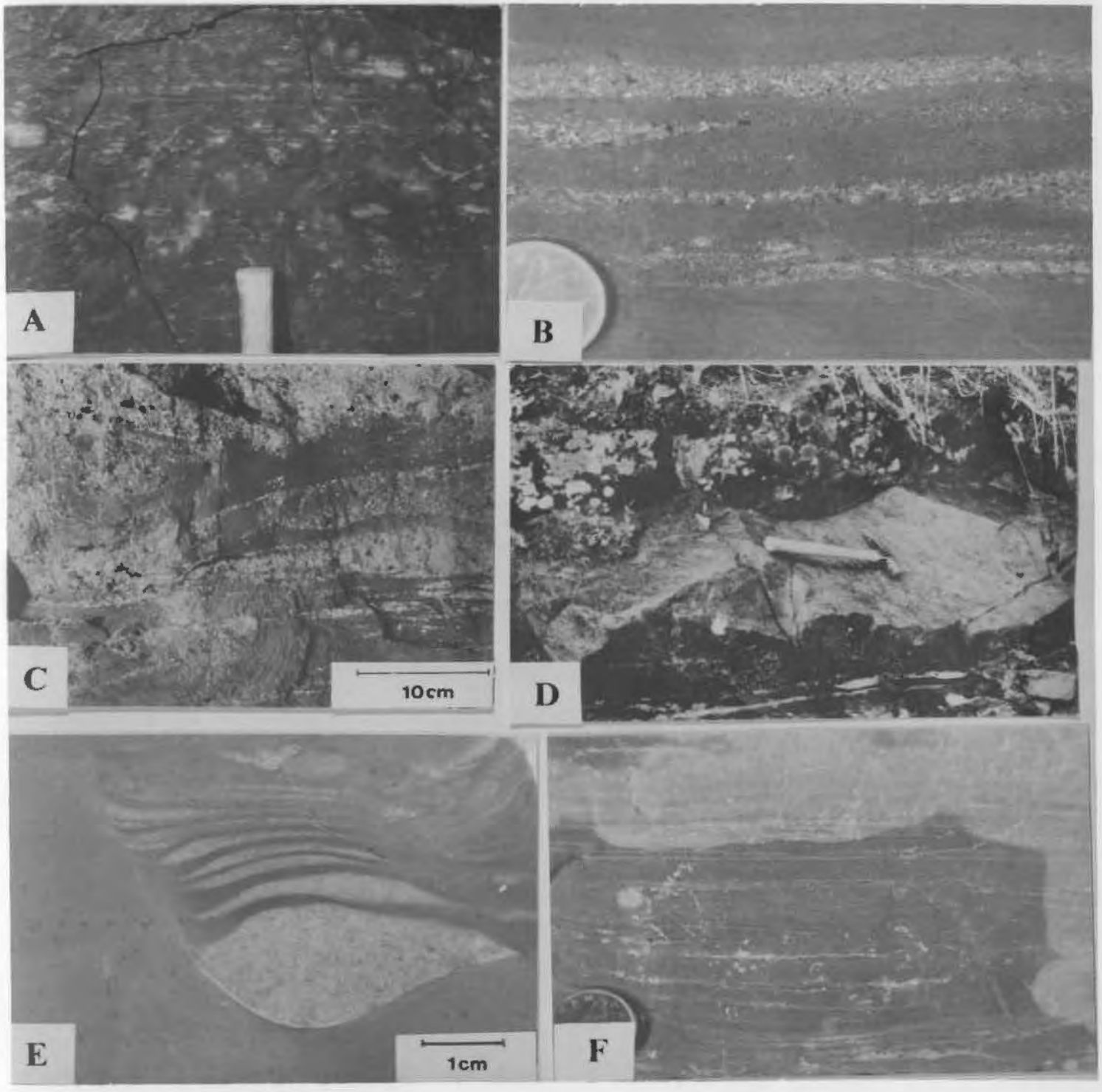
A
B
C
10cm
D
E
1cm
F

Interpretation

The green heterolithic facies is considered to a low-energy,subtidal marine deposit based on its structures, fine-grained nature and drab colour. Thinly laminated bedding with graded silt laminae, flaser bedding and lenticular bedding may reflect alternating periods of deposition in fairweather and storm conditions. Johnston (1978) postulated that mud layers resembling those of this facies are suspension deposits produced during tranquil periods and that graded silt and sand laminations are the result of fallout of coarser material suspended during storms.

The large symmetrical ripples are interpreted to be generated in relatively deep-water by wave action. Reineck and Singh (1973) noted that deep water wave ripples tend to be larger than shallow-water wave ripples because open-ocean waves have larger orbital diameters and thus can generate larger bedforms. The massive sand beds, with mudchip conglomerate at their baes, are high-energy deposits and are possibly related to intense wave action produced during storms or to strong tidal currents (cf. Johnston, 1978).

Red Heterolithic Facies

Description

This facies is the most abundant, and is present in member A and the lower part of member C (Fig. 3.2). It consists of red, pink, and purple sandstone, polymictic to oligomictic conglomerate, mudchip conglomerate, and minor amounts of red siltstone and mudstone. The sandstone is medium to coarse grained, moderate to well sorted, and contains angular to subrounded clasts set in a sericite matrix. Finely-disseminated hematite along grain boundaries imparts the red colour to the rock, and either silica or carbonate act as cement.

Individual sandstone beds range in thickness from 0.2 m to 2.0 m and average 0.5 m. Thinner beds, less than 0.4 m, are characterized by ripple lamination, parallel lamination and mud flasers (Fig. 3.4A). Most of the thicker beds appear structureless, but occasionally visible are small- to medium-scale sets of planar and trough crossbedding, and 'ball and pillow' structures. Some of the crossbeds contain reactivation surfaces (cf. Harms et al., 1965); others form herringbone units (Fig. 3.4B). Paleocurrent data from this facies are not abundant (localities V and Z, Fig. 3.1). At locality Z the distribution of crossbedding is bimodal-bipolar.

Red mudchip conglomerates, containing clasts up to 20 cm in diameter, occur throughout this facies. The clasts tend either to be localized near the bases of sandstone beds (Fig. 3.4C), or dispersed in the crossbedding foresets (Fig. 3.4D). Immediately above the carbonate facies of section J (Fig. 3.2) and at locality W (Fig. 3.1) there is a 2 m thick bed of purple-coloured, calcite-cemented, massive polymictic conglomerate with granule-sized, angular clasts. At locality Y (Fig.

FIGURE 3.4

Red Heterolithic Facies

A. Mud flasers with various rippled forms.

B. Small-scale planar and trough crossbedding with bimodal-bipolar current orientations. Darker sandstone is cemented with iron oxide and calcium carbonate while the lighter-coloured sandstone is cemented by silica.

C. Mud-chip conglomerate developed at the base of a massive sandstone bed.

D. Mudchips isolated on the foresets of crossbedding overlying a rippled sandy bed with mud flasers and mudchips.

E. Mudcracks developed in a thin mudstone bed and infilled with sandstone.

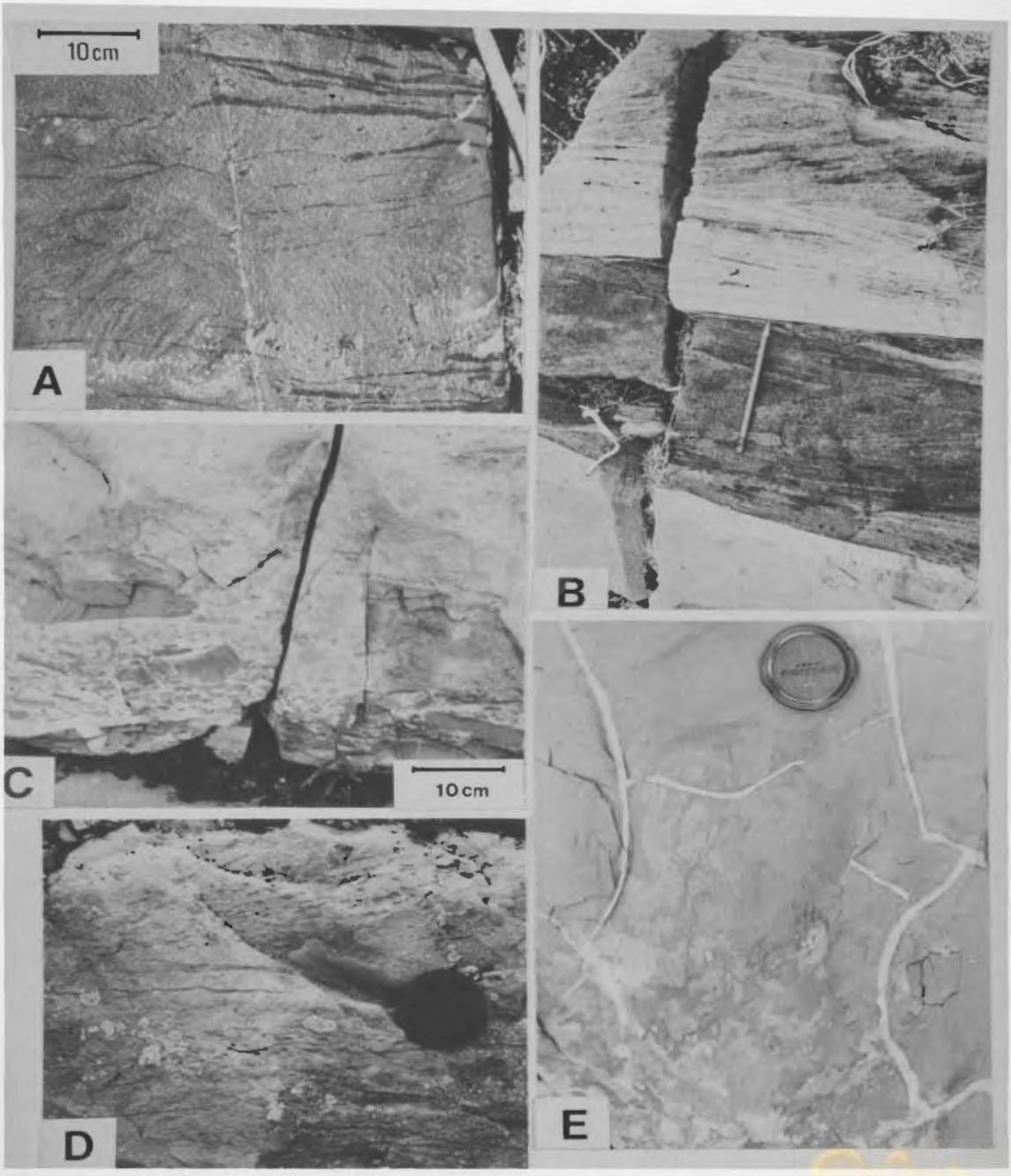
10cm
A
B
C
10cm
D
E

3.1), an oligomictic conglomerate composed of clast-supported, rounded, quartzite granules and pebbles set in a red, sandy, matrix was observed.

Fine-grained material in this facies is rare and limited to thin, parallel-laminated beds of red siltstone and mudstone less than 5 cm thick. Occasionally these mudstones contain polygonal mudcracks (Fig. 3.4E).

Interpretation

Types of lithologies and sedimentary structures found in the heterolithic facies suggest that deposition occurred in a predominately sandy, intertidal environment. Herringbone crossbedding, with reactivation surfaces, and crossbedding with a bimodal-bipolar distribution, are features commonly produced by reversing tidal currents (Reineck and Singh, 1973). This interpretation is further supported by an abundance of flaser bedding, which is produced in tidal shorelines by alternating periods of sand deposition and the fallout of fine-grained mud during slack water (Reineck and Wunderlich, 1968). The polygonal mudcracks indicate that, during low-water stages, the mud flats were subaerially exposed. The subsequent incorporation of these dried and cracked muds into mudchip conglomerates may have occurred within tidal channels (Klein, 1977). The granule and pebble conglomerate may have accumulated on beaches.

Carbonate Facies

This facies forms about 30% of member A (Fig. 3.2) and is subdivided into a pisolite subfacies and a fine-grained subfacies.

Pisolitic Subfacies

Description

This subfacies is composed of pisolitic floatstone, pisolitic rudstone, and minor calcarenite and dolarenite.

The pisolitic floatstone is characterized by individual pisoliths, composed of calcite or dolomite, dispersed as discrete units in a calclutite or dololutite matrix, or by distinct sheets of pisoliths (one clast thick) surrounded by a silty micrite (Fig. 3.5A). It is most commonly green or brown in colour and forms beds between 10 cm and 2 m thick. Pisoliths range in shape from ellipsoidal to spherical, through to irregular polygons, and average about 1 cm in diameter but can attain a maximum diameter of 4 cm. Pisoliths are defined by continuous and discontinuous laminations (Fig. 3.5B) which surround an intraclastic nucleus. Peloids, intraclasts and ooids are often bound onto the laminae and a fenestral porosity is developed between laminations. Occasionally, several pisoliths will combine to form a single compound pisolith which shares common outer laminations (Fig. 3.5A). At locality Z, alternating beds of pisolitic floatstone and red mudstone form distinctive cycles (Fig. 3.5B,C) averaging about 20 cm in thickness. Groups of these cycles are separated by low-angle unconformities.

Pisolitic rudstone is characterized by abundant contacts between individual pisoliths, a red colouration, a predominantly dolomitic composition, and a lack of fine-grained matrix. Beds of pisolitic rudstone range from 30 cm to 1.0 m in thickness and are often associated with doloarenite and crossbedded sandstone (Fig. 3.5D). Pisoliths within the rudstone are well sorted, less than 2 cm in diameter, and usually show evidence of abrasion and fracturing.

FIGURE 3.5

Carbonate Facies I

A. Pisolitic floatstone with individual pisoliths concentrated along a specific horizon. 'CP' is a compound pisolith. Top is up.

B. Cycles of pisolitic floatstone and mudstone. Groups of cycles are separated by a low-angle discordance.

C. Detail of a cycle. An horizon of similar-sized pisoliths is concentrated at the base of a pisolitic floatstone (P.F.) bed above a mudstone (M.S.) bed.

D. Massive bed of pisolitic rudstone grading upward into red crossbedded sandstone with opposed current directions.

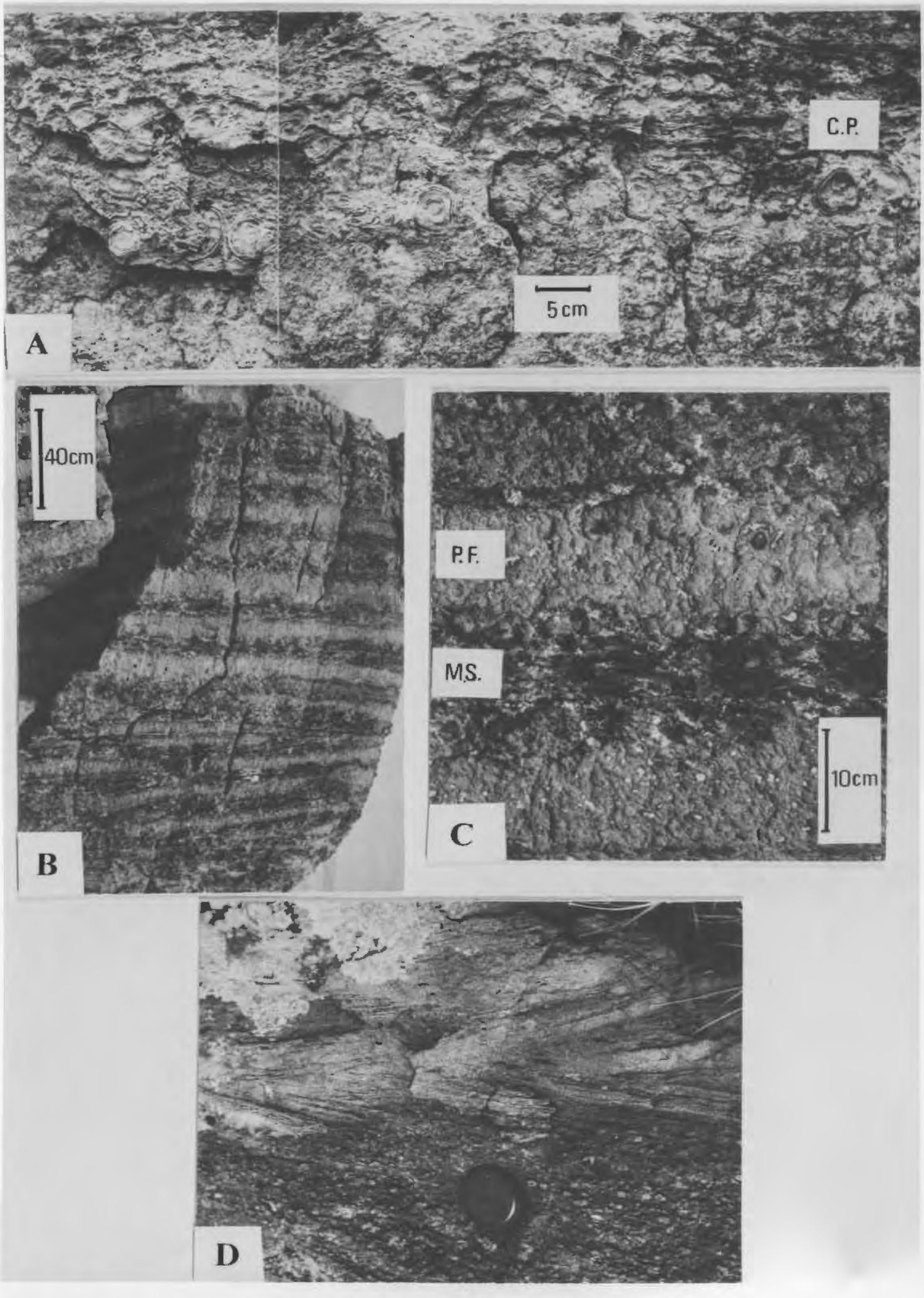
C.P.
5 cm
A
40cm
B
P.F.
M.S.
10cm
C
D

An interpisolitic porosity developed within rudstone is infilled by at least three generations of cement. The first is an isopachous, fibrous, calcite cement (Fig. 3.6A) which is followed by a coarse, blocky calcite, sparry cement and finally by a reddish quartz cement. Although extensive dolomitization often destroys the internal structure of the pisoliths, the original pisolitic character of the rock is preserved by the characteristic interpisolitic cement pattern (Fig. 3.6B).

The thin beds of red dolarenite and calcarenite associated with the pisolitic rudstone are grainstones and packstones composed of fragments of pisoliths, peloids, ooids, mudchips and siliciclastic detritus. Some packstones contain a well-developed vuggy porosity which has been infilled by geopetal muds, and by calcite and silica cement (Fig. 3.6C).

Interpretation

Pisoliths of this subfacies are probably algal in origin. Morphologically these pisoliths, with their irregular shape and laminations defined by variation in grain size, resemble the algal pisoliths described by Gebelein (1967) and Peryt and Piatkowski (1977). Absent are any features which would suggest an inorganic origin for the pisoliths; the pisolitic subfacies lacks the extensive replacement textures, laminar bedding and distinctive profiles commonly associated with pisoliths of caliche origin (James, 1972) and there is no evidence such as polygonal fitting, consistent downward elongation, reverse grading and perched inclusions to suggest that the pisoliths were produced by vadose marine processes (Dunham, 1969; Esteban, 1976).

FIGURE 3.6

Carbonate Facies II

Photomicrograph of pisolitic rudstone cemented by a fibrous, radial calcite cement and sparry cement. Pisoliths have distinct (D) and indistinct (I) laminations. 'V' is volcanic fragment.

Dolomitized pisolitic mudstone overlain by brecciated cryptalgal laminations. The interpisolith porosity of the rudstone is infilled with calcite.

Dolomitic grainstone with well-developed vuggy porosity which has been infilled with geopetal micrite (G) and calcite.

Polished slab of chaotic breccia composed of dolomicrite clasts dispersed in silty dolomicrite.

Small hemispherical algal stromatolite composed of fine-grained carbonate and chert.

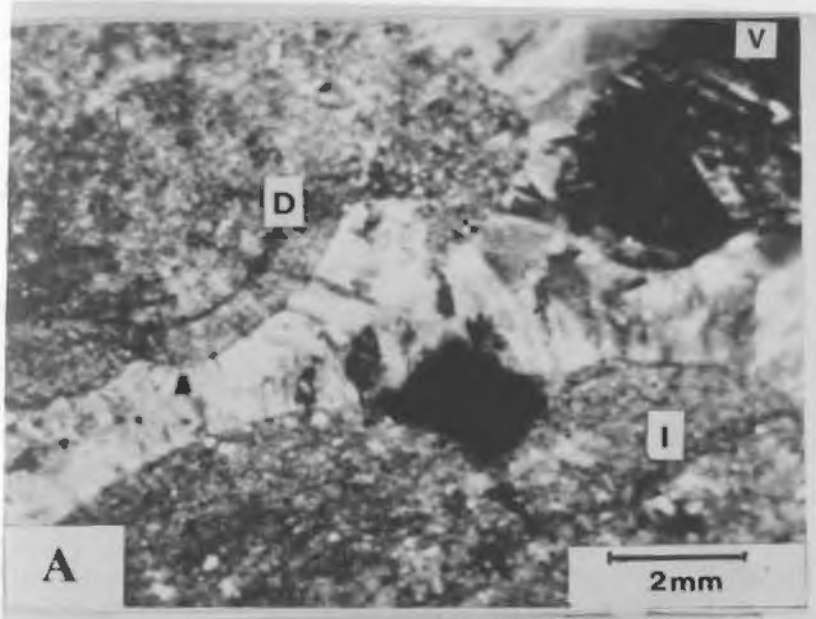
V
D
I
A
2mm

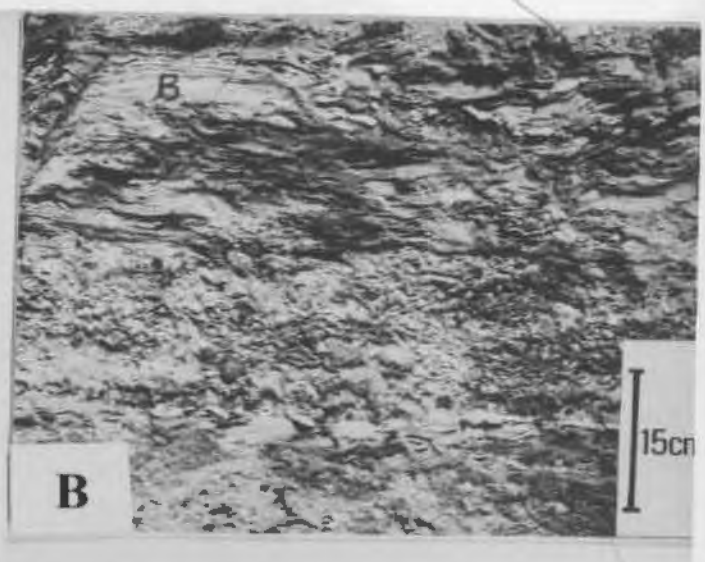
B
15cm
B

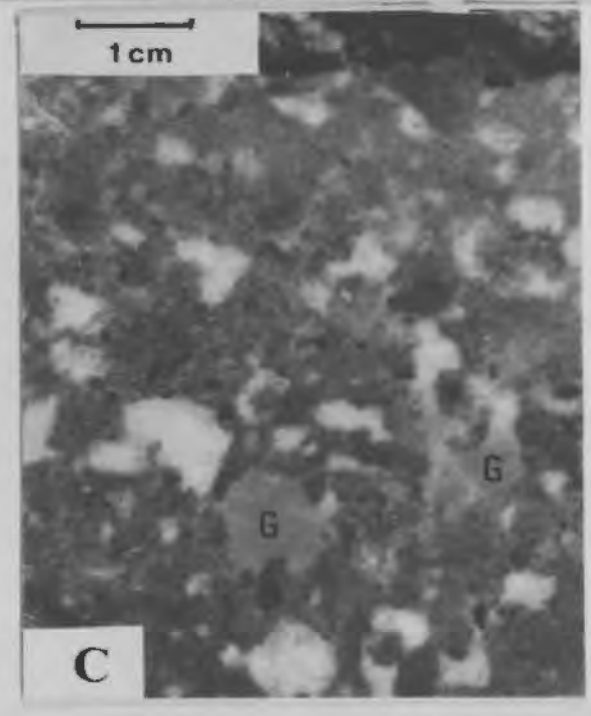
1 cm
G
G
C

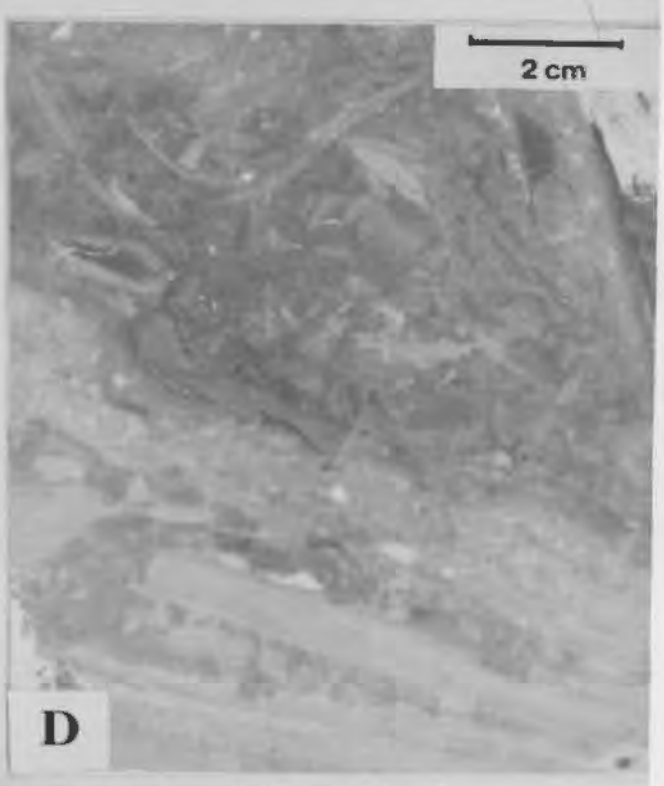
2 cm
D

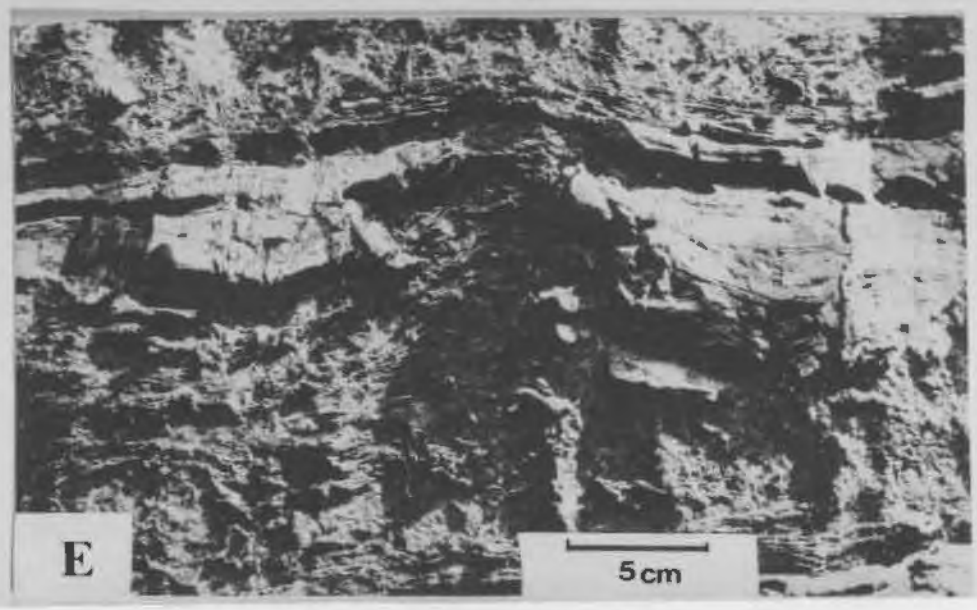
E
5cm

The pisolitic floatstone is interpreted to be a low-energy, shallow, subtidal deposit because of its abundant muddy matrix, poor sorting of pisoliths and its close association with fine-grained siliciclastics. Pisolith-rich horizons probably represent the *in situ* growth positions of pisoliths on a muddy substrate (Gebelein, 1967).

The cycles of alternating pisolitic floatstone and red, fine-grained, silicilcastic debris were produced when terrigenous material was introduced at regular intervals, and thus inhibited the growth of pisoliths. The minor angular unconformities which separate groups of cycles may record periods of storm-induced erosion.

The pisolitic rudstone probably represents tidal channel deposition. Tidal currents were responsible for the winnowing out of the fine-grained matrix material, improving the sorting of the pisoliths and abrading the pisoliths. A tidal origin is further supported by its close association with herringbone-crossbedded calcarenite and siliciclastic sandstone. The presence of isopachous, fibrous, calcite, cements surrounding the pisoliths suggests that cementation occurred in a submarine environment (James *et al.*, 1976).

Fine-grained Subfacies

Description

This subfacies is composed of varicoloured micrite, dolomicrite, cryptalgal laminite and minor bedded chert.

Buff, green and red micrite, dolomicrite and silty micrite are interbedded with the pisolitic subfacies and the green heterolithic facies. Beds are less than 0.5 m thick and are either massive or exhibit thinly-laminated parallel to slightly undulose bedding.

Edgewise conglomerates occur at the bases of some beds (Fig. 3.6D). At locality T, a 2 m-thick massive bed of pink dolomicrite with numerous thin beds of red chert was observed.

The cryptalgal laminate is composed of red or green, finely-laminated micrite, dolomicrite, and fine-grained grainstone. The laminations are of uniform thickness (about 2 mm), either planar or wavy in cross-section, and have a well developed microscopic fenestral fabric. Sporadically developed within the laminite are small bulbous stromatolitic forms (Fig. 3.6E), mudcracks and teepee structures (cf. Wilson, 1975).

Interpretation

Cryptalgal laminites and small domal stromatolites are characteristic of low-energy tidal flat deposits (Gebelein, 1976). The laminations are formed by the binding of carbonate muds by flat algal mats (Logan et al., 1974). The breccia layers associated with the laminates were produced by storms, or during periods of subaerial exposure.

The beds of massive and thinly laminated, fine-grained carbonate are probably low-energy, shallow, subtidal, lagoonal deposits.

Crossbedded Sandstone Facies

Description

This facies forms the upper part of member C, outcrops at section H (Fig. 3.1), and is characterized by large-scale, planar-tabular and planar wedge-shaped crossbedding (Fig. 3.7A,B). These sandstones are medium to coarse grained (Fig. 3.7C), moderately well-sorted, and

FIGURE 3.7

Crossbedded Sandstone Facies

A. Upper portion of a thick planar-tabular crossbed overlain by siltstone. Hammer handle points to top of bed.

B. Parallel-laminated and rippled sandstone overlying a planar-crossbedded sandstone. White botches are reduction spots.

C. The scoured base of a crossbed unit illustrating the coarseness of the sandstone. White botches are reduction spots.

Petrography

D. Photomicrograph of a silica- and calcite-cemented sandstone from member A. 'I' is an iron formation ooid with a radial fabric derived from the Sokoman Formation. 'C' is chert, also from the Sokoman Formation. 'V' is a felsic volcanic fragment derived from the Nimish Formation.

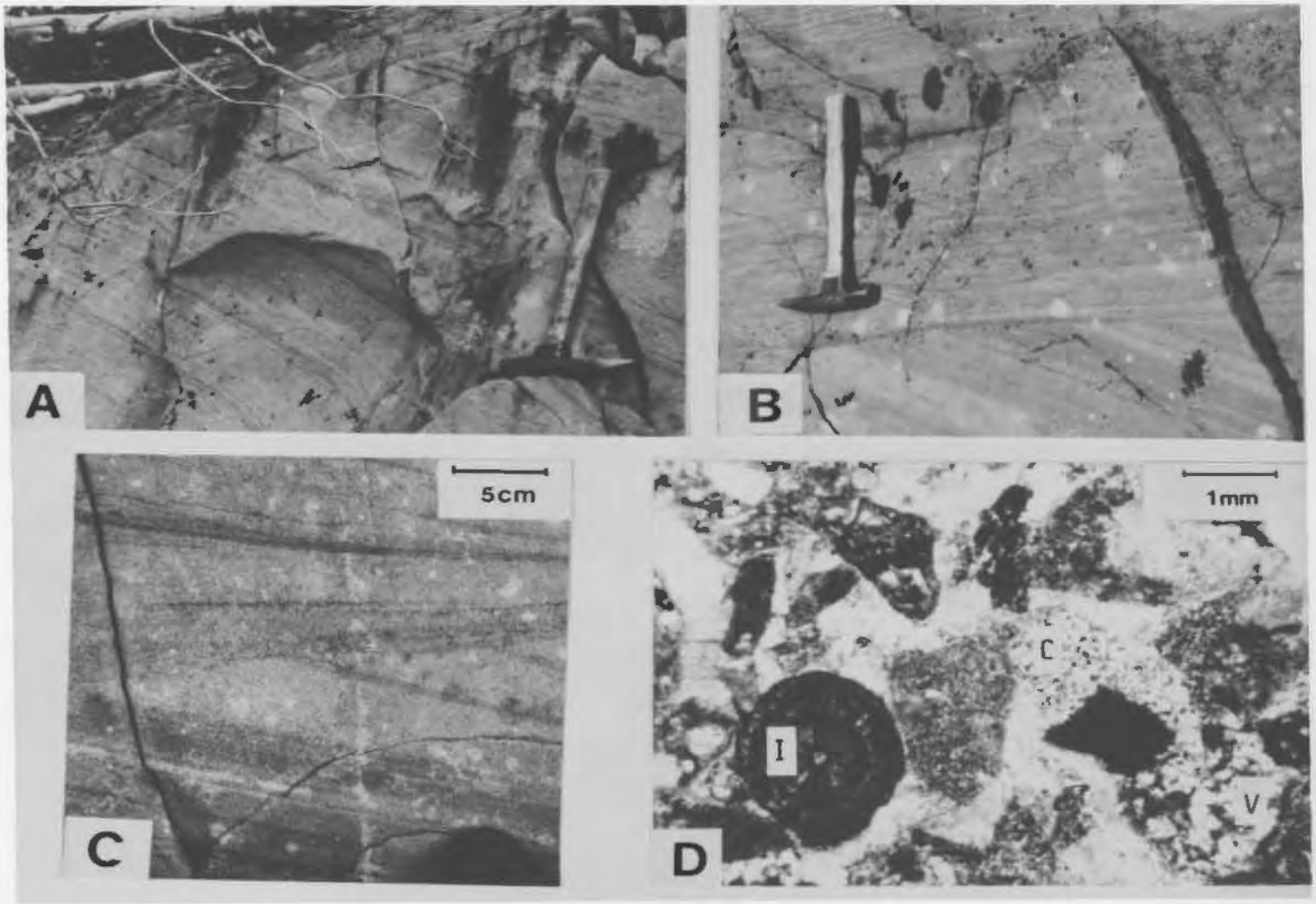
A
B
5cm
C
1mm
C
I
V
D

contain subangular to subrounded clasts. The normal red colouration has been changed to a buff tint in many isolated irregular patches (Fig. 3.7B,C).

Crossbed sets range in thickness from 0.5 m to 2 m (Fig. 3.7A, B) and can be traced laterally for up to 20 m. Foresets dip at angles between 22° and 30° and have a strong unimodal orientation, indicating that paleoflow was directed to the east (Fig. 3.1). Laminations within the sets range between 0.5 and 3 cm thick and are defined by alternations in grain size. Granule-sized mudchips and small-scale contortions occur at the bases of some crossbeds.

Associated with this facies are some small to medium-scale trough crossbeds, parallel and ripple-laminated bedding (Fig. 3.7B) and a few intercalations of siltstone containing calcareous nodules.

Interpretation

Examples of large-scale planar crossbedding with unimodal paleocurrent distribution occur in fluvial (Coleman, 1969), eolian (McKee, 1979) and shallow-marine (Anderton, 1976) depositional environments. A fluvial origin is considered most likely for this facies because the textures and structures commonly associated with the other two possibilities are absent.

The angularity, coarseness and moderate degree of sorting of the constituent clasts contrasts with the fine- to medium-grained, well-rounded and well-sorted sands typical of eolian deposits (McKee, 1979). A shallow marine origin is also ruled out because sedimentary structures typical of wave and tidal activity, such as reactiviation surfaces and flaser bedding, are absent.

The lack of fine-grained lithologies and the strongly unimodal paleocurrent distribution suggests that deposition occurred in braided rather than meandering fluvial channels. According to Miall's (1976) classification of braided stream deposits, an abundance of planar-crossbedded sandstone is typical of non-cyclic, sandy, braided rivers which develop on the distal portion of a braided alluvial plain.

PETROGRAPHY

Thirteen thin sections of medium-grained sandstone were point counted to determine their modal composition (Appendix A). The QFR plot of modal composition (Fig. 3.8A) demonstrates that the rock fragment content decreases markedly from member A through to member C. Member A contains abundant rock fragments composed of mafic volcanic, felsic volcanic, iron formation, chert and quartzite lithologies (Fig. 3.7D). The felsic volcanic fragments are distinctive and have a pervasive spherulitic alteration texture with numerous iron-oxide specks (Fig. 3.7D). In addition, the fragments become bright yellow when a sodium cobaltinitrite stain is applied (Dickson, 1966), and thus are probably potassium rich.

The sandstones of members B and C contain a significantly lower portion of rock fragments and are composed prodominantly of quartz, plagioclase, chert and orthoclase. The trend of decreasing rock fragment content with stratigraphic height within the formation, is independent of grain size variations, because only medium-grained sandstones were chosen for point counting.

Major element geochemistry shows that the sandstones of members B and C plot in the ferromagnesian-potassic field (Fig. 3.8B) of the

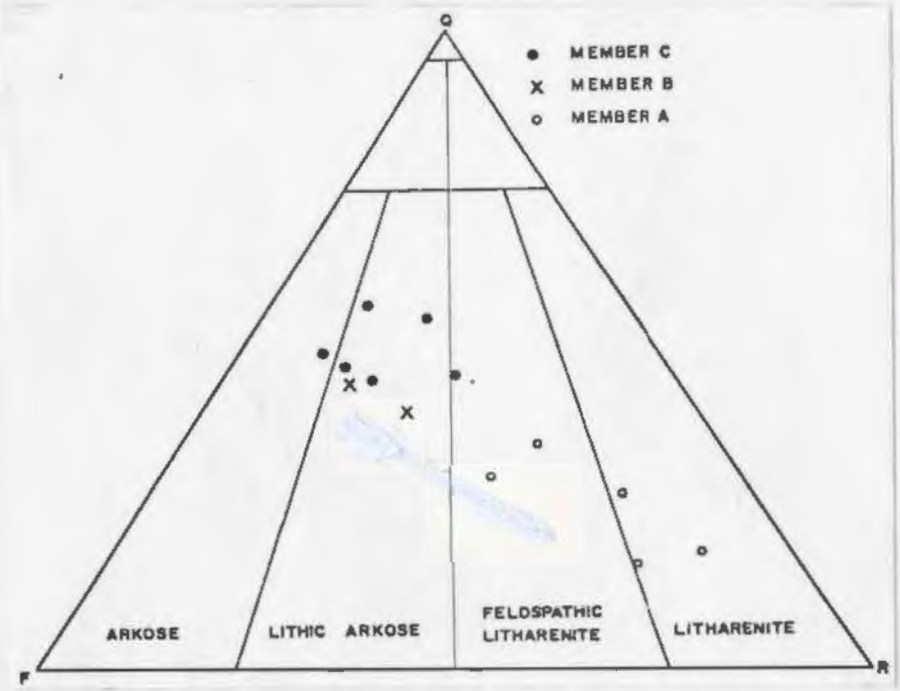

Fig. 3.8A A quartz (Q), feldspar (F) and rock fragment (R) diagram for 13 medium-grained sandstones of the Tamarack River Formation. 200 grain-counts per sample. Sandstone classification according to

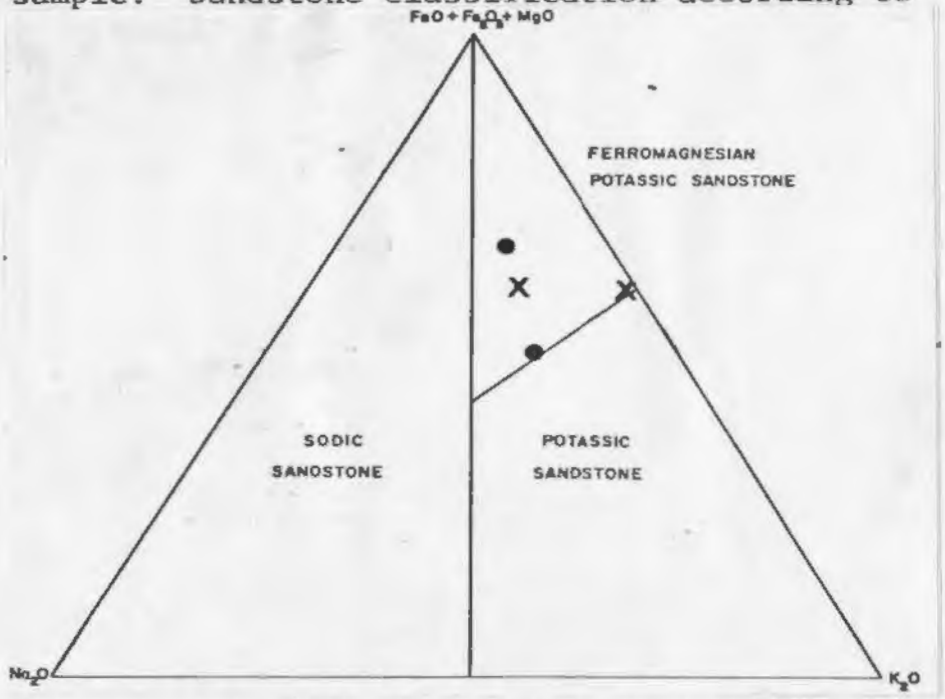

Fig. 3.8B Ternary plot of Na_2O, $FeO + Fe_2O_3 + K_2O$ for chemical analyses of four Tamarack River Formation sandstones. Chemical fields are from Blatt et al (1972, p. 318).

Blatt, et al., (1972) classification. X-ray diffraction indicates that the mudstones of member B are composed of chlorite, sericite and quartz with possibly minor feldspar and illite.

The unique rock fragments in the sandstones of member A suggest that the bulk of the detritus deposited in the lower part of the Tamarack River Formation was derived from the underlying Knob Lake Group (Ware, 1979). Both the chert and iron formation clasts originated from the Sokoman Formation and the quartzite grains probably came from the Wishart Formation, whereas the Nimish Formation, must have supplied the volcanic fragments, because this detritus contains the same alteration textures and potassium enrichment noted by Evans (1979).

The presence of Nimish Formation volcanic clasts places constraints on the sediment dispersal pattern operating during deposition of the lower part of the Tamarack River Formation. Because the Nimish Formation only occurs north of the Tamarack River Formation, volcanic detritus in the lower member must have been deposited by a southward-flowing dispersal system. The litharenites and lithic arkoses of members B and C contain fewer rock fragments than member A and are composed predominantly of quartz, chert, plagioclase, orthoclase, and microcline, with accessory mica and heavy minerals.

The lack of a major lithic component in the sandstone of the two upper members may in part be due to the destruction of rock fragments by increased reworking, or it could also reflect a change in provenance. Within member C, the easterly-directed paleocurrents and the approximate equal proportions of quartz and feldspar suggest that the detritus in the upper portion of the formation was derived from the granite gneisses of the Superior Province (Fig. 1.1).

Redbeds make up about 70% of the Tamarack River Formation (Fig. 3.2) and are interpreted to have been deposited in either a fluvial or an intertidal environment. Their red pigmentation is considered to be of diagenetic origin; iron was released during the hydrolysis of volcanic or silicate clasts and precipitated in the ferric state under oxidizing conditions (cf. Hubert and Reed, 1978). The subtidal rocks are predominantly green and their pigmentation is believed to be due to the reduction of ferric iron by decaying organic matter, bacteria, or H_2S on the sea floor, and its incorporation into authigenic pyrite as ferrous iron (Berner, 1971). In some places, the primary green colouration of the subtidal lithologies has been oxidized to a red pigmentation by later diagenetic processes.

STRATIGRAPHY

The basal contact of the Tamarack River Formation with the Knob Lake Group is not exposed, but an unconformable relationship may be inferred from clast content. The presence of a distinctive rock fragment suite, which must have originated from the Knob Lake Group, indicates that at least part of the Knob Lake Group was uplifted and eroded prior to or during deposition of the Tamarack River Formation.

Due to poor exposure, the internal stratigraphic relationships of the formation are not well understood. However, it is believed that the three measured sections can be combined (Fig. 9A) to define a composite type section for the formation. This belief is based on four observations:

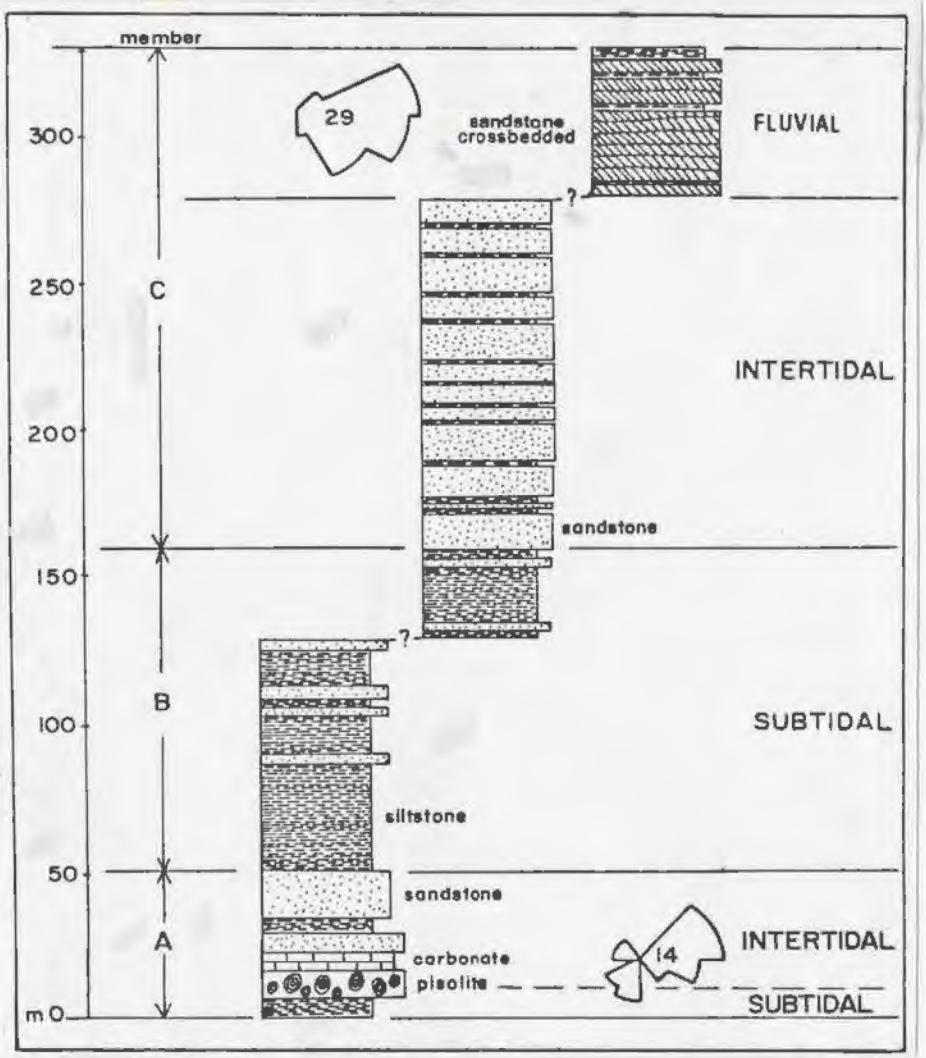

Fig. 3.9A Summary stratigraphic section for the Tamarack River Formation with facies interpretation and paleocurrent data.

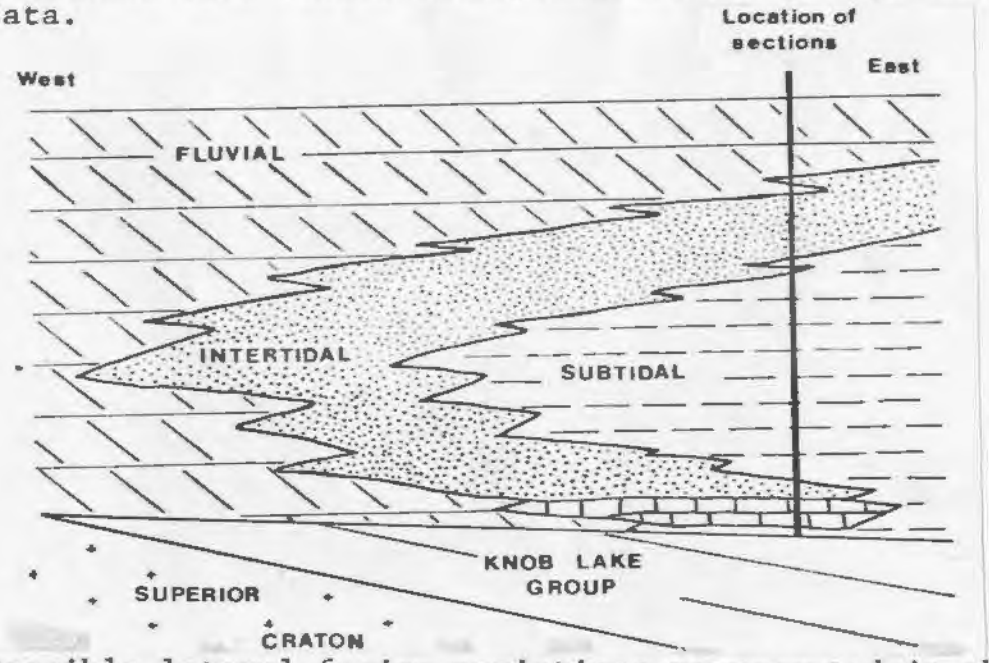

Fig. 3.9B Possible lateral facies variations represented in the Tamarack River Formation.

1. The upper part of section J is lithologically similar to the lower part of section I and likewise the upper part of section I is similar to the lower part of section H (Fig. 3.2).
2. A realistic map pattern can be drawn which reconciles this proposed stratigraphy and all the available structural data (Fig. 2.3 in back pocket).
3. Because the three measured sections are located west of the Sakit Lake Fault and are aligned north-south, subparallel to the major structural trends of the Labrador Trough, it is unlikely that any major structural features separate the sections.
4. It is considered improbable that the three sections are lateral, time-equivalent, facies variations of each other because it is unlikely that a shallow-marine to fluvial depositional regime could produce three distinctive sections, all over 60 m thick, with a maximum of only 12 km separating the sections.

DEPOSITIONAL HISTORY

The Tamarack River Formation is interpreted to record two transgressive-regressive cycles (Fig. 3.9B). The initial transgression is represented by the basal shallow-marine green siltstone of member A (Fig. 3.9A). As sea-level fell, the input of clastic detritus decreased. The siltstone grades upward into the subtidal pisolitic floatstone, dololutite and calcilutite, and the intertidal pisolitic rudstone, packstone, grainstone and cryptalgal laminite. Renewed influx of siliciclastic detritus inhibited generation of calcareous sediment, and intertidal red-sandstone with minor mudchip conglomerate and mudstone were deposited.

To account for the large volume of volcaniclastic material in the lower member, it is proposed that the paleodispersion pattern was directed southward.

The second transgression was initiated by a relative sea-level rise. The intertidal sandstones fine upward into the green shallow-marine siltstones of member B. The trend of crests of large-scale ripples suggests that the paleoshoreline trended in a NE-SW direction. The final regression is marked by the return of coastal conditions and the deposition of the red intertidal sandstones of member C. These sandstones are overlain by the crossbedded, red, sandstone facies which was deposited under braided fluvial conditions on an easterly-dipping paleoslope (Fig. 3.9A). The thickness and the easterly directed paleocurrent pattern of these fluvial deposits, plus an abundance of quartz and feldspar clasts which were probably derived from a granitic terrane, suggest that this member may have onlapped in a westerly direction to rest directly on the Superior Province craton (Fig. 3.9B).

The coastal to shallow-marine and fluvial nature of the sediments and their associated paleocurrent patterns suggest that the Tamarack River Formation is a miogeoclinal deposit which accumulated along the eastern margin of the Superior Province craton. The paleodispersal systems extant during deposition were directed either away from, or parallel to, the craton. The formation forms the third sequence of miogeoclinal deposits which developed in the Labrador Trough during Aphebian times. The first and second sequences are represented by the lower and upper parts of the Knob Lake Group.

CORRELATION

The Tamarack River Formation may be correlative with strata in the northern Labrador Trough. South of Ungava Bay (Fig. 3.10), a 400 m sequence of fluvial to shallow-marine, clastic and chemical sediments belonging to the Chioak, Abner, and Larch River Formations has been mapped by Dimroth et al., (1970). These strata have been interpreted as the third miogeoclinal cycle or sequence present in the northern part of the Trough (Dimroth et al., 1970). This northern sequence appears to rest unconformably on the iron formation of the Fenimore Formation (Dressler, 1979; Benard, 1965) which is believed to be correlative with the Sokoman Formation (Fig. 3.10), the second-sequence iron formation of the central Trough. Both the Tamarack River Formation and the strata of the Chioak, Abner and Larch River Formations are relatively thin, shallow marine to fluvial deposits which appear to rest unconformably on second-sequence rocks of the Labrador Trough. Taken together, these formations may be the remnants of an extensive third miogeoclinal sequence which developed in the Labrador Trough during Late Aphebian time.

SUMMARY

The Tamarack River Formation is a Late Aphebian sedimentary sequence which rests unconformably on the upper Knob Lake Group in the south-central Labrador Trough. The formation is divided into three informal stratigraphic members and four depositional facies. The green heterolithic facies consists of subtidal siltstone, and contains flaser and parallel-laminated bedding, with minor sandstone and mudstone. The

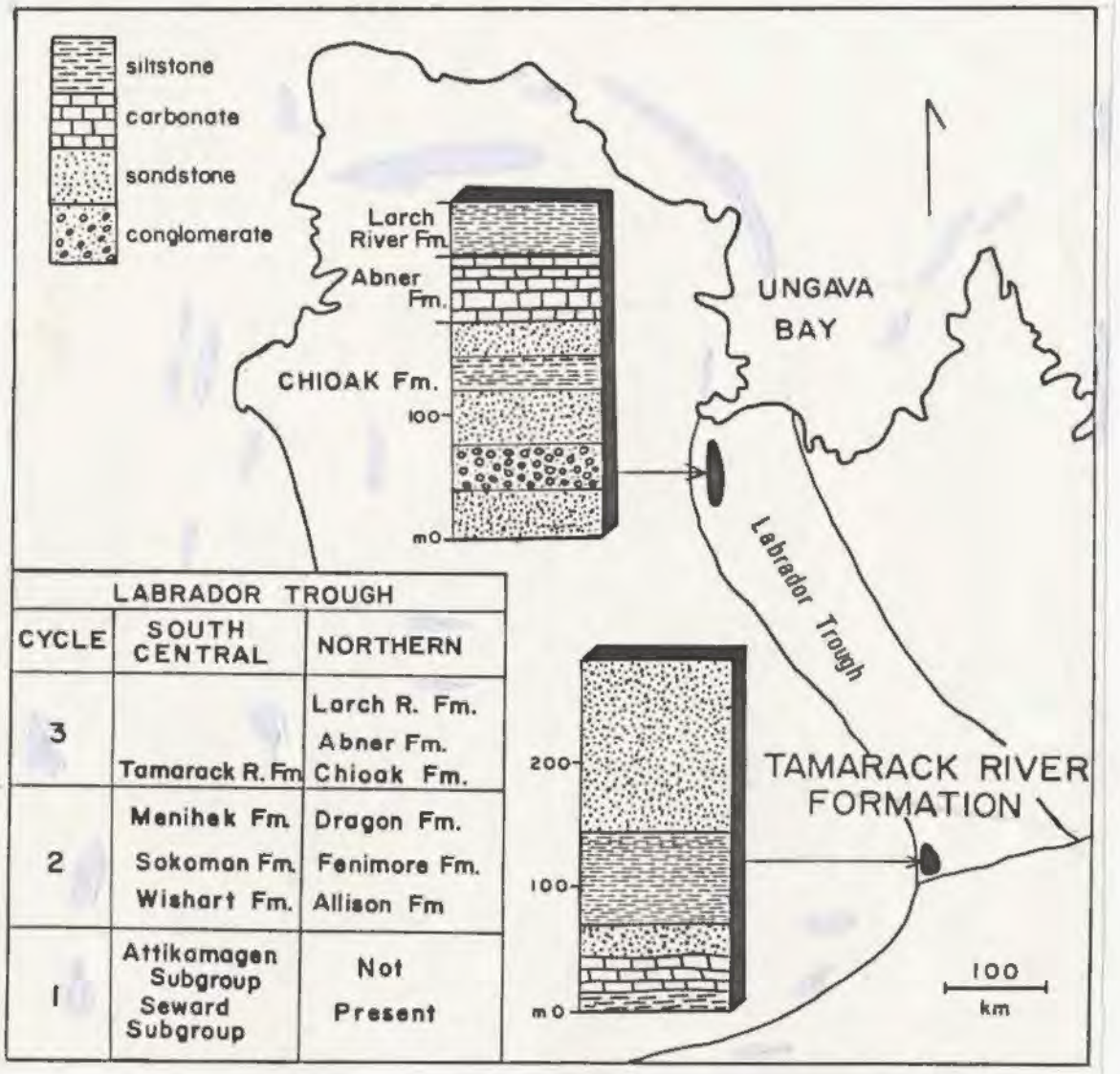

LABRADOR TROUGH		
CYCLE	SOUTH CENTRAL	NORTHERN
3	Tamarack R. Fm.	Larch R. Fm. Abner Fm. Chioak Fm.
2	Menihek Fm. Sokoman Fm. Wishart Fm.	Dragon Fm. Fenimore Fm. Allison Fm
1	Attikamagen Subgroup Seward Subgroup	Not Present

Fig. 3.10: Possible third sequence sediments of the Labrador Trough; the Chioak, Abner, and Larch River Formations of the northern trough, and the Tamarack River Formation of the south-central trough. The stratigraphy of northern Labrador is adapted from the descriptions of Dimroth et.al., (1970).

red heterolithic facies is composed of intertidal sandstone with abundant mudchip conglomerate, herringbone crossbedding, and minor amounts of mudcracked mudstone. The carbonate facies consists of pisolitic floatstone, calcilutite and dololutite of subtidal origin and intertidal pisolitic rudstone, cryptalgal laminite, packstone, and grainstone. The crossbedded red sandstone facies is characterized by large-scale, planar crossbedding and is probably a fluvial deposit. Member A records a regressive cycle; basal beds of subtidal siltstone pass upward into intertidal algal carbonate and clastic lithologies. As sea-level rose, subtidal conditions returned and the siltstones of member B were deposited. These fine-grained lithologies were in turn overlain by intertidal and fluvial clastics of member C.

Distinctive clast lithologies in member A suggest that its clastic detritus was derived from an uplifted area to the north, underlain by volcanics of the Knob Lake Group. With increasing stratigraphic height within the formation, the sandstones progressively become more mineralogically mature. Paleocurrents and clast lithologies of member C indicate that its provenance was the Superior Province, to the west.

The Tamarack River Formation is Aphebian in age because it was deformed along with the underlying Knob Lake Group during the Hudsonian Orogeny. The formation is interpreted to have been deposited along the eastern margin of the Superior Province craton, and to represent the third miogeoclinal sequence of Aphebian age recognized in the southern Labrador Trough. The lithologically similar Chioak, Abner, and Larch River Formations of the northern Labrador Trough may be correlative with the Tamarack River Formation, because they appear to occupy the same stratigraphic position.

CHAPTER 4 - SIMS FORMATION

INTRODUCTION

The Paleohelikian Sims Formation is a 700-m thick sequence of conglomerate, arkose and quartzarenite which rests unconformably on deformed Aphebian strata. The formation is exposed in four major outliers; Muriel, Sims, MacLean, and Evening outliers, and covers a total area of about 500 sq.km. (Fig. 2.3, in pocket). The three northern outliers are gently folded (Section A-A', Fig. 2.3) and essentially unmetamorphosed, but Evening outlier was moderately deformed during the Grenvillian Orogeny (Section B-B', Fig. 2.3) and contains a well-developed metamorphic fabric which obscures most primary sedimentary structures (Ware and Wardle, 1979).

The formation is subdivided into three informal members: member A, basal conglomerate; member B, arkose; member C, quartzarenite and conglomeratic quartzarenite. Seven stratigraphic sections were measured through the formation (Fig. 4.1), and although no one section provides continuous exposure of all the component members, section C, located on the northeast side of Sims outlier (Fig. 4.1), is designated as the formation's type section. A useful reference section that can serve as a field standard for the basal conglomerate of member A is the section in the northwest side of Muriel outlier (section A, Fig. 4.1).

Member A, the basal conglomerate, rests unconformably on either the Knob Lake Group or the Tamarack River Formation. It is a maximum of 30 m thick and is exposed only in Muriel outlier and two small unnamed outliers northeast of Muriel outlier (Fig. 2.3).

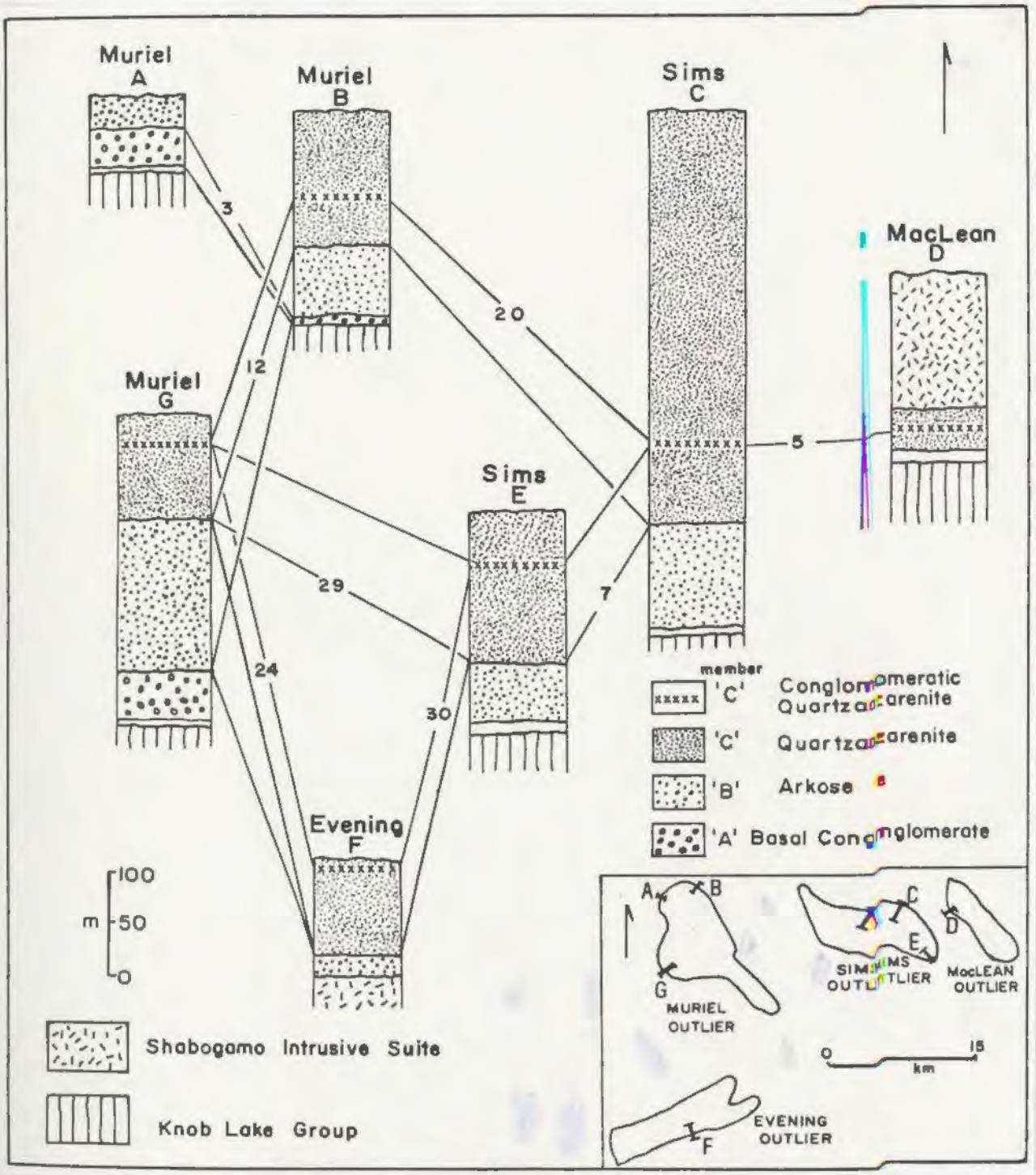

Fig. 4.1: Correlation of measured stratigraphic sections through the Sims Formation. Numbers refer to distance between sections in kilometres. The unpatterned interval at or near the base of some sections indicates that the basal contact is not exposed.

Member B consists of red arkose with minor siltstone and mudstone In Muriel outlier, the basal conglomerate of member A fines upward and grades into the arkose, but in Sims outlier, member B appears to rest directly in the Knob Lake Group (section C, Fig. 4.1). The most continuous exposure through the member is the 150 m thick section G in Muriel outlier (Fig. 4.1). Member B thins eastward, being only 100 m thick in Sims outlier, and is not exposed in MacLean outlier.

The upper unit, member C, is a thick, tabular deposit of well-indurated quartzarenite with minor quartz granule and pebble conglomerate. The member forms the prominent summits of all the outliers and is best exposed at section C in the eastern flank of Sims outlier (Fig. 4.1), where it attains a thickness of over 500 m. Other useful stratigraphic sections through this member are sections A, B and E (Fig. 4.1). The lower contact of the member is a 30 m-thick transition zone where red arkose and pink subarkose of member B intertongue with quartzarenite. The exact boundary is arbitrarily chosen to be the first-one-metre thick bed of quartzarenite. However, on MacLean outlier, this transition zone is not exposed and the quartzarenite may rest directly on the Knob Lake Group (Fig. 2.3). The beds of conglomeratic quartzarenite are located between 75 and 100 m above the base of member C. They are less than 25 m thick and form a useful marker bed which is present in all outliers (Fig. 4.1).

The angular unconformity which separates the Sims and Tamarack River Formations is strikingly apparent on aerial photographs of northern Muriel outlier (Fig. 4.2A). In addition, along the northern and western flanks of Muriel outlier, there are numerous locations

FIGURE 4.2

Sims Formation

A. Stereo pair of aerial photographs of northern Muriel outlier showing the angular unconformity between the Tamarack River and Sims Formations. A, B and J are measured stratigraphic sections.

B. Cross-section of the oligomictic breccia developed at the base of section B. Flat-lying oligomictic breccia facies rests unconformably on steep easterly-dipping sandstones of the Wishart Formation.

Oligomictic Breccia Facies

C. Clast-supported oligomictic breccia showing angularity of framework clasts.

D. Crude stratification developed in the coarse-grained matrix of the clast-supported breccia. The quartzite clasts are stained dark red with iron oxide and contain quartz veins.

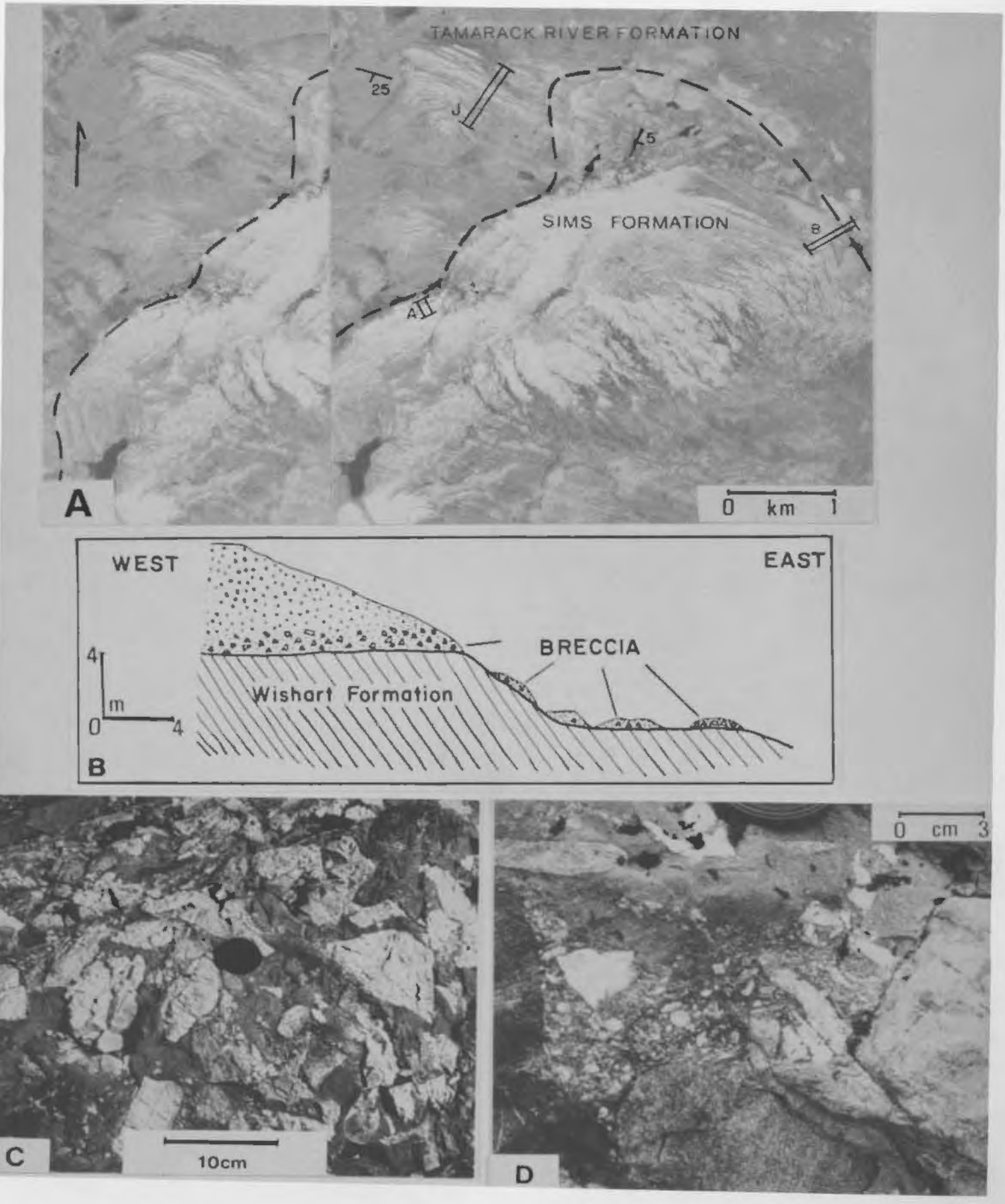
TAMARACK RIVER FORMATION
25
J
5
SIMS FORMATION
8
A
A
0 km 1
WEST
EAST
4
m
0
4
BRECCIA
Wishart Formation
B
C
10cm
D
0 cm 3

(sections I, J, H and locality U, Fig. 3.1) where only a few metres of cover separate the two formations. The contact between the Sims Formation and Knob Lake Group is exposed at the base of section B (Figs. 4.1 and 4.2A).

The Sims Formation was deposited between 1.75 Ga and 1.4 Ga and thus is Paleohelikian in age. The 1.75 Ga maximum is the age of the Hudsonian orogeny which deformed the underlying Aphebian rocks (Stockwell, 1970). The 1.4 Ga minimum is the age of the Shabogamo Intrusive Suite (Brookes et al., 1981) which locally intrudes the Sims Formation.

FACIES

The Sims Formation is divided into five major facies (Table 4.1). Member A is composed of an oligomictic breccia facies and a polymictic conglomerate facies. Member B constitutes the arkose facies and member C is divided into a quartzarenite facies and a conglomeratic quartzarenite facies.

Member A

Oligomictic Breccia Facies: Description

A thin oligomictic breccia belonging to member A was deposited unconformably on an irregular paleotopographic surface developed on the Wishart Formation at the base of section B on the northeast flank of Muriel outlier (Fig. 4.1). This paleotopographic surface appears to have the form of a small hill or ridge with a slope dipping eastward at about 30° (Fig. 4.2B). The quartzite below the unconformity is extensively

TABLE 4.1

Facies of the Sims Formation

facies abundance (%)	distribution	lithology abundance (%)	sedimentary structures	diagenetic structures	depositional environment
oligomictic breccia (T)	member A section B Muriel outlier	breccia (90), sandstone (10)	clast-supported and matrix-supported breccia, with matrix stratification.		talus slope
polymictic conglomeratic (5)	member A Muriel outlier	clast-supported cgl. (80), matrix-supported cgl. (10), sandstone (10), dolomicrite (T).	clast imbrication, crossbedding, and mudcracks.	stylolites, red-coloured matrix.	proximal braided alluvial plain, with playa lakes
arkose (25)	member B Muriel, Sims, Evening outliers	sandstone (90), siltstone and mudstone (8), granular cgl. (2).	crossbedding, ripples, channels, mudcracks, synsedimentary faulting and folding.	red colouration with buff reduction spots.	distal braided alluvial plain
quartzarenite (65)	member C all outliers	sandstone (98), siltstone (2).	ripple marks, crossbedding, planar bedding, parting and current lineations, pull-aparts and planar erosional surfaces.	concretions, iron-oxide dendrites, iron oxide bands.	coastal, near shore and shallow marine.
conglomeratic quartzarenite (5)	member C all outliers	granular cgl (80), coarse sandstone (15), pebble cgl (5). mudstone (T).	planar crossbedding, scour pockets, and lag deposits.	concretions.	beach backshore.

T = Trace

fractured, contains numerous quartz veins, and is locally stained red by iron oxide. The overlying breccia is up to 4 m thick and is composed of very angular clasts of Wishart Formation quartzite. Clasts are up to 1 m in diameter, have no preferred orientation, are poorly sorted, and are either matrix supported or form an intact framework (Fig. 4.2C). The matrix is a friable, poorly-sorted, coarse red sandstone. In places within the clast-supported breccia, a crude internal stratification is developed in the matrix between clasts (Fig. 4.2D), or a shelter porosity is preserved beneath larger clasts. The breccia fines abruptly upward into the coarse- and medium-grained arkoses of member B.

Polymictic Conglomerate Facies: Description

This facies forms the bulk of member A and is best exposed at section A (Fig. 4.1). It is composed of clast-supported conglomerate with minor amounts of matrix-supported conglomerate, red sandstone, red mudstone, and pink dolomicrite.

The clast-supported conglomerate consists of subrounded to rounded, boulder- to granule-sized clasts set in a red sandstone matrix (Fig. 4.3A,B). Clasts are poorly to moderately well sorted, commonly imbricated and locally define a crude horizontal stratification. Individual beds are between 0.5 and 2 m thick and extend laterally for up to 25 m. Basal contacts are erosional and have up to 0.25 m of relief. Stacked conglomerate units reach 5 m in thickness. The matrix is a medium- to coarse-grained, poorly sorted litharenite, which is cemented either by silica or dolomite.

FIGURE 4.3

Polymictic Conglomerate Facies

A: Imbricated, clast-supported, boulder to pebble conglomerate with a red sandstone matrix (1 km east of section A).

B: Clast-supported pebble conglomerate with crude horizontal stratification and interbedded planar crossbedded sandstone (top of section A).

C: Matrix-supported conglomerate with a sandy matrix and cemented by silica (section A).

D: Matrix-supported conglomerate demonstrating reverse grading. Clasts are angular Wishart Formation quartzite. The sandy matrix is cemented by carbonate and differential weathering gives the clasts a positive relief.

E: Carbonate-cemented, crossbedded, pebbly sandstone, overlying dolomicrite with abundant stylolitic surfaces (section A).

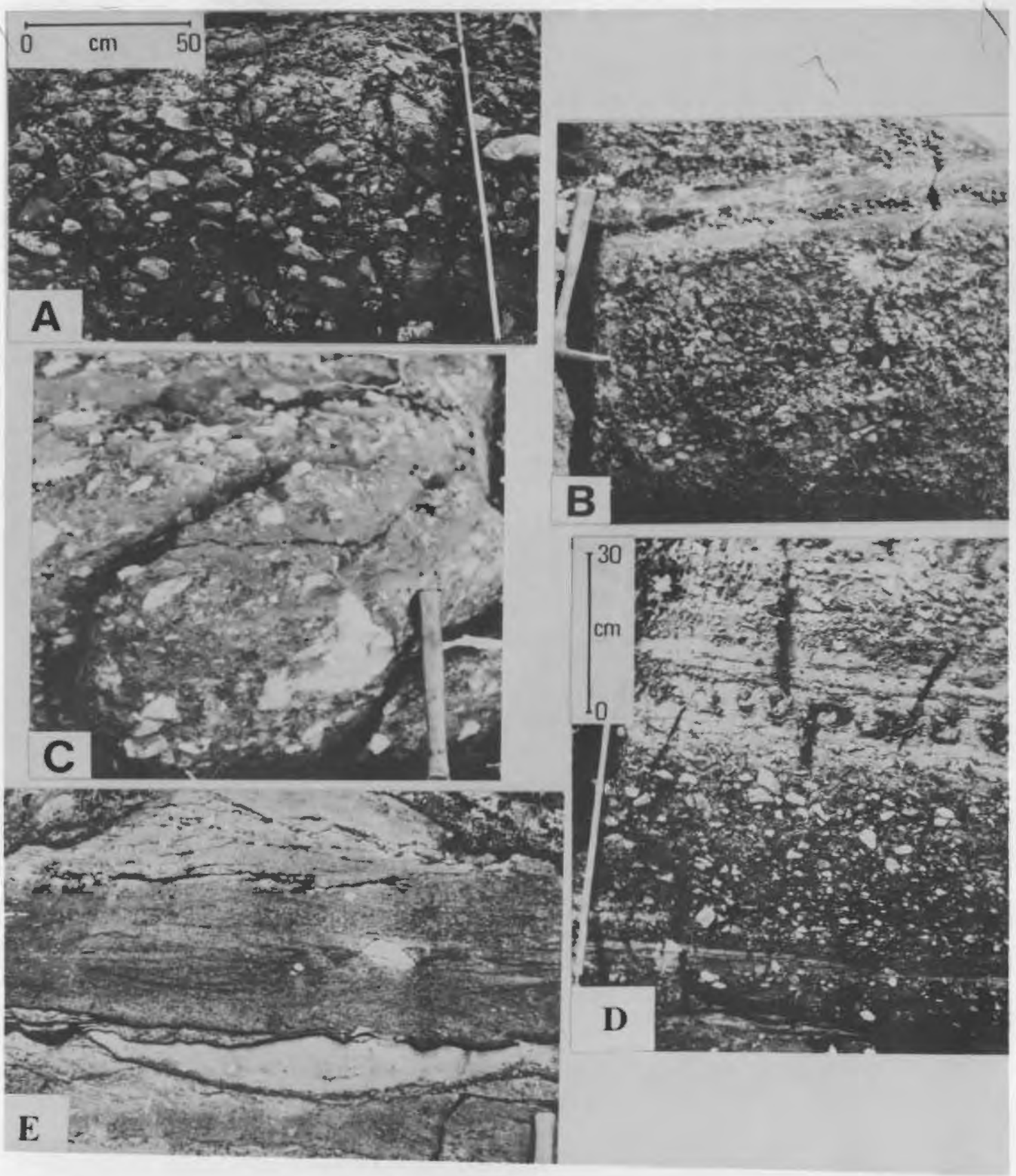
0 cm 50
A
B
C
30
cm
0
D
E

Matrix-supported conglomerates are uncommon; only two beds, each less than 1 m thick were measured in section A (Fig. 4.3C,D). Clasts are up to 30 cm in diameter, poorly sorted, lack imbrication, and are dispersed in a matrix of red sandstone, siltstone and pink dolomicrite. Characteristically, the clasts are distinctly more angular than those of the clast-supported conglomerate. In places, reverse grading of clasts is visible (Fig. 4.3D).

The dominant clast lithologies are quartzite, iron formation, vein quartz, carbonate and chert with a minor amount of siltstone, granite and volcanic clasts. Consistent dispersal patterns emerge based on clast types, when pebble-count histograms are plotted on a map of Muriel outlier (Fig. 4.4). On the eastern flank, conglomerates are dominated by a single lithology, quartzite, iron formation or carbonate; the conglomerates on the western side have roughly the same portions of each of these lithologies. Maximum clast size and estimated sorting values also show an east-west variation within the outlier (Fig. 4.4). Clasts on the eastern flank are poorly sorted and are up to 0.5 m in diameter, whereas those on the western flank are moderately well sorted, better founded, and less than 0.15 m in diameter.

Minor amounts of pebbly sandstone, red sandstone, pink dolomicrite and red mudstone are interbedded with the two types of conglomerates. The pebbly sandstone contains planar and trough crossbeds which average 0.3 m in set thickness, and have foreset slopes in the range of 17° to 25°. The pebbles and granules of the pebbly sandstones are either isolated in the foresets of the crossbeds or concentrated as basal lag deposits. The sandstones are coarse to medium grained, poorly to moderately sorted litharenites, and are either crossbedded or parallel

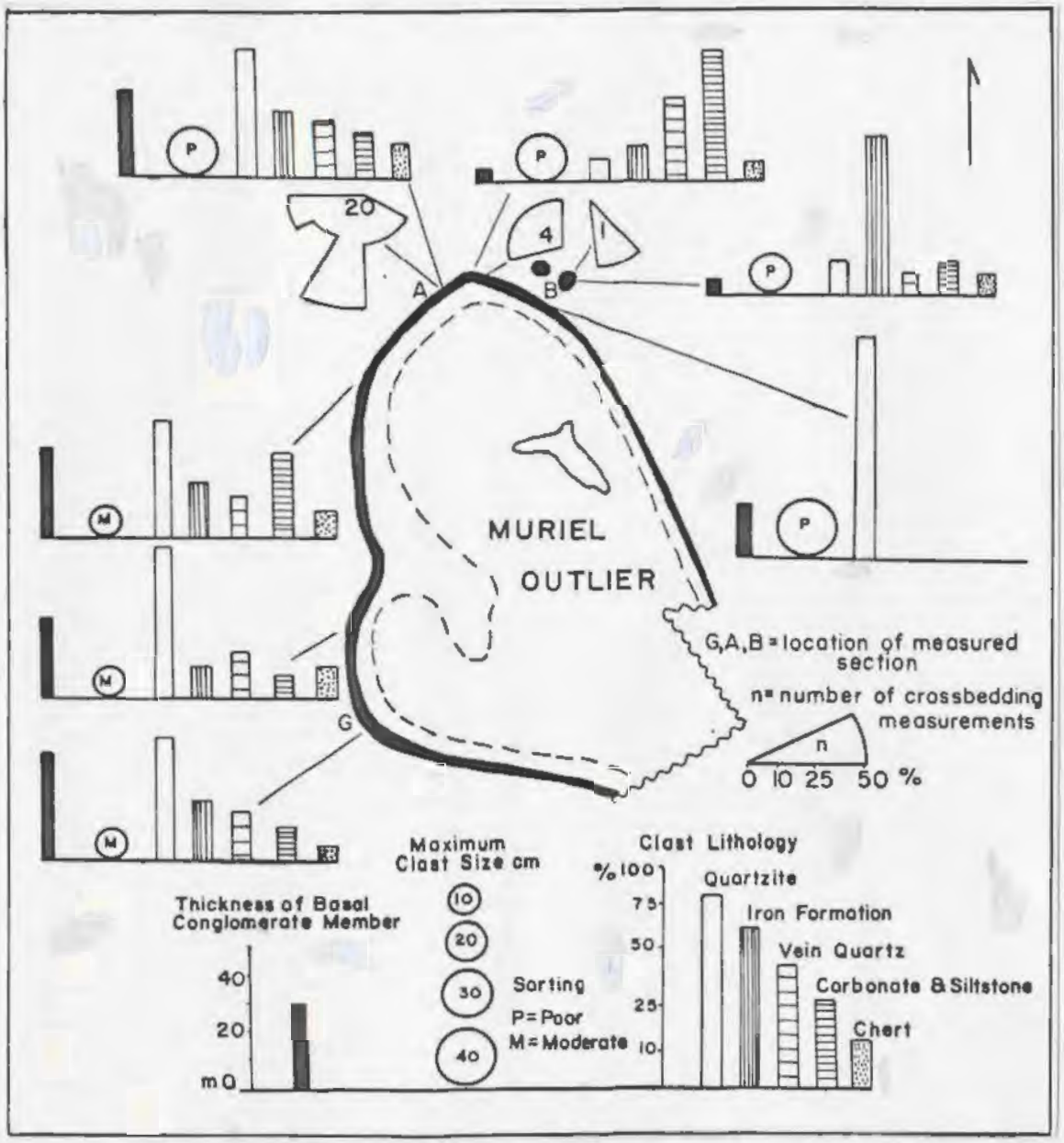

Fig. 4.4: Sketch map of Muriel outlier illustrating the distribution of paleocurrent data and thickness variations of member A. Pebble count histograms are based on 100 counts per locality and exclude granite and volcanic clasts which total less than 5%. Maximum clast size records the average of the ten largest clasts. Sorting values are visual estimates.

laminated. Crossbedding measured at section A indicates a southward flow direction. At nearby localities, however, paleocurrents trend northwestward and southeastward (Fig. 4.4).

At the base of section A (Fig. 4.5) there are thin beds of pink, silty dolomicrite (Fig. 4.3E) and mudcracked mudstone. The dolomicrite contains abundant stylolites but no visible primary structures.

Member A: Interpretation

The oligomictic breccia facies is interpreted as remnants of a talus slope deposit that accumulated adjacent to a low, eastward-sloping hill. This is supported by the nature of the breccia, the morphology of the paleotopographic surface and the close proximity to a fault zone. The angularity, coarseness and poor sorting of the breccia indicates that the clasts were not transported any appreciable distance. The localized development in the clast-supported breccia of crude stratification within the matrix indicates that the clasts were originally deposited without any significant matrix content, possibly as rock slides (Gardiner, 1976). The matrix was introduced later when sediment-laden water filtered down into the interstices of the breccia and deposited its load, gradually filling the void spaces as internal sediment. In some isolated voids beneath larger clasts, sediment was unable to penetrate, and shelter porosity developed.

Examples of ancient talus slope deposits are rare in the geologic record, and this has been attributed by Reineck and Singh (1973) to their low preservation potential. Neilson (1968) however, describes Devonian rockfall deposits in Norway which are interbedded with alluvial fan deposits. The Norwegian example is also believed to be fault

controlled, but is more extensive, thicker, and finer grained than the Sims Formation example.

The polymictic conglomerate facies is interpreted to have been deposited on a proximal, braided, alluvial plain (Fig. 4.5). Beds of coarse-grained, massive- to crudely-stratified, clast-supported conglomerate are a common deposit of gravelly braided streams (Boothroyd and Ashley, 1975). They are upper flow regime deposits which were produced by the migration of longitudinal bars on channel bottoms (Rust, 1972). During a falling-water stage, sand infiltrates this coarse framework, as transverse bars or dunes migrate over the tops of the gravel bars. These sandy bedforms, if preserved, would leave a record of either parallel lamination or planar and trough crossbedding (Boothroyd and Ashley, 1975).

The poorly-sorted, matrix-supported conglomerates with angular clasts were probably deposited by debris flows generated during flood conditions (cf. Miall, 1978). The thin mudstone beds are interpreted to be overbank deposits which were occasionally subaerially exposed, to produce mudcracks. The beds of dolomicrite may have accumulated in small playa lakes or ponds which developed in inter-channel areas during semiarid or arid periods (cf. Kendall, 1979). The dolomite in the lower parts of the polymictic conglomerate facies may have formed during dry seasons, when the groundwater within the conglomerate evaporated, allowing carbonate minerals to precipitate within the matrix as a cement (Kendall, 1979).

Member B

Arkose Facies: Description

This facies is up to 150 m thick, widespread, and consists of crossbedded and planar-bedded red arkose and subarkose, with minor

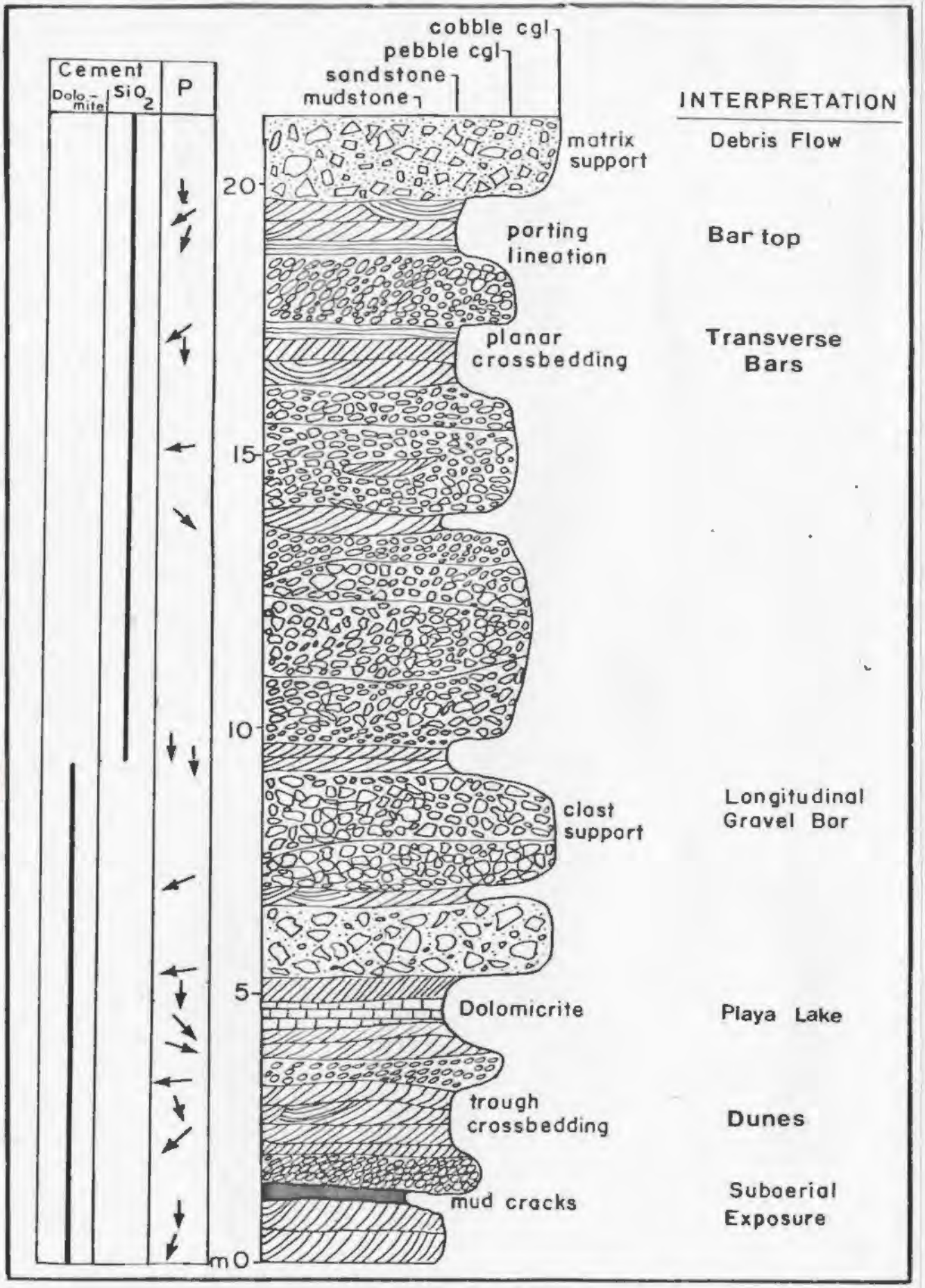

Fig. 4.5: Descriptive-interpretive stratigraphic section through the polymictic conglomerate facies of member A (section A). Paleocurrent data (P) are from crossbedding.

amounts of granule conglomerate, siltstone and mudstone. Sandstones are coarse to fine grained, poorly sorted to moderately well sorted, and contain angular to subrounded grains. Red colouration results from a fine coating of hematite on grain surfaces, and has been locally converted to a buff colour in reduction spots or along bedding and fracture planes.

Medium- to large-scale, planar-tabular crossbedding is the most common sedimentary structure (Fig. 4.6A and 4.6B). In the lower parts of member B, crossbedding ranges in thickness from .25 to 1 m and forms cosets up to 2 m thick (Fig. 4.6B). In the upper portion of member B, individual sets are thicker, ranging up to 2 m, and can be traced laterally for over 50 m (Fig. 4.6A). Foreset laminae dip at angles between 18° and 25° and are either straight or curved in cross-section. Trough crossbedding is less common, being restricted to the lower portions of the member. Troughs average about 25 cm in thickness. The overall distribution of all paleocurrent measurements obtained from both planar and trough crossbedding orientations have a broad unimodal pattern which trends northwestward (Fig. 4.7). However, at the outcrop level there is often a wide variation in directions obtained from adjacent sets of planar and trough crossbeds. Approximately 95% of the measurements were from planar crossbeds; the other 5% were from the axes of trough crossbeds.

A few thinning- and fining-upward cycles, ranging in thickness from 50 cm to 2 m, occur at the base of section G (Fig. 4.1). Within a cycle, the lowermost beds are up to 25 cm thick and consist of cross-bedded mudchip conglomerate, granule conglomerate and/or, coarse-grained sandstone (Fig. 4.6B). These rest on an erosional surface and pass upward into thinner units of crossbedded and planar-bedded,

FIGURE 4.6

Arkose Facies I

A. Large-scale planar-tabular crossbedding with curved foresets. Near the top of section G.

B. Sets of medium-scale planar crossbedding separated by parallel-laminated sandstone (section B).

C. A sequence with planar crossbedding at the base and trough crossbedding at the top (section G).

D. Rippled sandstone interbedded with minor amounts of siltstone and mudstone.

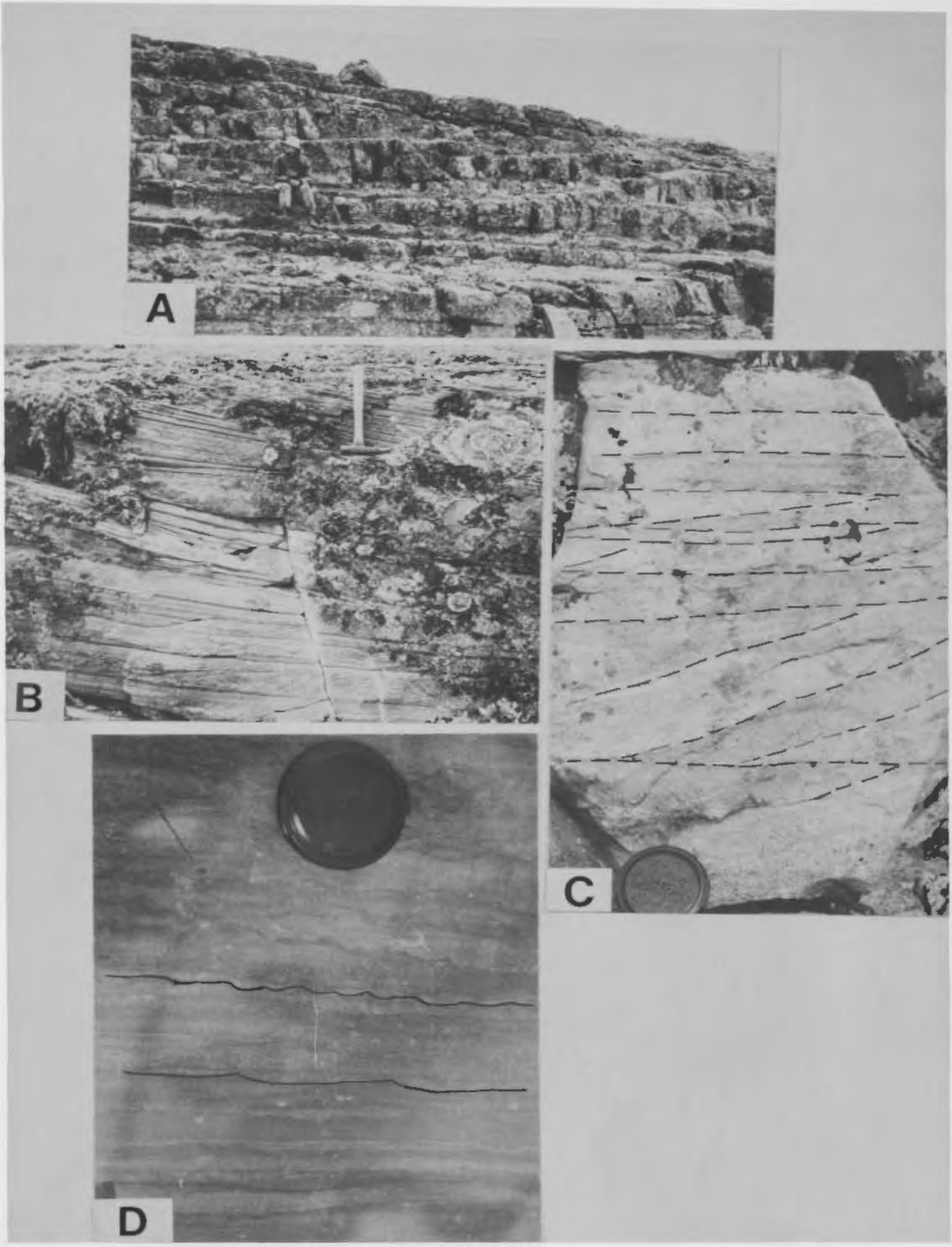
A
B
C
D

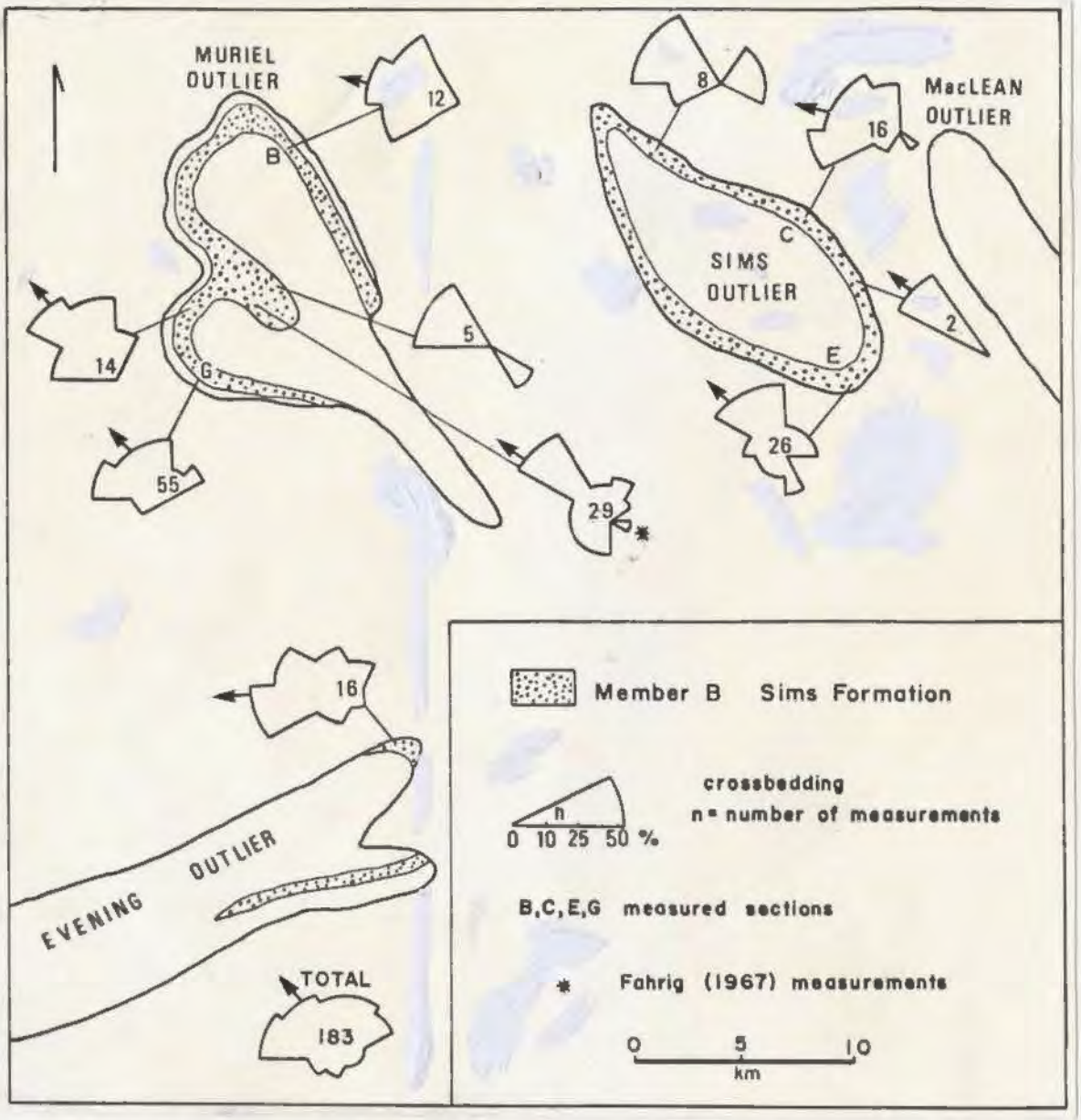

Fig. 4.7: Paleocurrent distribution for crossbedding of member B. Vector means (arrows) are only calculated for unimodal distributions. Data from Evening outlier has been corrected for tectonic tilt.

FIGURE 4.8

Arkose Facies II

A. A channel surface draped by mudchip conglomerate and eroded into a thin mudstone bed (section B).

B. Asymmetrical current ripples with superimposed mudcracks (section E).

C. Syn-sedimentary high-angle faults in a planar bedded, fine-graided arkose. Beds above and below this zone are parallel and continuous.

D. Convolute bedding in laminated sandstone and siltstone.

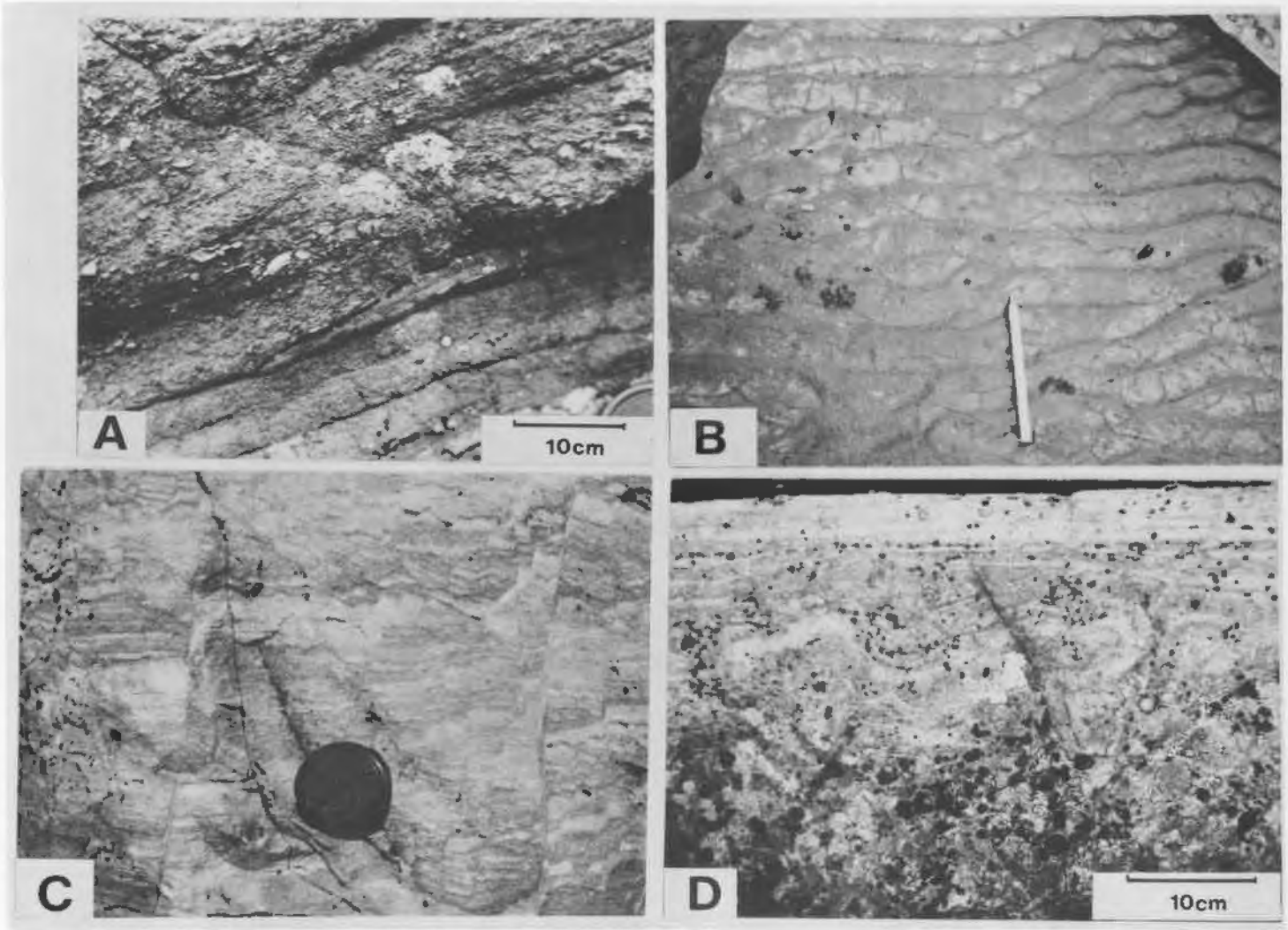
A
10cm
B
C
D
10cm

medium-grained sandstone (Fig. 4.6C) and finally into interbedded rippled sandstone, siltstone and mudstone (Fig. 6D).

Fine-grained lithologies make up less than 5% of the sections. Mudstones are thin, commonly cut by erosional surfaces (Fig. 4.8A) and often mudcracked (Fig. 4.8B). Soft-sediment deformation structures such as recumbently-folded crossbedding, high-angle syn-sedimentary faulting (Fig. 4.8C) and convoluted bedding (Fig. 4.8D) are sporadically developed within the facies.

Member B: Interpretation

The tabular-geometry, unimodal, predominantly northwesterly-directed paleocurrent distribution, and textural and mineralogical immaturity, are features which suggest deposition in a sandy fluvial regime located in the distral portions of a northwestward-dipping alluvial plain (Fig. 4.9). This fluvial system was probably a braided stream of low-sinouisty type, because fine-grained material is lacking (cf. Moody-Stuart, 1966) and the distinctive point bar cycles characteristic of meandering rivers are not recognized (cf. Walker and Cant, 1979).

The planar crossbeds developed when the avalanche faces of transverse bars migrated downstream within the braid system (Fig. 4.9). The trough crossbeds were produced by migration of dunes in channels. The broad distribution of paleocurrent directions and the difference in paleoflow directions obtained from adjacent sets of trough and planar crossbeds suggest that these bars were oriented at oblique angles to the main channel direction (Cant and Walker, 1978). Superficially, the thick crossbed sets common to this facies resemble lateral accretion crossbedding; however, this crossbedding consistently exhibits foreset

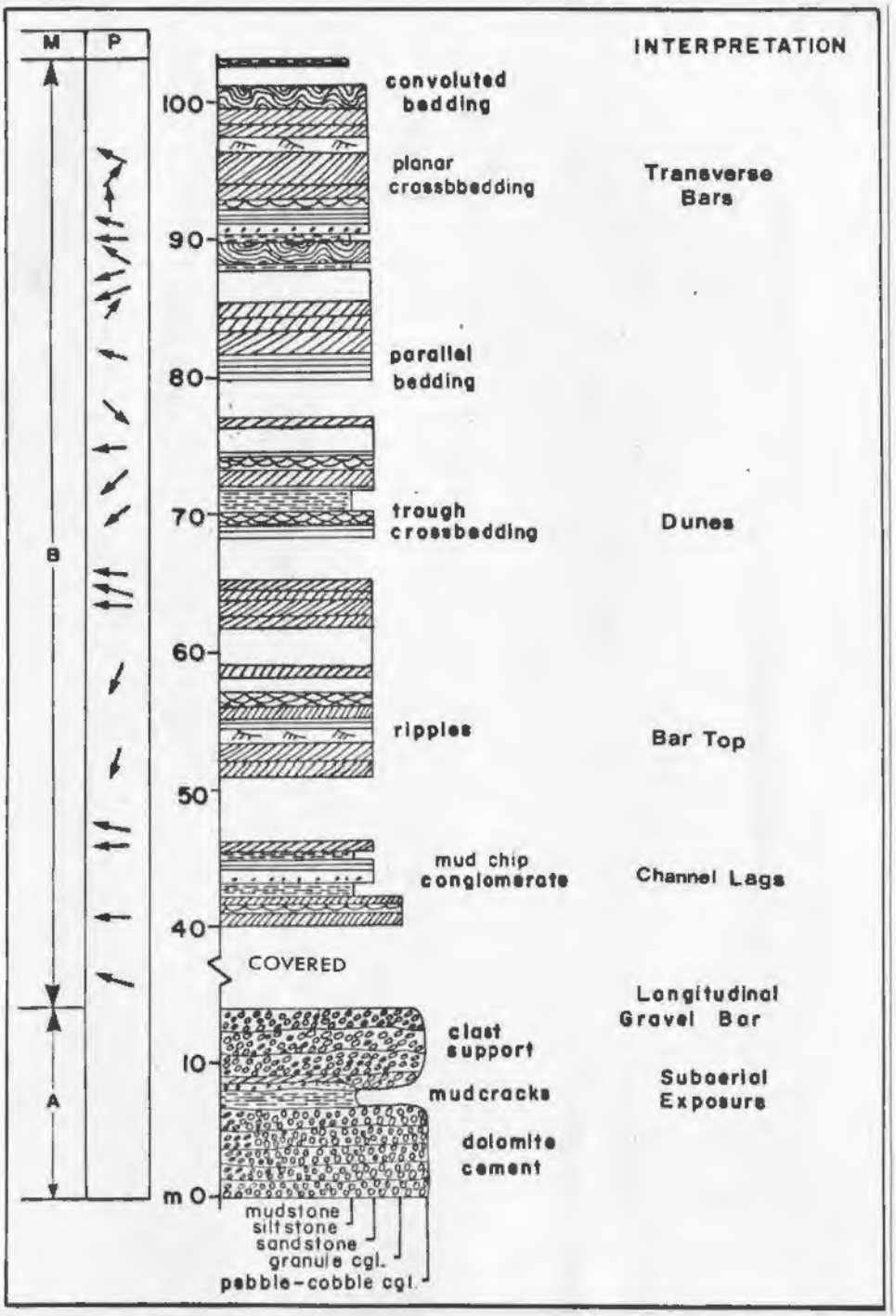

Fig. 4.9: Generalized, descriptive, interpretive, stratigraphic section of members (M) A and B at section G (S.W. Muriel outlier) Paleocurrent (P) data are from planar crossbedding. Member A represents proximal braided river deposits whereas member B represents the lateral distal equivalents.

dips greater than 15° and lacks any lateral grain size variation, both of which are uncharacteristic of lateral accretion crossbedding (cf. Walker and Cant, 1979). The cross-laminated sandstones and siltstones are bar top deposits (cf. Miall, 1978) and the massive mudstones, with evidence for subaerial exposure, are probably the remnants of overbank deposits. Locally these mudstones are eroded and preserved as basal lags of channel deposits.

Soft-sediment deformation structures are common in fluvial regimes. The overturned crossbedding was probably produced by strong shear on the bed during flood (cf. Long, 1978); the synsedimentary faulting may have formed when a channel undercut its bank (cf. Reineck and Singh, 1973) and the convolute bedding may have been produced by dewatering or liquefaction (cf. Blatt et al., 1972).

The vertical profile of sedimentary structures in member B (Fig. 4.9) resembles Miall's (1978) Platt River type of braided streams, being dominated by planar crossbedding and having a noncyclic depositional style.

Member C

Quartzarenite Facies: Description

This facies forms about 90% of the member (Fig. 4.10) and consists of very mature, well-indurated quartzarenite that ranges in colour from white and light orange through to pink and light purple. Overgrowths of authigenic silica are prevalent throughout the sandstones, and act as a cement which practically obliterates all original grain boundaries. Where visible, the original clasts are subangular to subrounded, fine to medium grained, and have a unimodal size distribution. Traces

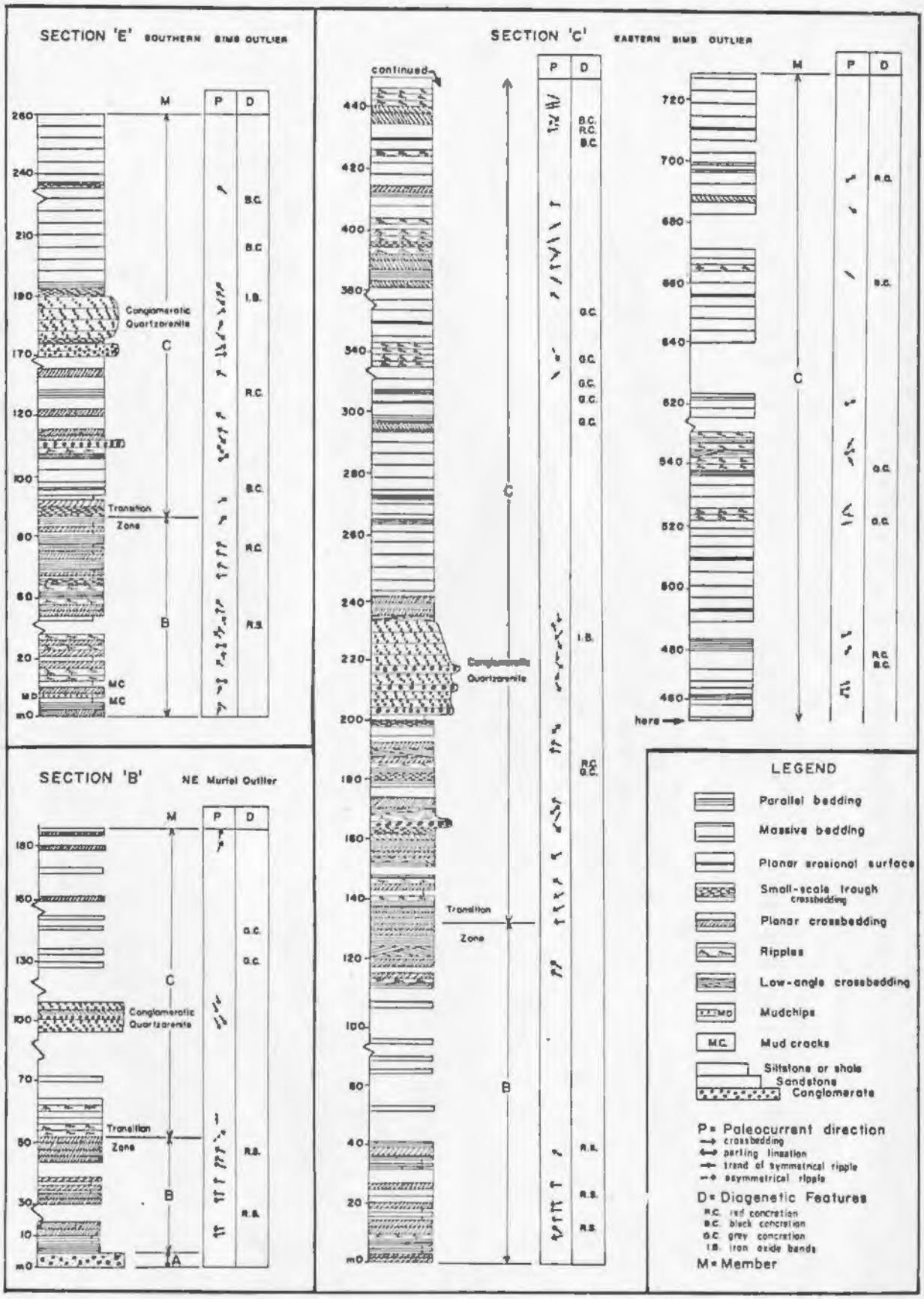

Fig. 4.10: Stratigraphic sections B, C, and E through the Sims Formation illustrating paleocurrent data (P) and the distribution of diagenetic structures (D).

of sericite surround the grains. Heavy mineral grains are scattered throughout the sandstones or are concentrated into distinct laminations.

Internal sedimentary structures cannot be discerned in about 70% of the exposures of this facies, due to an absence of grain-size variation, presence of lichen cover and diagenetic alteration. Such beds were logged as massive (Fig. 4.10), but truly structureless beds are probably rare. Radiographs of some apparently massive slabs revealed internal structures usually defined by heavy minerals (Fig. 4.11A). In many examples the only discernable feature of a bed is the flat or undulating nature of the bedding plane. Flat and laterally persistent bedding surfaces, up to 0.5 km^2 in area, are especially abundant in the upper parts of the member (Fig. 4.10). Some undulating bedding planes in the upper parts of the member exhibit shapes which resemble large sandwaves with bedform amplitudes greater than 2 m.

A wide variety of ripple marks is present. They are most abundant in the lower and middle parts of the member (Fig. 4.10). Varieties present, in order of abundance, are as follows: symmetrical ripples (85%), asymmetrical ripples (10%) and interference ripples (5%) (Fig. 4.11B). Also noted were a few examples of double-crested ripples (4.11C), flat-topped ripples (Fig. 4.11C) and ladderback ripples. Megaripples (Fig. 4.11D) are rare bedding-plane structures. Wavelengths of the majority of the ripples range between 5 and 10 cm and the amplitudes range from 1 to 3 cm. At a few localities it was recognized that some of the asymmetrical ripples were produced by wave action, based on their internal laminations and lack of crest bifurcations on extensive rippled bedding planes (Reineck and Singh, 1973). In excess of 250 paleoflow determinations were obtained from the

FIGURE 4.11

Quartzarenite Facies I

A. X-ray photograph of a slab of rippled quartzarenite. Bedding is just visible and is defined by concentrations of heavy minerals.

B. Two sets of symmetrical ripples intersecting at an oblique angle to form interference ripples.

C. Flat-topped symmetrical ripples with weakly developed double crests between the major crests.

D. Large megaripples with sinuous crests.

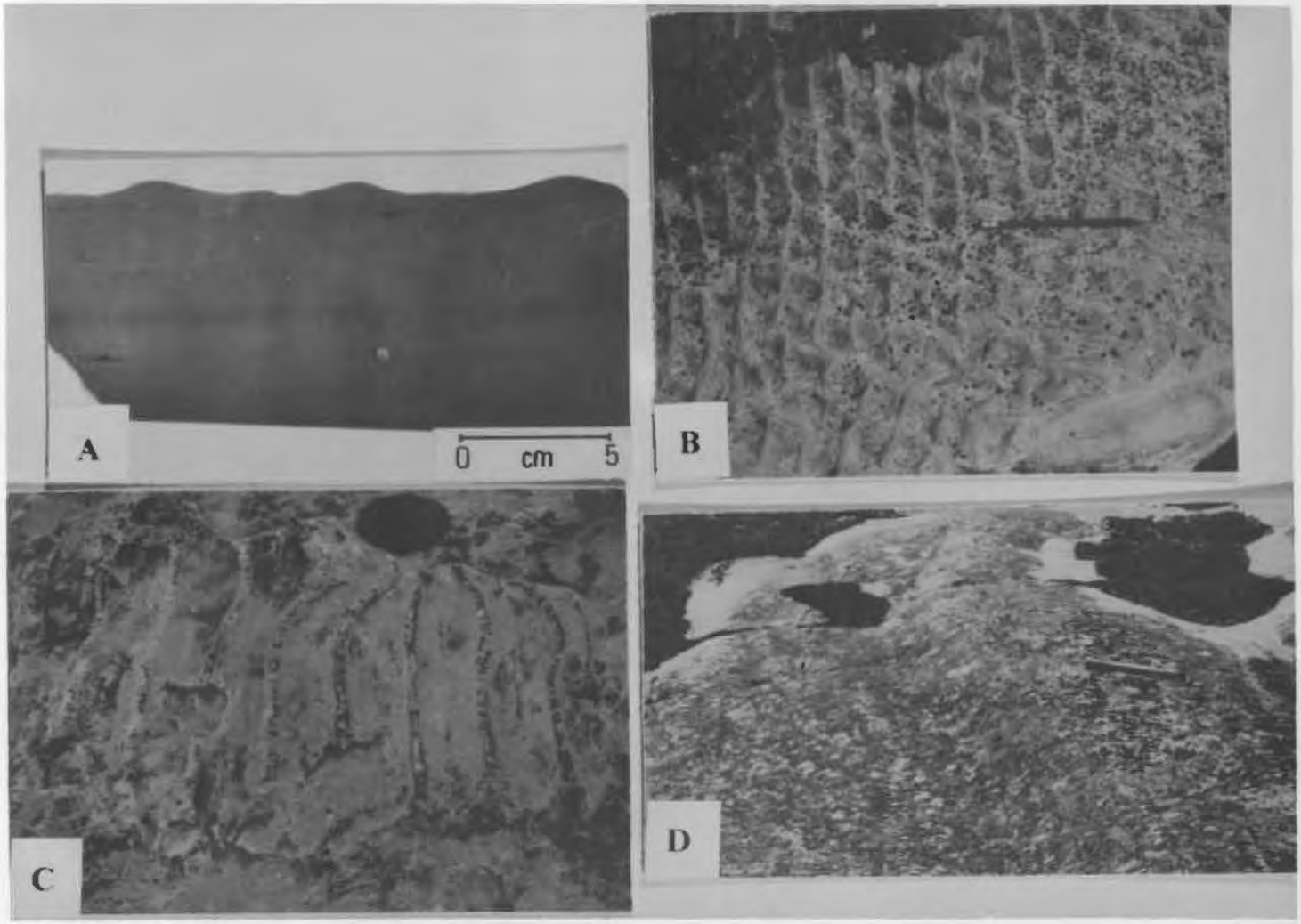
A
0 cm 5
B
C
D

ripples (Fig. 4.12). In Sims outlier, the average trend of symmetrical ripple crests is directed NE-SW whereas, in Muriel outlier, the trend is predominantly NW-SE. The paleoflow direction inferred from asymmetrical ripples, of both current or wave variety, is directed toward the southeast.

The facies consists of equal proportions of medium-scale planar-tabular crossbeds (Fig. 4.13A) and small-scale trough crossbeds (Fig. 4.13B). Trough crossbeds range in thickness from 15 to 40 cm and form cosets up to 2 m thick. The basal lamination of a set is commonly marked by a heavy mineral layer (Fig. 4.13B). Planar crossbeds tend to be thicker, up to 1 m, and in most places have a tabular geometry (Fig. 4.13A). Foreset angles are in the 20° to 25° range. Occasionally, reactivation surfaces and herringbone patterns were noted. Paleocurrent data obtained from the crossbedding illustrate a variety of distributions including strongly unimodal, bimodal, and polymodal (Fig. 4.12). Between the transition zone and the conglomeratic quartzarenite facies, paleocurrents are unimodal and directed on average to the west or northwest. Above the conglomeratic quartzarenite facies, the paleocurrent distributions are bimodal or polymodal (Fig. 4.10). When all data are compliled into a single plot, a polymodal distribution results,with a prominent southeasterly mode and subordinate northwesterly and northeasterly modes (Fig. 4.12).

Sets of planar-bedded quartzarenite, up to 1.5 m thick, containing low-angle truncations, current lineation and parting lineation (Fig. 4.13C) occur throughout the lower third of the member. Laminations are between 5 and 30 mm thick, and are composed of alternating laminae of well-sorted, fine- and medium-grained quartz. Locally, heavy minerals

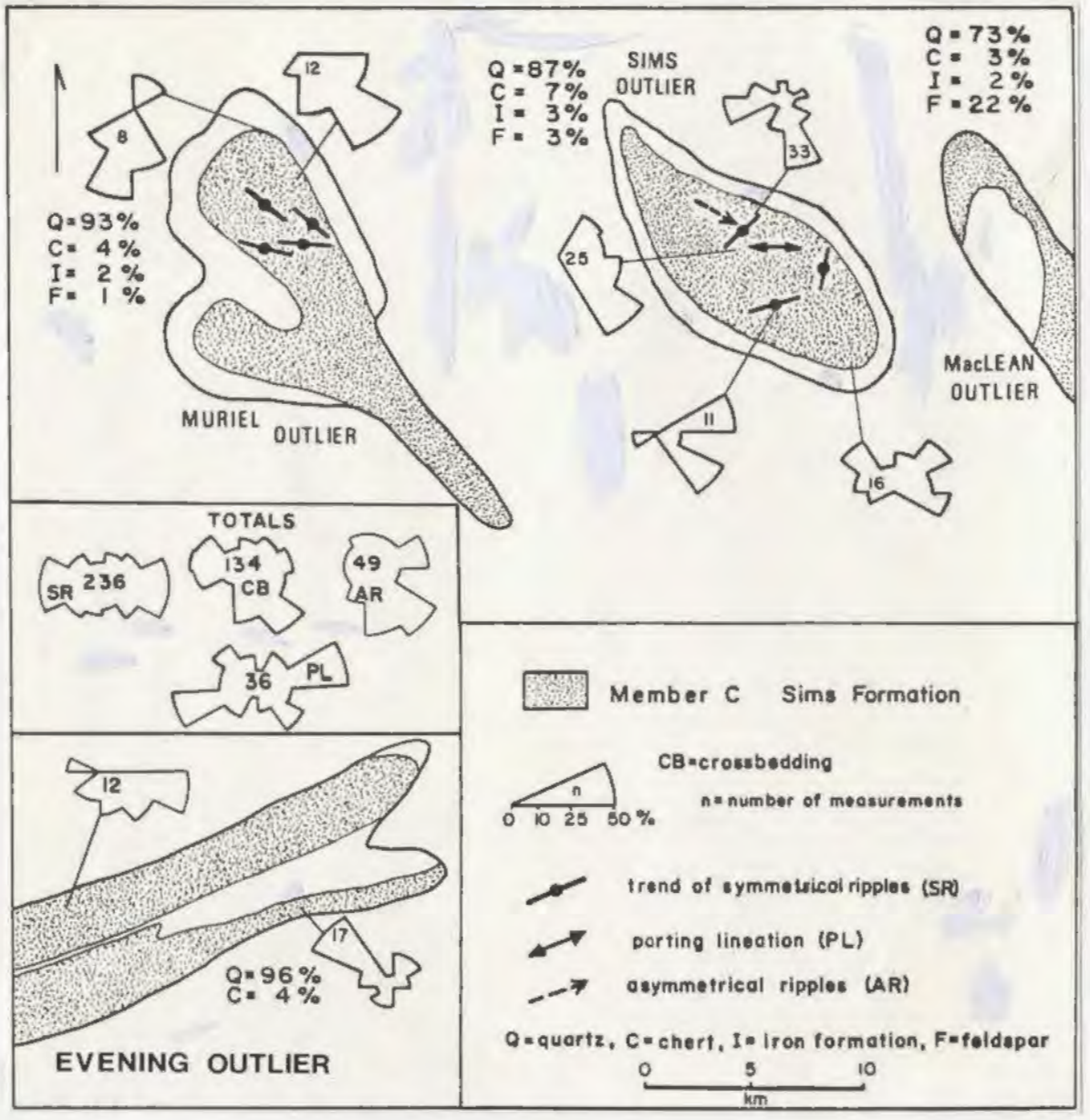

Fig. 4.12: Paleocurrent and clast type dispersion for member C. Trends of parting lineation (PL), crest lines of symmetrical ripplies (SR), and current direction for asymmetrical ripples (AR) are based on the average of a minimum of ten readings per station. Evening outlier crossbedding measurements have been corrected for tectonic tilt. Clast dispersion data are based on the average of four samples per outlier, with 100 point counts of granule-sized material per sample.

FIGURE 4.13

Quartzarenite Facies II

A: Planar crossbedding with opposed current directions separated by planar bedded quartzarenite (section C).

B: Small-scale trough crossbedding with numerous heavy mineral laminations (section B).

C: Primary current lineation defined by heavy mineral grains and parting lineation (section C).

D: Local breccia developed in planar-bedded quartzarenite with heavy-mineral lamination. The quartzarenite infilling is massive and is free of heavy minerals (section C).

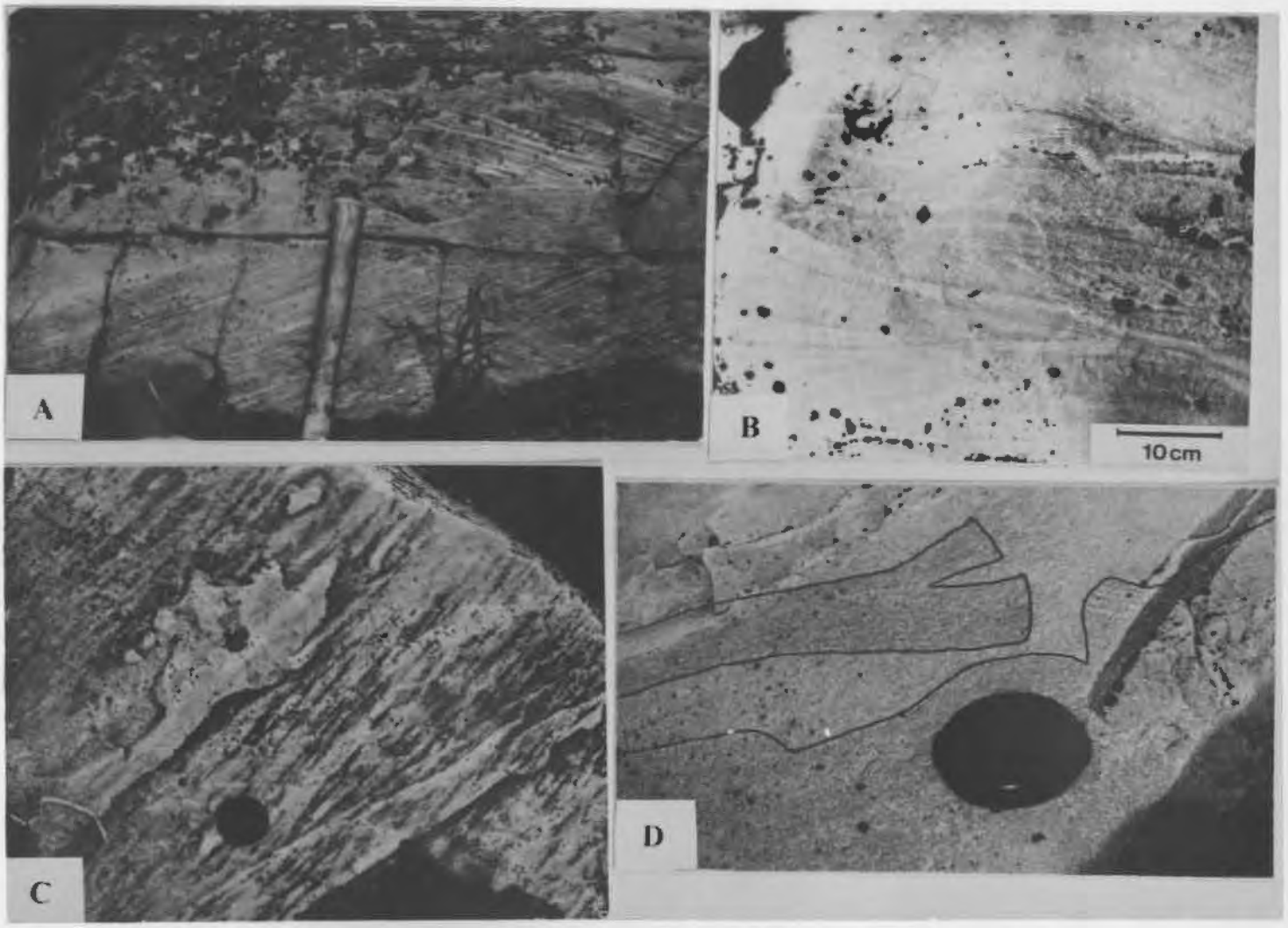
A
B
10cm
C
D

are concentrated in parallel-laminated beds up to 3 cm in thickness. Paleocurrent measurements of the orientation of the parting and current lineations in Sims outlier have a strong east-west trend (Fig. 4.12). At the base of section C, a large-scale semi-lithified fragment composed of planar beds has been ripped up and detached along a bedding plane (Fig. 4.13D).

Conglomeratic Quartzarenite: Description

This facies crops out on all outliers between 75 and 90 m above the base of member C (Fig. 4.1) and ranges in thickness from 20 m on Muriel outlier to 40 m on Sims outlier (Fig. 4.10). In addition, 4 m of this facies are present in Sims outlier about 30 m above the base of the member (Fig. 4.10). The facies consists of granule conglomerate, pebble conglomerate, planar-bedded sandstone, and minor red mudstone.

The granule conglomerate forms sets of planar-tabular crossbedding from .25 to 1 m thick (Fig. 4.14A). In cross-section, the foresets of the crossbeds are either straight, concave up or convex up, and are defined internally by layers, up to 10 cm thick, of well-rounded, well-sorted clasts which exhibit both normal and reverse grading (Fig. 4.14B). Toward the top of the facies, crossbed set thickness decreases and a greater portion of planar-bedded quartzarenite is interbedded with the granule conglomerate. Paleocurrent measurements of the crossbedding are directed primarily southward or southeastward with a few isolated sets indicating transport toward the northwest (Fig. 4.10). The conglomerate is composed of vein quartz, with minor chert, iron formation and feldspar. The percent abundance of each clast type is plotted in Figure 4.12. In the western outliers, vein quartz dominates, however the

FIGURE 4.14

Conglomeratic Quartzarenite Facies

A. Large-scale planar crossbedding dipping to the left, formed by inclined beds of granule conglomerate and coarse-grained sand.

B. Thin beds of normally-graded and reversely-graded granular and coarse-grained sandy material at the base of a large-scale-planar crossbed.

C. Small-scale, steep-sided scour pockets containing concentrations of pebbles. The underlying quartzarenite contains numerous calcareous concretions which tend to weather out, forming pock marks.

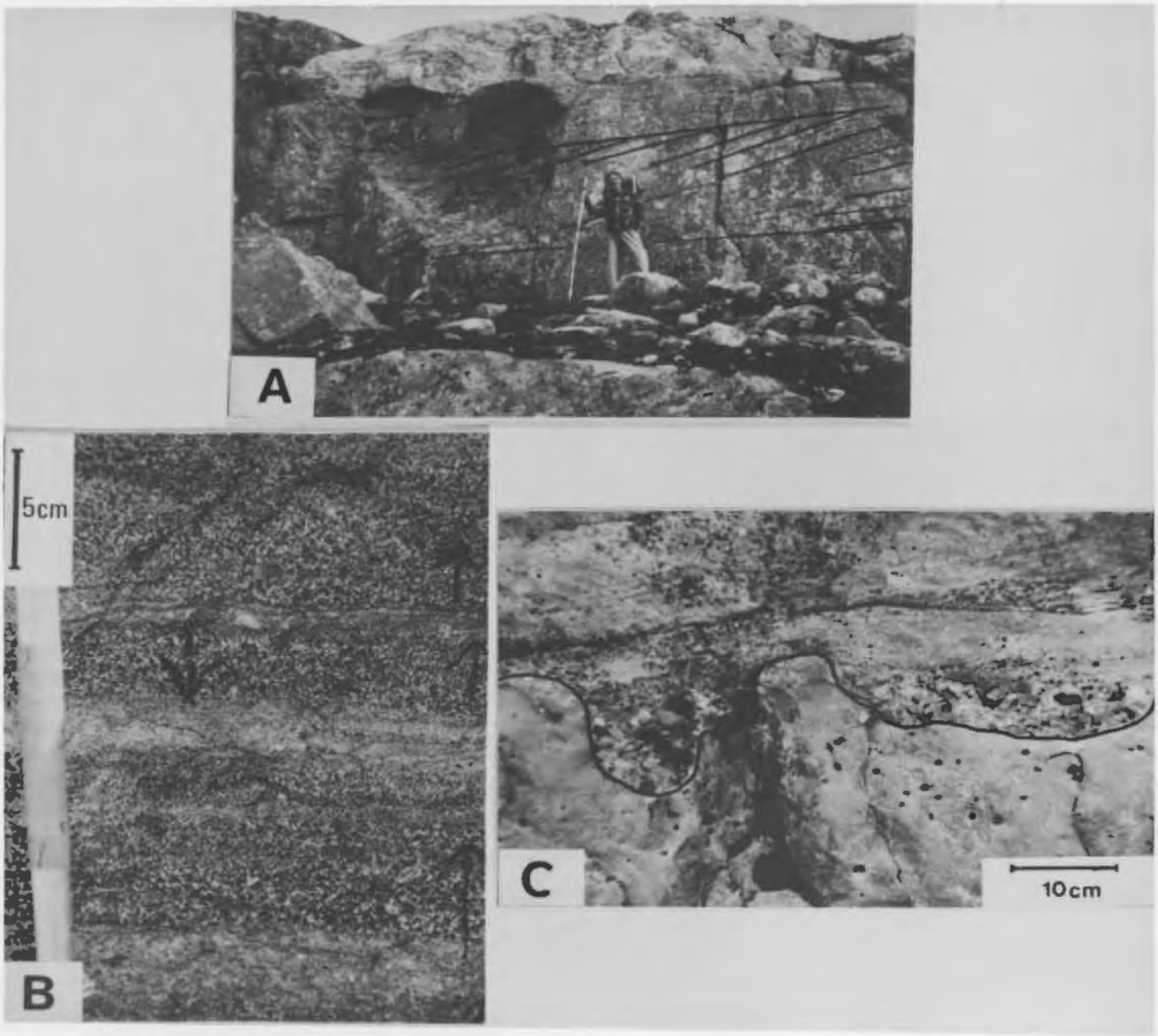
A
5cm
B
C
10cm

conglomerate of MacLean outlier contains significant amounts of kaolinitized potassium feldspar.

The lower portion of the facies contains numerous thin beds of pebble conglomerate with vein quartz, jasper, iron formation and quartzite clasts. Two types of pebble conglomerates were noted, both composed of well-rounded clasts less than 10 cm in diameter. The most common type is composed of a single layer of tightly-packed or dispersed pebbles resting on an extensive flat surface (cf. Anderton, 1976). At the base of this facies at section C, this type of conglomerate rests on a thin bed of red mudstone (Fig. 4.10). In the other type of conglomerate, pebbles are concentrated into isolated steep-sided channels up to 40 cm deep and 1.5 m wide (Fig. 4.14C). The steep scour pockets were produced either by soft sediment deformation or by erosion of cemented pre-conglomerate sands.

Member C: Interpretation

Member C was deposited in a broad spectrum of environments which include fluvial, lagoonal, beach, nearshore, and shallow marine (Fig. 4.15). The sandstone of member owes its mineralogical and textural maturity to extensive mechanical abrasion produced by fluvial and coastal processes, or by extensive weathering processes which removed all but the quartz clasts (cf. Pettijohn et. al 1972). The interval of quartzarenite between the base of the member and the conglomeratic quartzarenite is probably of fluvial origin because its predominantly northwestward-directed crossbedding distribution is identical to the paleocurrent trend in the underlying fluvial arkose of member B. In addition this interval lacks the abundant ripple marks and parting lineations which occur above the conglomeratic quartzarenite.

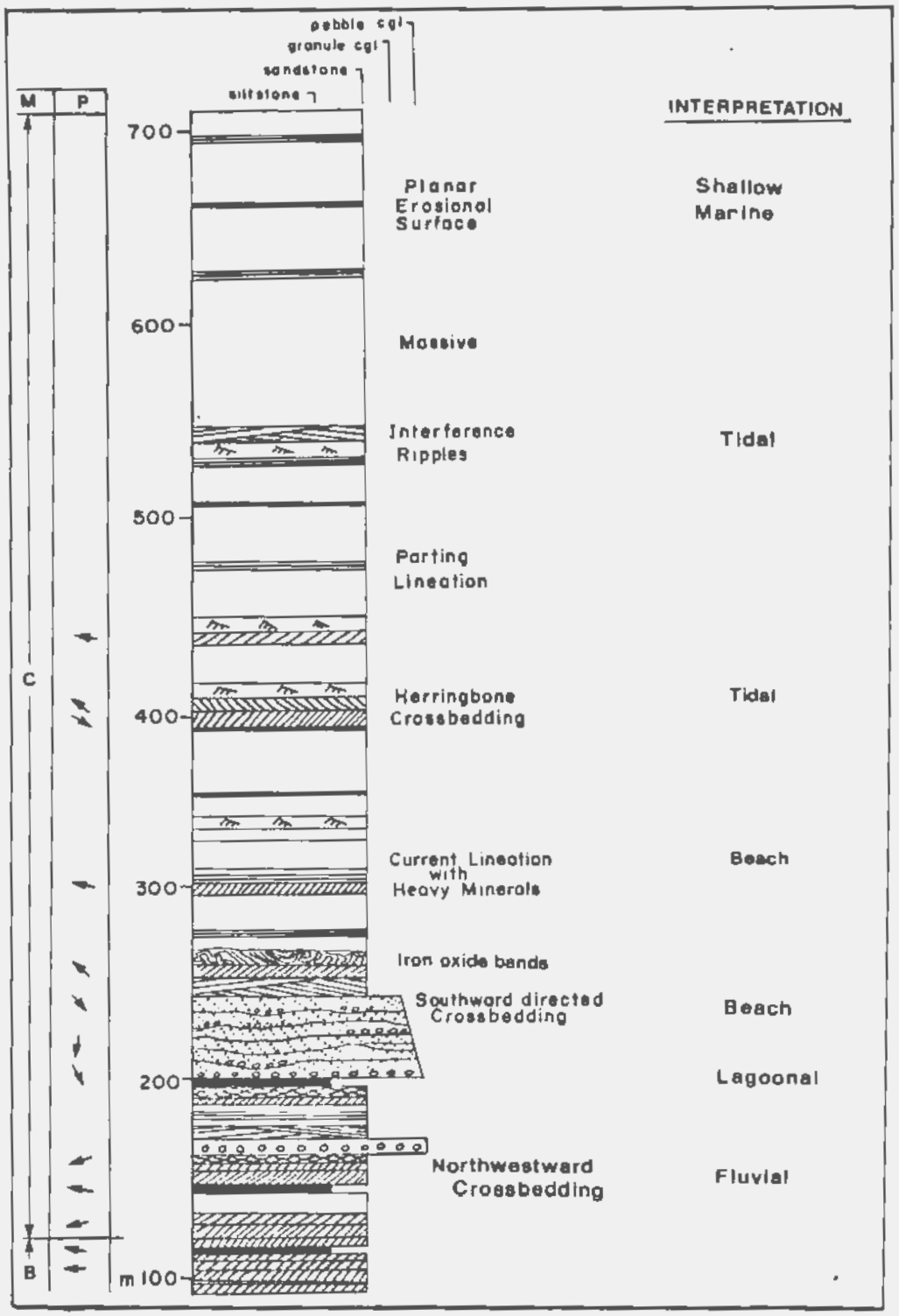

Fig. 4.15: Generalized descriptive-interpretive stratigraphic section of member C. Taken from section C, eastern Sims outlier.

Based on its lithology, blanket-like geometry and sedimentary structures, the conglomeratic quartzarenite facies is interpreted to be a coarse-grained beach deposit. The thin, laterally-persistent pebble layers are interpreted to represent transgressive beach-gravel lags which were produced by surf winnowing as an advancing sea encroached over a pebbly sand beach (cf. Clifton, 1979). The small channels containing pebble conglomerate are similar to structures described by Clifton (1981) and interpreted as being produced by stream gullies which cut across a beach. The sets of large-scale, southeastward-directed planar crossbedding may have been produced by the landward migration of beach ridges (cf. Hayes and Kana, 1976). The couples of granule and sand resemble the landward dipping ramp stratification of beach ridges (cf. Orford and Carter, 1982) or swash bars and the interbedded planar sandstones are interpreted as foreshore deposits produced in the swash zone (cf. Clifton et al., 1971). The overall thinning of the conglomerate unit in a westerly direction and the abundance of potassium feldspar clasts in MacLean outlier suggests that its detritus was derived from the east. The locally developed thin beds of red siltstone at the base of the conglomerate may be the remnants of backshore lagoonal sediments.

The two hundred metres of quartzarenite above the conglomeratic quartzarenite were deposited under conditions which fluctuated between coastal and nearshore marine. Planar-bedded sandstones containing parting lineations, low-angle truncations, and numerous heavy mineral concentrations are typically developed on the foreshore (cf. Clifton et al., 1971). The high ratio of wave ripples to current ripples is characteristic of foreshore and shoreface zones of beach deposition (cf. Reineck and Singh, 1973). This coastline was probably influenced to

some extent by tidal processes, based on the presence of herringbone crossbedding, reactivation surfaces within individual crossbeds, and the various types of ripple marks. The flat-topped, ladderback, and double-crested ripples are only formed during the ebb stages of tidal cycles (Reineck and Singh, 1973). The tidal range was probably small, less than 4 m, because the widespread fine-grained tidal flat deposits which typify macrotidal coastlines (Hayes and Kana, 1976) are absent.

There is no compelling evidence to suggest that a major barrier system was present during the deposition of the conglomerate and the quartzarenite facies. They lack the extensive lagoonal deposits, dominant seaward-directed paleocurrents, and the fining-upward cycles which characterize barrier islands (Reinson, 1979). The lagoonal siltstones are very limited in extent and probably accumulatedin small depressions located behind beaches. However, due to the transgressive nature of the overall stratigraphic sequence, it is possible that landward migration of the barrier bar complex has completely eroded all the remains of the lagoons (cf. Reinson, 1979).

The upper parts of member C appear to have been deposited in deeper water; i.e. the shallow marine zone. Sedimentary structures are rare and limited to extensive planar surfaces. Anderton (1976) suggested that such surfaces may be produced by submarine subtidal erosion.

Numerous studies of recent coastal and shallow-marine sediments (cited in Potter and Pettijohn, 1963) indicate that the average trend of wave-ripple crests parallels the coastline. The divergence in average ripple trends for member C in Sims and Muriel outliers suggests that the trend of the coastline for the two outliers was different (Fig. 4.12), and that member C was deposited in a broad embayment which opened northward.

DIAGENESIS

Megascopic diagenetic structures such as concretions, iron-oxide dendrites and iron-oxide bands occur in member C. Descriptions of these structures are given in Table 4.2, and their locations are shown in Fig. 4.1.

Concretions are very abundant (Fig. 4.16 A,B) and have a wide range of shapes, colours, compositions and concentrations (Table 4.2). They were formed by localized, concentric cementation around a nucleus in the pores of an unlithified host (cf. Pettijohn, 1976), prior to the introduction of the pervasive silica cement. X-ray and microprobe analyses indicate that the red concretions are cemented by hematite and contain traces of Na- and Mg- bearing tourmaline (Fig. 4.16C). The black concretions were probably originally cemented by siderite which has been subsequently altered to limonite; the grey concretions are cemented by calcium carbonate. The variation in composition suggests that the solutions which produced the concretions had a wide range of ionic species in solution and that precipitation of the cements occurred under fluctuating Eh and pH conditions (Berner, 1971). The age of the concretion growth is unknown, but it must predate the introduction of widespread silica cement which destroyed the sands porosity.

Iron-oxide dendrites (Fig. 4.16D) are rare and only occur in areas with high concentrations of red concretions. They are thought to have formed when Fe-rich solutions circulated through pores of the sandstone and precipitated out as a ferric iron cement at the tip of the dendrite (van Straaten, 1978). Their hematite composition indicates

TABLE 4.2

Diagenetic structures of member C

	concretions	iron-oxide dendrites	iron-oxide bands
size shape	Spherical, ellispoidal to irregular polygons. Diameter between 3 mm to 10 cm.	Tree-like with broad base and tapered top. Up to 25 cm long and 5 cm wide.	Thin, continuous, closely spaced bands forming irregularly curved surfaces which are continuous for up to 20 m.
colour	Varicoloured, most commonly red, black to blue and grey. Locally orange, brown or a combination of colours.	Red.	Red.
occurrence	Very common, density variable and can form up to 60% of a bed. Often concentrated within discrete horizons, Grey concretions more common near base, and red and blue more common near top.	Rare, only on bedding planes or at right-angles to bedding. Associated with concretions.	Very rare, only in upper 10 m of conglomeratic quartz-arenite.
composition	Grey cemented by calcite. Red cemented by hematite. Blue to black possibly cemented by siderite which has been altered to limonite.	Hematite.	Hematite.

FIGURE 4.16

Diagnesis

A. Small red concretions averaging about 2 cm in diameter and forming about 40% of a quartzarenite bed.

B. Grey concretions cemented by calcite and weathering out of a quartzarenite sample. Scale in centimetres.

C. Photomicrograph of a blue concretion formed in a quartzarenite with extensive overgrowths of quartz. The opaque material between grains imparts the colour to the concretion. Authigenic tourmaline crystals (T) have formed within the cements.

D. Bedding-plane view of red-coloured iron-oxide dendrites. Pencil for scale.

E. Irregular curved, red, iron oxide bands crosscutting thinly-laminated quartzarenite.

F. A red concretion (right) truncating iron-oxide bands. Bedding is parallel to the top of the slab.

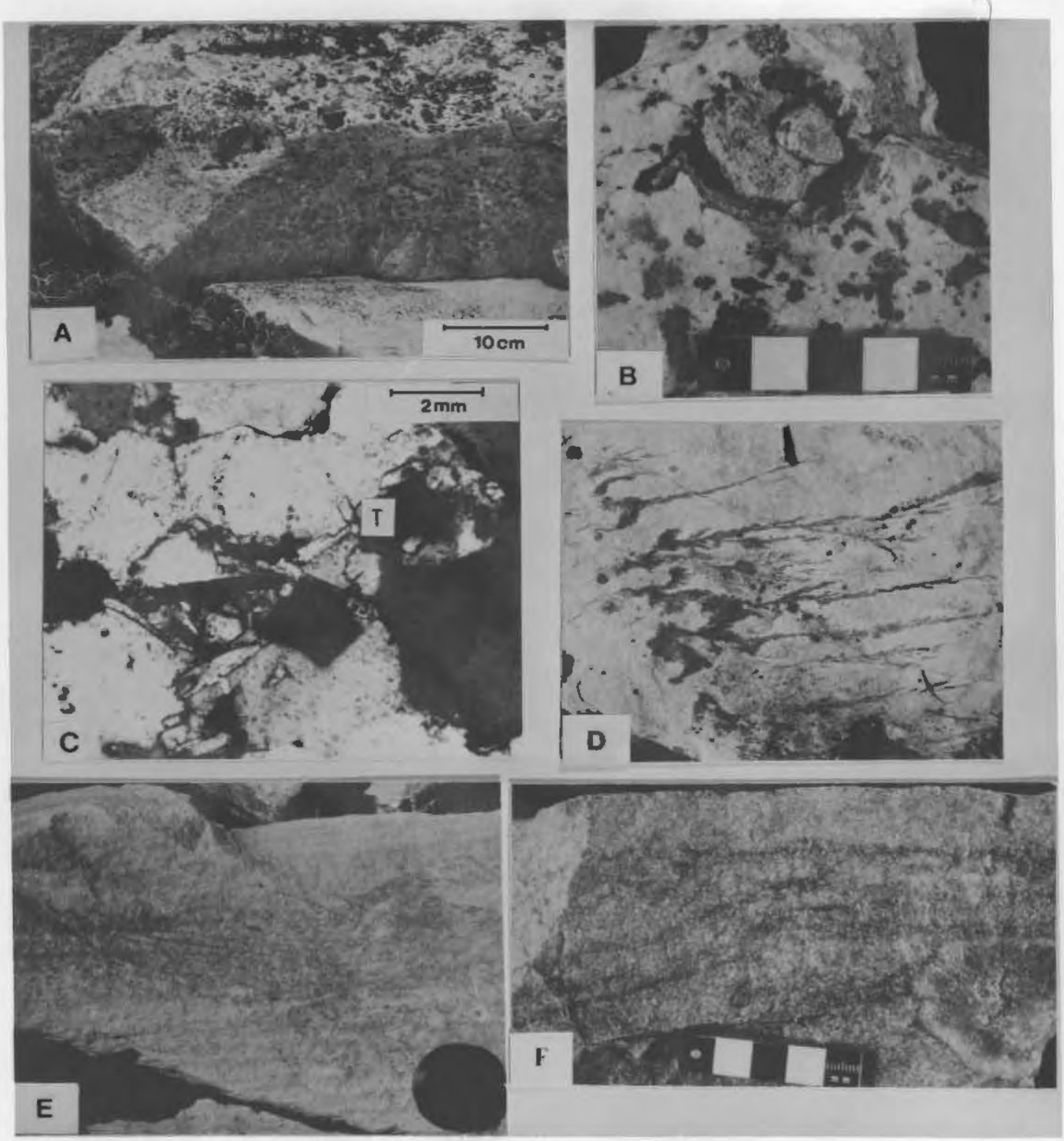
A
10cm
B
2mm
T
C
D
E
F

that precipitation occurred under oxidizing conditions (Berner, 1971). Although the age of dendrite growth is not known, their close association with red concretions suggests that they developed contemporaneously.

Curved iron-oxide bands (Fig. 4.16E) occur in the upper portion of the conglomeratic quartzarenite facies (Fig. 4.2). These bands never intersect one another, are laterally continuous for distances of up to 20 m and in places are truncated by concretions (Fig. 4.16F). Their geometry is reminiscent of the roll-front type of uranium deposit common in the southwestern United States (Gabelman, 1977). The bands were probably formed when an iron-rich solution encountered a zone where a physical or chemical change occurred, allowing iron oxide to precipitate in the pores of the quartzarenite (Gabelman, 1977). The disintegration of heavy minerals may have been the source for the iron in solution. The relative age relationships and the restrictions of these bands to strata interpreted to be beach deposits suggests that the bands are early diagenetic features and may have been formed by the mixing of fresh and marine waters.

PETROGRAPHY

Thirty-six thin sections of sandstone (Appendix A), twenty-three rock slabs (Fig. 4.12) and outcrops of conglomerate (Fig. 4.4) were point-counted. In addition, five sandstone were analyzed chemically (Appendix B). When the modal composition of the sandstones are plotted on a QFR diagram (Fig. 4.17A), a consistent trend emerges. Sandstones become more mineralogically mature with increasing stratigraphic height.

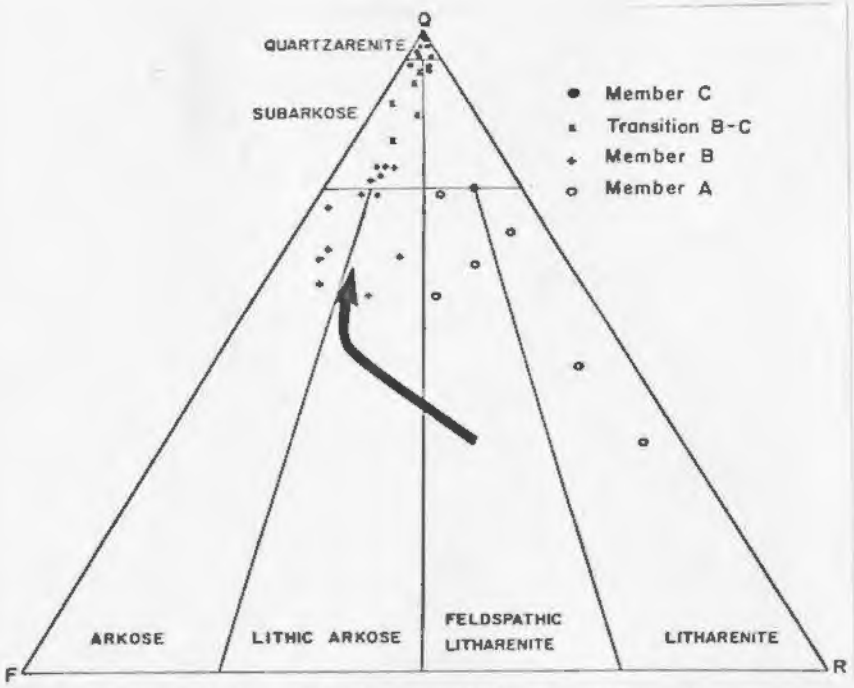

Fig. 4.17A: A quartz (Q), feldspar (F), and rock fragment and chert (R) diagram for thirty-five fine- to coarse-grained sandstones of the Sims Formation. Two hundred grain counts per sample. Sandstone classification according to Folk (1967).

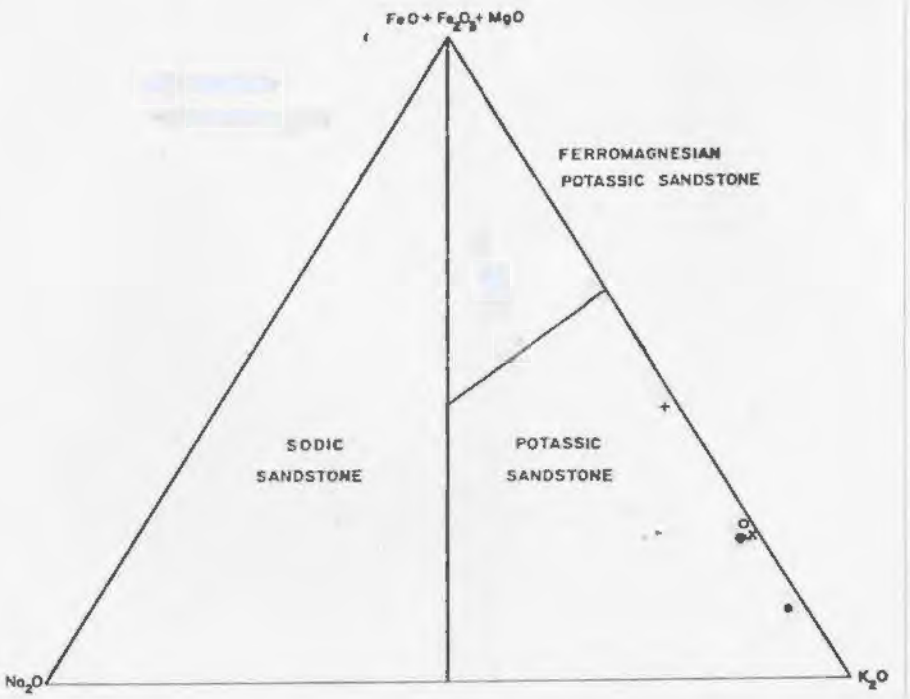

Fig. 4.17B: Ternary plot of Na_2O, $FeO + Fe_2O_3 + MgO$, and K_2O for chemical analyses of five Sims Formation sandstones. Chemical fields are according to Blatt et. al. (P 318, 1972).

This trend is paralleled by an increase in textural maturity; i.e. roundness and sorting values, and a change from red colouration in members A and B to a predominantly white colour in member C.

The red sandstones interbedded with the conglomerate of member A are litharenites and feldspathic litharenites (Fig. 4.17A) and are rich in angular grains of quartz, feldspar and a wide variety of rock fragments including chert, quartzite, iron formation, volcanics and carbonates. In the arkose, lithic arkose , and subarkose of member B and the transition zone with member C, the percentage of rock fragments decreases. These sandstones are composed predominantly of subangular to subrounded quartz, chert, plagioclase, microcline and muscovite and contain heavy minerals such as magnetite, rutile, tourmaline, zircon, apatite and epidote. With increasing stratigraphic height, the amount of feldspar decreases. The quartzarenite of member C is composed of over 95% quartz with only traces of chert and orthoclase. The heavy mineral suite is composed of rutile, tourmaline and zircon. Chemically, the quartzarenite is consistently over 95% SiO_2 (Appendix B).

These petrographic trends are controlled by depositional facies. The rapid deposition characteristic of fluvial environments allowed preservation of the abundant feldspars, rock fragments, and unstable heavy minerals found in the conglomerates and arkose of members A and B. In supermature quartzarenite of member C, most feldspars and rock fragments have been removed by the extensive mechanical and chemical weathering processes which occur in coastal and shallow-marine environments (Pettijohn et al., 1972).

Colouration of the formation also reflects the degree of mineralogical maturity. The red colour of the arkose was probably

produced when free iron was released during the diagenesis of Fe-bearing silicates and was subsequently precipitated under oxidizing conditions as ferric iron (Berner, 1971). However, this process could not operate in the white- to pale-coloured quartzarenite, because either this lithology lacked any significant concentrations of Fe-bearing silicate detritus, or early diagenetic processes removed the Fe-silicate suite. The sericite which surrounds most grains may represent the only traces left of these unstable lithologies.

Clast lithologies present in the conglomerates (Fig. 4.4) and sandstones (Fig. 4.17A) were derived from erosion of the Knob Lake Group and the Eastern Basement Complex. The quartzite clasts were derived from the Wishart Formation; the iron formation and chert from the Sokoman Formation; the volanics from the Nimish Formation; the carbonate and siltstone rock fragments from the Tamarack River Formation; and the granite and potassium feldspar from the Eastern Basement Complex. This exclusive continental provenance for the formation is further supported by the potassium-rich nature of sandstones (Fig. 4.17B). This type of sandstone, according to Blatt et al., (1972), most commonly accumulates on stable granitic cratons.

DEPOSITIONAL HISTORY

A summary of the interpreted depositional environments for the Sims Formation is presented in Figure 4.18. The basal conglomerates only outcrop in Muriel outlier and their deposition was initiated by a minor reactivation of the Sakit Lake Fault (Fig. 4.19), a major northwest-trending Aphebian structure. In the vicinty of the fault, the

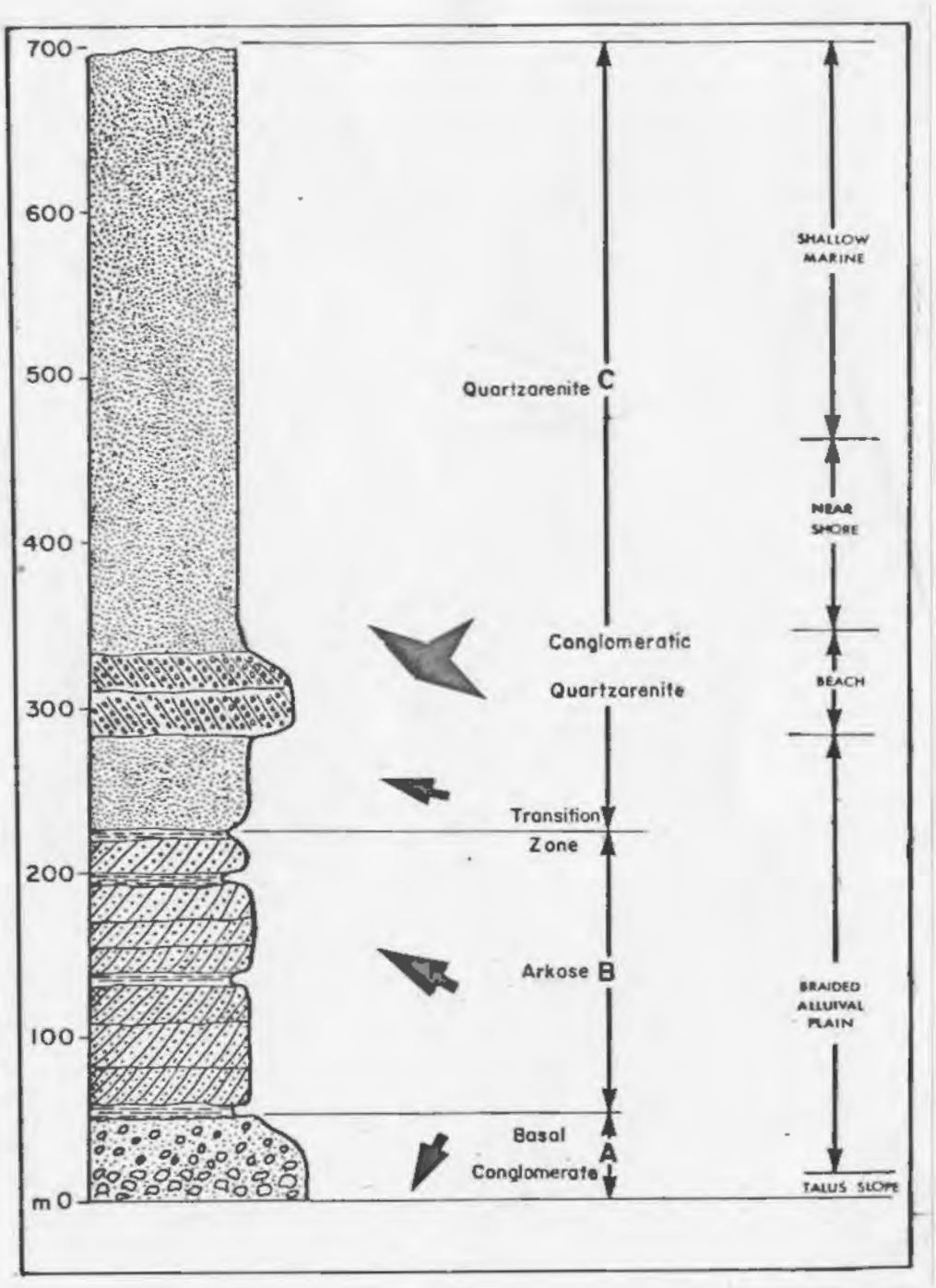

Fig. 4.18: Generalized stratigraphic section for the Sims Formation illustrating the facies interpretation, and a summary of the paleocurrent directions obtained from crossbedding, shown by arrows.

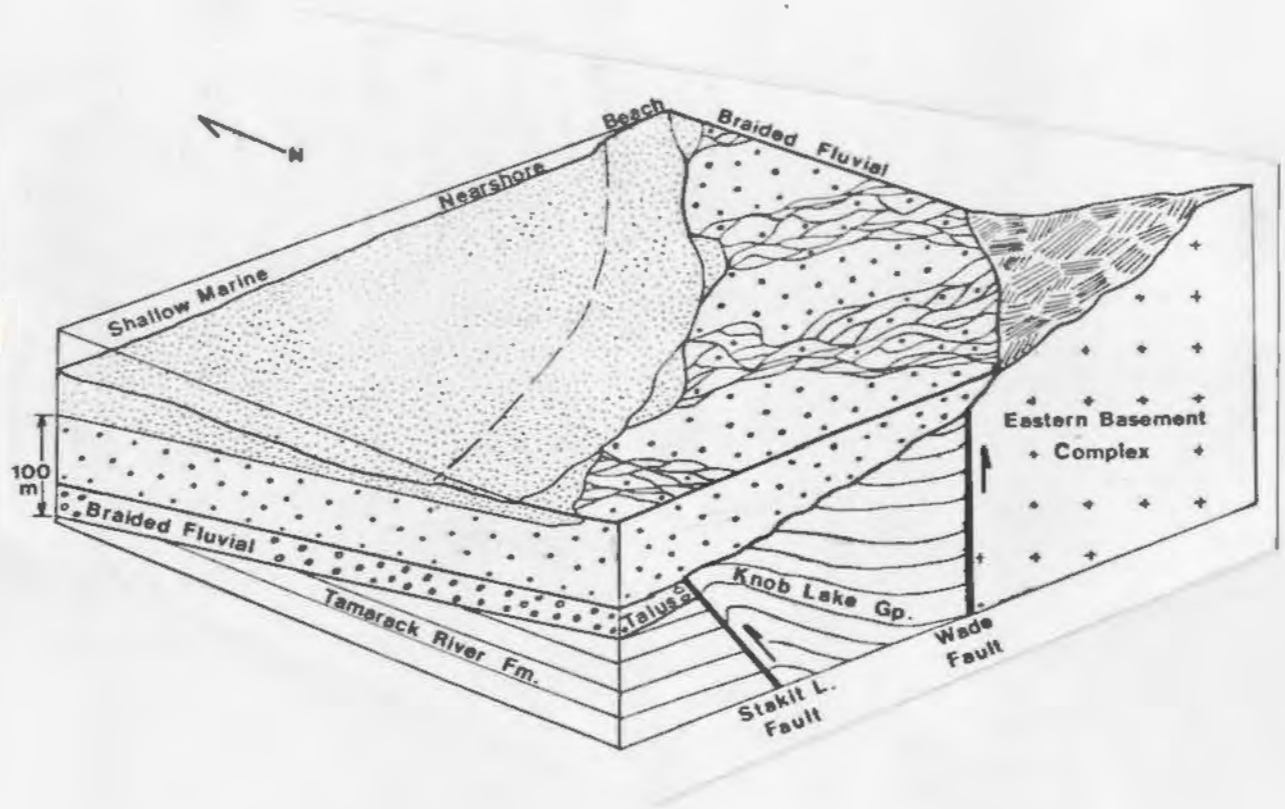

Fig. 4.19: Paleogeographic reconstruction for the Sims Formation during the initial deposition of the quartzarenite facies.

paleotopography was rugged and a thin veneer of coarse, talus-slope breccia accumulated adjacent to a small scarp. Westward within Muriel outlier, the breccia passes laterally into a 30 m thickness of better-sorted and finer-grained polymictic conglomerate which was deposited in the proximal regions of an alluvial fan. The dolomicrite inter-bedded with the conglomerates is believed to be of lacustrine origin and suggests that the climate was arid or semiarid (cf. Kendall, 1969). Periodically, heavy rains could have caused debris flows to spread onto the fan.

In Muriel outlier, the conglomerates fine abruptly upward (Fig. 4.18) into the arkose facies of member B; in Sims outlier, the arkose appears to rest directly on Aphebian strata. This facies was deposited by non-cyclic sandy braided rivers which were located in the distal portions of a northwestward-dipping alluvial plain (Fig. 4.19). The arkoses gradually became more mineralogically mature and pass upward into the thick, quartzarenites of member C. The lower portion of the quartzarenite is interpreted to be of fluvial origin, because its paleocurrent pattern is similar to that in the underlying arkose facies These sandstones owe their maturity either to mechanical abrasion produced by combination of fluvial and coastal processes or to extensive chemical weathering. The overlying conglomeratic quartzarenite is a high-energy sand and gravel beach deposit characterized by transgressive lags and southeasterly-directed migration of beach berms. The minor red mudstones immediately below the conglomerate may represent the remnants of lagoonal deposits. The middle portion of the quartzarenite facies contains abundant ripple marks, crossbedding, and parting

lineation and is interpreted as being deposited in foreshore and nearshore environments. The orientation of ripples suggests that this facies accumulated in a broad northward-facing coastal embayment. The upper portion of the quartzarenite lacks visible structures and is probably a shallow shelf deposit.

Overall, the Sims Formation is a transgressive sequence which continually onlaps in an easterly direction towards its source terrane. There are some minor regressive pulses, the most notable being responsible for the deposition of the fluvial quartzarenite. The great thickness of coastal and shallow marine quartzarenite implies that relative sea level rose slowly and steadily (Kraft, 1978), and that large amounts of sediment were carried to the coast, where wave and tidal processes produced high degrees of mineralogical and textural maturity. The cause of this relative sea level rise is unknown, but it is possible that subtle but persistent vertical movements on the Wade Lake fault, located just to the east of MacLean outlier (Fig. 4.19), could have gradually lowered the depositional basin with respect to its source terrane, the Eastern Basement Complex, at a rate that allowed coastal processes to produce the high degree of maturity. A similar thick, transgressive quartzarenite succession is the Lower Paleozoic Peninsula Formation, South Africa, which Hobday and Tankard (1978) interpret as a transgressive barrier bar and shallow marine shelf deposit. Likewise they attribute the great thickness of the Peninula Formation, over 750 m, to a high volume of clastic input, coupled with a steady and gradual subsidence.

Placed in a tectonic framework, the Sims Formation may represent a post-orogenic molasse deposit which accumulated in a foreland basin that

developed on the western side of the Labrador Trough, after the Hudsonian Orogeny. The formation bears some similarities to the Mesozoic-Tertiary Western Canadian foreland basin (Miall, 1982). In both cases, sedimentation was actively controlled by tectonic processes, the resulting clastic wedges were derived mainly from the uplifted orogen, and the underlying strata have undergone considerable amounts of compressional deformation (Fig. 4.19).

CORRELATION

Considering the shallow-marine nature of thick upper member of the Sims Formation, it is likely that the Sims Formation once covered an extensive portion of the Canadian Shield and that correlative strata should be present in adjacent areas of Labrador and Quebec. Within Labrador, the other major Paleohelikian sedimentary sequences are the Blueberry Lake Group (Wardle and Bailey, 1981) located about 20 km west of Evening Lake (Fig. 4.20), and the Bruce River and Letitia Lake Groups (Smyth et al. , 1978) both located in the Central Mineral Belt, 400 km to the west. These three groups are composed of great thicknesses of terrestrial volcanics and associated volcaniclastic sediments (Brookes et al., 1981), and are probably not contemporaneous with the Sims Formation. However, the Sims Formation may be correlative with the widely scattered and undated outliers of the Sakami Formation (Donaldson, 1970) which rest unconformably on the Archean gneisses of the Superior Province in northern Quebec (Fig. 4.20), between 400-800 km north and west of the Sims Formation. The Sakami Formation reaches a maximum thickness of 500 m (Fig. 4.20) and is divided into a lower zone of terrestrial conglomerate, arkose and red shale and an upper zone of

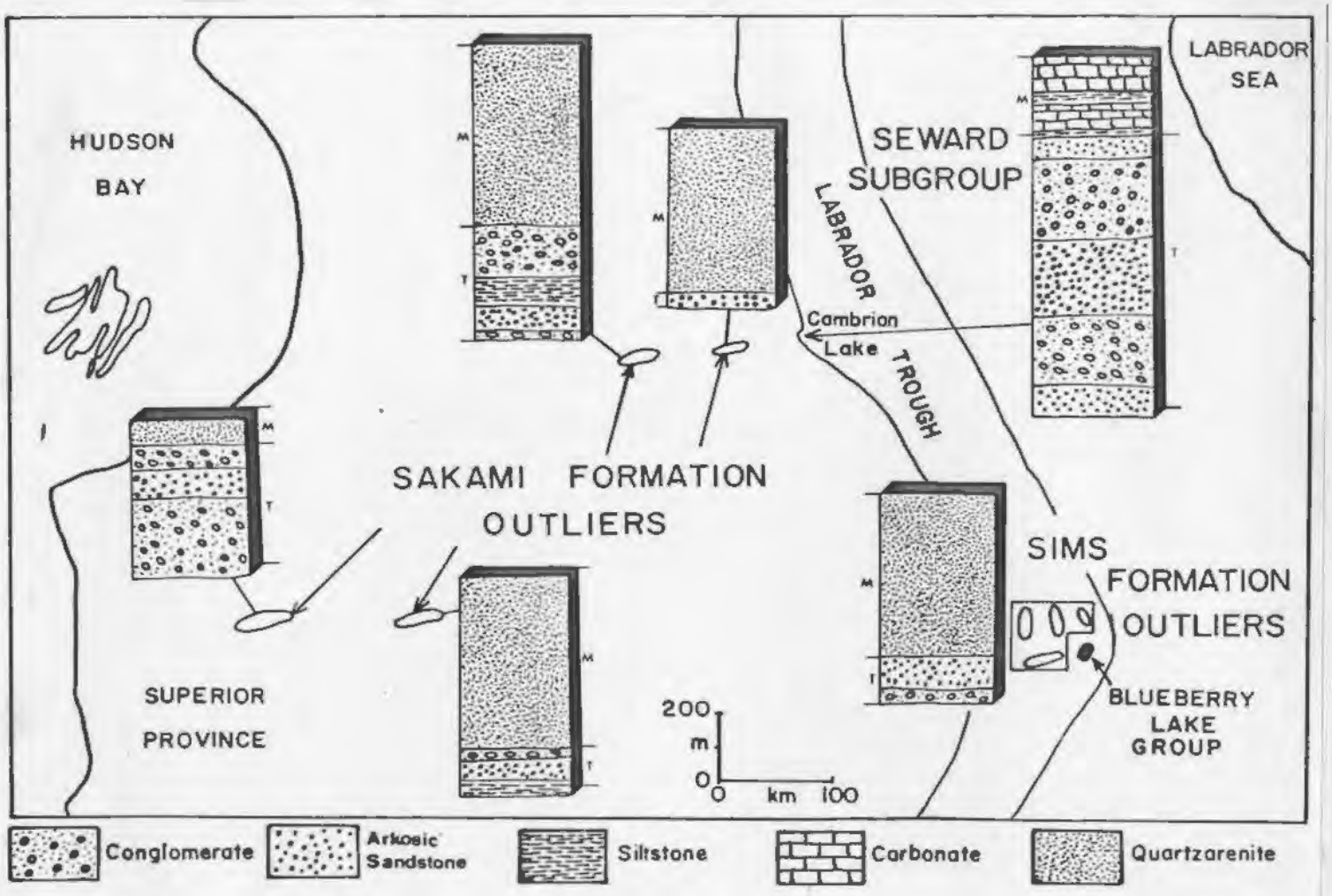

Fig. 4.20 Stratigraphic sections of the Sims Formation, the four major outliers of the Sakami Formation (Eade, 1960) and the Seward Subgroup in the Cambrian Lake area (Dimroth, 1979).
M = marine sediments; T = terrestial sediments

shallow marine quartzarenite (Eade, 1966). The internal stratigraphy of the Sakami Formation is very consistent from outlier to outlier and contains the same terrestrial to marine transition observed in the Sims Formation.

Previously Eade (1966), and Clark and Owen (1981) correlated the Sakami Formation with the Aphebian Seward Subgroup of the Cambrian Lake area of the Labrador Trough (Fig. 4.20). This correlation was based on lithological similarities and the proximity of the northwest outlier of the Sakami Formation to the Seward Subgroup of the Cambrian Lake area. However, the Sakami Formation and Seward Subgroup may be significantly different in age. The Sakami Formation, when compared with the Seward Subgroup, has a much greater ratio of quartzarenite to arkose, is a somewhat thinner sequence (Fig. 4.22), and contains iron formation pebbles (Eade, 1966) which may have been derived from the erosion of Labrador Trough strata.

If the correlation between the Sims and Sakami Formation is correct, then it follows that during Paleohelikian time, terrestrial deposits of varying thickness accumulated in isolated fault-controlled basins developed on the eastern parts of the Superior and Churchill cratons. Eventually these red beds were transgressed by a thick and widespread accumulation of coastal to shallow marine quartzarenites, which may have completely covered the eastern Canadian Shield.

SUMMARY

The Sims Formation is a Paleohelikian clastic sequence which rests unconformably on Aphebian foreland strata of the Labrador Trough. It consists of a thin, lower interval of terrestrial redbeds and a thick, upper unit of coastal to shallow marine quartzarenite.

Reactivation of Aphebian faults initiated the accumulation of the redbeds and in one area produced a talus-slope breccia adjacent to a fault scarp. The overlying conglomerate and arkose are braided river deposits which developed on a widespread, northwestward-dipping alluvial plain. The presence of interbedded playa lake deposits suggests that the climate was arid. These redbeds were transgressed by a thick blanket of quartzarenite, which was deposited in a broad spectrum of environments including: fluvial, lagoonal, beach, shoreface, nearshore and shallow marine. Consistently throughout its deposition, the formation onlapped in an easterly direction and derived its detritus from an uplifted area to the east or southeast, which was underlain by the Knob Lake Group and the Eastern Basement Complex.

The Sims Formation may be a post-orogenic, foreland molasse deposit correlative with the undated, but lithologically similar Sakami Formation of northern Quebec.

CHAPTER 5

CONCLUSIONS

Tamarack River Formation

1. The Tamarack River Formation is a newly recognized sedimentary sequence of Late Aphebian age which rests unconformably on the Knob Lake Group, in the south-central portion of the Labrador Trough. The formation is divided into three informal members and four depositional facies.
2. The formation records two transgressive-regressive pulses. The initial transgression is recorded by the shallow-marine siltstone facies. As relative sea level lowered and clastic supply decreased, these siltstones grade into the intertidal to subtidal carbonate facies. With renewed clastic input, a red sandstone facies of beach and tidal flat origin was deposited. The second transgression was initiated by a relative sea level rise which caused the return of shallow marine shelf conditions. The final regression is characterized by the development of coastal sandstones and a thick unit of fluvial sandstones.
3. Paleocurrent and petrographic data suggest that the paleodispersion pattern of the formation changed with time. During the deposition of lower units, sediments were derived from the north, whereas for the upper units, clastic detritus originated from the Superior Province in the west.
4. The formation was deposited along the western margin of the Superior Province and represents the third Aphebian miogeoclinal sequence or cycle that is recognized in southern Labrador Trough. The Tamarack River Formation may be correlative to strata in the northern Labrador Trough which occupy the same third-cycle stratigraphic position.

Sims Formation

1. The Sims Formation is a Paleohelikian clastic sequence which rests unconformably on Aphebian strata of the Labrador Trough. The formation is divided into three informal members and five depositional facies. It consists of a thin, lower interval of terrestial redbeds and thick upper unit of coastal to shallow marine quartzarenite.
2. Reactivation of Aphebian faults initiated the accumulation of redbeds and produced a talus-slope breccia facies and a braided fluvial conglomerate facies. These conglomerates fine upward into the braided fluvial arkose facies. These redbeds were overlain by a thick blanket of quartzarenite and conglomeratic quartzarenite which was deposited in a broad spectrum of environments including ; fluvial, lagoonal, beach, shoreface, nearshore and shallow marine.
3. The formation represents a major transgressive pulse and throughout its deposition it continually onlapped in an easterly direction. Clastic input was from an uplifted area to the east or southeast.
4. The Sims Formation may represent a post-orogenic molasse deposit which accumulated in a foreland basin that developed on the western side of the Labrador Trough, after the Hudsonian Orogeny. The formation may be correlative witb the undated but lithologically similar Sakami Formation of northern Quebec.

REFERENCES

Allen, J. R. L., 1963; The classification of cross-stratified units with notes on their origin. Sedimentology, 2, 93-114.

Anderton, R., 1976; Tidal-shelf sedimentation: an example from the Scottish Dalradian. Sedimentology, 23, 429-458.

Banks, N. L., 1973; Innerelv member: Late Precambrian marine shelf deposit, east Finmark. Norges geol. Unders, 288, 7-25.

Baird, D. M., 1950; The Geology of the Evening Lake - South Gabbro Lake areas, southwestern Labrador. Unpub. report, Iron Ore Co. Can., Montreal, 1-47.

Beland, R., 1949; The geology of the Gabbro Lake area. Unpub. report, Labrador Mining and Exploration Co., Montreal, 1-26.

Berard, J., 1965; Berard Lake area, New Quebec. Quebec Dept. Nat. Resources, Report 111, 1-139.

Berger, G. W. and D. York, 1980; Reinterpretation of the North American apparent polar wandering curve for the interval 800-1500 Ma. Can. J. Earth Sci., 17, 1229-1235.

Berner, R. A., 1971; Principles of Chemical Sedimentology. McGraw-Hill, N.Y., 1-240.

Blatt, H., G. V. Middleton and R. C. Murray, 1972; Origin of Sedimentary Rocks. Prentice Hall, Englewood Cliffs, N.J., 1-634.

Boothroyd, J. C. and G. M. Ashley, 1975; Process, bar morphology and sedimentary structures on braided outwash fans, northeastern Gulf of Alaska. In: A. V. Jopling and B. C. McDonald (editors); Glaciofluvial and glaciolacustrine sedimentation. Soc. Econ. Paleo. Min., Special Publ. 23; 193-222.

Brooks, C., R. J. Wardle and T. Rivers, 1981; Geology and geochronology of the Helikian magmatism, western Labrador. Can. J. Earth Sci., 18, 1211-1227.

Busch, D. J., 1978; Uranium exploration in the western Labrador Concession. Brinex, Toronto, G-78018, 1-39.

Carmichael, I. S. E., F. J. Turner and J. Verhoogen, 1974; Igneous Petrology, McGraw-Hill Co., N.Y., 1-739.

Clark, T. and J. V. Owen, 1981; Sedimentary geology of the Cambrian Lake area, northern Quebec. Geol. Soc. Can., Annual meeting Abstracts, 6.

Clifton, H. E., 1981; Progradational sequences in Miocene shoreline deposits, southeastern Caliente Range, California. J. Sed. Petrology, 51, 165-184.

Clifton, H. E., R. E. Hunter and R. L. Phillipps, 1971; Depositional structures and processes in the non-barred high-energy nearshore. J. Sed. Petrology, 41, 651-670.

Coleman, J. M., 1969; Brahmaputra River: channel processes and sedimentation. Sed. Geol., 3, 129-239.

Dallmeyer, R. D., 1980; $^{40}Ar/^{39}Ar$ radiometric dating in western Labrador. Internal Report, Nfld. Dept. Mines and Energy, 1-8.

Dickson, J. A. D., 1966; Staining technique. J. Sed. Petrology, 36, 491-505.

Dimroth, E., 1978; Labrador Trough area between latitudes 54°30' and 56°30'. Quebec Dept. Nat. Resources, Report 163, 1-396.

Dimroth, E., D. R. A. Baragar, R. Bergeron and G.D. Jackson, 1970; The filling of the Circum-Ungava Geosyncline. In: A. E. Baer (ed); Basins and geosynclines of the Canadian Shield. Geol. Surv. Can., Paper 70-40, 45-142.

Donaldson, J. A., 1970; The Labrador subprovince. In: R. J. W. Douglas (ed.); Geology and economic minerals of Canada. Geol. Surv. Can., Economic Geology Report, 1, 101-107.

Dressler, B., 1979; Region de la Fosse du Labrador (56°30'- 57°15'). Quebec Dept. Nat. Resources, Report 195, 1-117.

Dunham, R. J. 1969; Vadose pisolite in the Capitan Reef (Permian), New Mexico and Texas. In: G. M. Friedman (ed); Depositional environments in carbonate rocks a symposium. Soc. Econ. Paleo. Min., Spec. Publ. 14, 182-191.

Eade, K. E., 1949; The Sims Lake area, Labrador. Unpubl. Report, Labrador Mining and Exploration Co., Montreal, 1-27.

Eade, K. E., 1966; Fort George River and Kaniapiskau River (westhalf) map areas, New Quebec. Geol. Surv. Can., Memoir 339, 1-84.

Emslie, R. F., E. Irving and J. K. Park, 1976; Further paleomagnetic results from the Michikamau Intrusion, Labrador. Can. J. Earth Sci., 13, 1052-1057.

Esteban, M., 1976; Vadose pisolite and caliche. Am. Assoc. Pet. Geol., 60, 2048-2057.

Evans, J., 1978; Geology and geochemistry of the Nimish Subgroup, Dyke Lake area. Nfld. Dept. Mines and Energy, Report 78-4, 1-39.

Evans, J., 1979; An alkalic volcanic suite of the Labrador Trough, Labrador,. Unpubl. M.Sc. thesis, Memorial University, Nfld., 1-382.

Fahrig, W. F., K. W. Christie and E. J. Schwartz, 1974; Paleomagnetism of the Mealy Mountain anorthosite suite and of the Shabogamo Gabbro, Labrador, Canada. Can. J. Earth Sci., 11, 18-29.

Fahrig, W. F., 1967; Shabogamo Lake map-area, Nfld.-Labrador and Quebec (23 GE½). Geol. Surv. Can., Memoir 354, 1-23.

Fisher, R. A., 1953; Dispersion on a sphere. Proc. R. Soc. London, 271, 295-305.

Folk, R. L., 1968; Petrology of sedimentary rocks. Heimpills, Austin, Texas, 1-170.

Frarey, M. J. 1961; Menihek Lakes, Nfld. and Quebec. Geol. Surv. Can., Map 1087A.

Fraser, J. A., 1952; Evening Lake area - Ray Lake area. Labrador. Iron Ore Co. Can., Montreal, 1-27.

Fryer, B. J., 1972; Age determinations in the Circum-Ungava Geosyncline and the evolution of PreCambrian banded iron formation. Can. J. Earth Sci., 9, 652-663.

Gabelman, J. W., 1977; Migration of uranium and thorium-exploration significance. Am. Assoc. Pet. Geol., Studies in Geol. 3, 1-237.

Garner, H. F., 1974; The Origin of Landscapes. Oxford University Press, London, 1-734.

Gebelein, C.D., 1976; Open marine subtidal and intertidal stromatolites (Florida, the Bahamas, and Bermuda). In: M. R. Walter (ed); Stromatolites, Elsevier, Amderdam, 381-388.

Goodwin, A. M., 1951; Metamorphism in rocks of the Evening Lake area. Unpubl. M.Sc. thesis, Univ. of Wisconsin, 1-137.

Gower, C. F., A. B. Ryan, D. G. Bailey and A. Thomas, 1980; The position of the Grenville Front in eastern and central Labrador. Can. J. Earth Sci., 17, 784-787.

Harms, J. C., J. B. Southard, D. R. Spearing, and R. G. Walker, 1975; Depositional environments as interpreted from primary sedimentary structures and stratification sequences. Soc. Econ. Paleo. Min., Short course 2, 1-161.

Harrison, J. M., J E. Howell and W. F. Fahrig, 1972; A geological cross-section of the Labrador miogeosyncline near Schefferville, Quebec. Geol. Surv. Can., paper 70-37, 1-48.

Hayes, M. O. and T. W. Kana, 1976; Terrigenous clastic depositional environments, some modern examples, Am. Assoc. Pet. Geol., Field course, 1-315.

Hobday, D. K. and A. J. Tankard, 1978; Transgressive-barrier and shallow-shelf interpretation of the Lower Paleozoic Peninsula Formation, South Africa. Geol. Soc. Am., 89, 1733-1744.

Hubert, J. F. and A. A. Reed, 1978; Red-bed diagenesis in the East Berlin Formation, Newark Group, Connecticut Valley. J. Sed. Petrology, 48, 175-184.

Irvine, T. N. and W. R. A. Baragar, 1971; A guide to the chemical classification of the common volcanic rocks. Can. J. Earth Sci., 8, 523-548.

Irving, E., 1964; Paleomagnetism. John Wiley and Sons Inc., N.Y., 1-399.

Jaeger, J. C., 1968; Cooling and solidification of igneous rocks. In: H. H. Hess and A. Poldervaart (editors); The Poldervaart treatise on rocks of basaltic composition. John Wiley and Sons, N.Y. 2, 503-536.

James, N. P., 1972; Holocene and Pleistocene calcareous crust (caliche) profiles, criteria for subaerial exposure. J. Sed. Petrology, 42, 817-836.

James, N. P, and R. N. Ginsburg, D. W. Marszalk and P. W. Choquette, 1976; Facies and fabric specificity of early subsea cements in shallow Belize (British Honduras) reefs. J. Sed. Petrology, 46, 523-544.

Johnson, H. D., 1978; Shallow siliciclastic seas. In: H. G. Reading (ed.); Sedimentary environments and facies. Blackwell, Oxford, 207-258.

Kendall, A. C., 1979; Continental and supratidal (sabka) evaporities. In: R.G. Walker (ed.); Facies models, Geosci. Can., Reprint series 1, 145-158.

Klein, G. de V., 1977; Tidal circulation model for deposition of clastic sediment in epeiric and mioclinal shelf seas. Sed. Geol., 18, 1-12.

Krough, T. E. and G. L. Davies, 1973; The significance of inherited zircons on the age and origin of igneous rocks - an investigation of the ages of the Labrador adamellites. Carnegie Inst. Wash., Yearbook 72, 610-613.

Levell, B. K. 1980; A late Precambrian tidal shelf deposit, the Lower Sandford Formation, Finnmark, North Norway. Sedimentology, 27, 539-557.

Long, D. G. F., 1978; Proterozoic stream deposits, some problems of recognition and interpretation of ancient sandy fluvial systems. In: A. D. Miall (ed.), Fluvial sedimentology. Can. Soc. Pet. Geol., Memoir 5, 313-342.

Logan, B. W., P. Hoffman, C. D. Gebelein, 1974; Algal mats, cryptalgal fabrics and structures, Hamelin Pool, Western Australia. In: Evolution and diagenesis of Quaternary carbonate sequences, Shark Bay. Western Australia. Amer. Assoc, Pet. Geol., Memoir 22, 140-193.

Low, A. P. 1896; Report on exploration in the Labrador peninsula along the Eastmain, Koksoak, Hamilton, Manikuagan and portions of other rivers in 1892-93-94-95. Geol. Surv. Can., Ann Rept. 8 pt L.

MacDonell, L. and J. L. Walker, 1975; Report on geochemical and geological exploration in the Labrador concession. Unpubl. report. B.P. Minerals Ltd., Toronto, 1-30.

McKee, E. D., 1979; Sedimentary structures in dunes. In: E. D. McKee (ed.) A study of global sand seas. U.S. Geol. Surv., Prof. pap. 1052, 83-136.

McMillian, R. H., 1978; Genetic aspects and classification of important Canadian uranium deposits. Can. Mining and Metall., Bull. 71, 800, 61-67.

Miall, A. D., 1978; Lithofacies types and vertical profile models in braided river deposits, a summary. In: A. D. Miall (ed.); Fluvial sedimentology. Can. Soc. Pet. Geol., Memoir 5, 597-604.

Miall, A. D. 1981; Alluvial sedimentary basins: tectonic setting and basin architecture. In: A. D. Miall (ed); Sedimentation and tectonics in alluvial basins. Geol. Assoc. Can., Paper 23, 1-34.

Moody-Stuart, M., 1966; High and low sinuosity stream deposits with examples form the Devonian of Spitsbergen. J. Sed. Petrology 36, 1102-1117.

Murthy, G.S., W. F. Fahrig and D. L. Jones, 1968; The paleomagetism of the Michikamau anorthositic intrusion. Can. J. Earth Sci., 5, 1139-1144.

Nilsen, T. H., 1968; The relationship of sedimentation to tectonics in Solund Devonian district of southwestern Norway. Nor. Geol. Unders., 259, 1-108.

Noel, N. and T. Rivers, 1980; Geological mapping in the McKay River - Gabbro Lake area. Western Labrador. In: R. V. Gibbons (ed); Report of Activities, 1979. Nfld. Dep. Mines and Energy, 80-1, 214-221.

Orford, J. D. and R. W. G. Carter, 1982; Crestal overtop and washover sedimentation on a fringing sandy gravel barrier coast, Carnsore Point, southeast Ireland. J. Sed. Petrology, 52, 265-278.

Peryt, T. M. and T. S. Piatkowski, 1977; Algal-vadose pisoliths in the Zechstein Limestone (Upper Permian) of Northern Poland. Sed. Geol., 19, 275-286.

Pettijohn, F. J., P. E. Potter and R. Siever, 1972; Sand and Sandstone Springer-Verlag, N.Y., 1-618.

Potter, P. E. and F. J. Pettijohn, 1963; Paleocurrents and basin analysis. Academic Press, N.Y., 1-372.

Pouliot, G., 1968; Paramorphisme de quartz dans le granophyre de l'intrusion de Muskox. T. N. O. Naturaliste Can., 95, 1272-1292.

Reineck, H. E. and I. B. Singh, 1973; Depositional Sedimentary Environments, Springer-Verlag, N.Y., 1-255.

Reineck, H. E. and F. Wunderlich, 1968; Classification and origin of flaser and lenticular bedding. Sedimentology, 11, 99-104.

Reinson, G.E., 1979; Facies Models 6. Barrier Island Sytems. In: R.G. Walker (ed.); Facies Models, Geosci. Con. Reprint series 1, 57-74.

Rivers, T., 1980a; Revised stratigraphic nomenclature for Aphebian and other rock units southern Labrador Trough, Grenville Province. Can. J. Earth Sci., 17, 668-670.

Rivers, T., 1980b; Geological mapping in the Evening-Lake Wightman Lake area, western Labrador. In: R. V. Gibbons (ed); Report of Activities, 1979. Nfld. Dept. Mines and Energy, Report 80-1, 201-205.

Rust, B. R., 1972; Structure and process in a braided river. Sedimentology, 18. 221-246.

Smyth, W. R., B. E. Marten and A. B. Ryan, 1978; A major Aphebian-Helikiam unconformity within the Central Mineral Belt of Labrador. Definition of new groups and metallogenic implications. Can. J. Earth Sci., 15, 1954-1966.

Stockwell, C. H., 1970; Geology of the Canadian Shield. In: R. J. W. Douglas (ed); Geology and economic minerals of Canada. Geol. Surv. Can., Economic Geol. Report 1, 44-54.

Tarling, D. H. 1971; Principles and Applications of Paleomagnetism. Chapmen and Hall, London, 1-164.

Taylor, F. C., 1979; Reconnaissance geology of a part of the Precambrian shield, northeastern Quebec, northern Labrador and Northwest Territories. Geol. Surv. Can., Memoir 393. 1-99.

Tiphane, M., 1951; Geology of South Menihek Lake area. Unpubl. report. Iron Ore Co. Can., 1-24.

van Straaten, L. M. J. U., 1978; Dendrites. Geol. Soc. London, 135, 137-151.

Walker, R. G. and D. J. Cant, 1979; Sandy Fluvial Systems. In: R. G. Walker (ed); Facies Models. Geosci. Can., reprint series 1, 23-32.

Wanless, R. K., R. D. Stevens, G. R. Lachance, and J. Y. H. Rimsaite, 1966; Age determinations and geological studies. Part 1 - isotopic ages. Geol. Surv. Can., Paper 64-17, 1-156.

Wardle, R. J., 1979; Geology of the eastern margin of the Labrador Trough. Nfld. Dept. Mines and Energy, Report 78-9, 1-22.

Wardle, R. J. and D. G. Bailey, 1981; Early Proterozoic sequences. In: F. H. A. Campbell (ed); Proterozoic Basins of Canada. Geol. Surv. Can., Paper 81-10, 331-360.

Ware, M. J., 1979; Geology of the Sims Lake - Evening Lake area, western Labrador. In: R. V. Gibbons (ed); Report of Activities, 1978. Nfld. Dept. of Mines and Energy, Report 79-1. 135-141.

Ware, M. J., 1980; Tamarack River Formation, Sims Lake - Menihek Lake area, western Labrador. In: R.V. Gibbons (ed); Report of Activities, 1979. Nfld. Dept. Mines and Energy, Report 80-1, 194-200.

Ware, M. J. and R. J. Wardle, 1979; Geology of the Sims - Evening Lake area, western Labrador, with emphasis on the Helikian Sims Group. Nfld. Dept. Mines and Energy, Report 79-5, 1-22.

Wilson, J. L. 1975, Carbonate Facies in Geologic History. Springer-Verlag, N.Y., 1-471.

Wynne-Edwards, H. R., 1960; Geology, Michikamau Lake (west half) Quebec-Nfld. Geol. Surv. Can., Map 2-1960.

Wynne-Edwards, H. R., 1961; Ossokmanuan Lake (west half) Nfld. Geol. Surv. Can., Map 17-1961.

Wynne-Edwards, H. R., 1972; The Grenville Province. In: R. A. Price and R. J. W. Douglas (editors); Variations in Tectonic Styles in Canada. Geol. Assoc. Can., Paper 11, 263-335.

APPENDIX A.

Unit	#	Q	QP	Iv	Ip	Sd	C	Sl	P	M	O	Mi	H
LE FER FORMATION	168	72	12	-	-	-	-	-	11	-	3	-	2
WISHART FORMATION	16	91	-	-	-	-	-	-	1	3	5	-	-
	16a	83	7	-	-	-	-	-	2	3	5	-	-
	13	90	8	-	-	-	-	-	-	-	2	-	-
	6	82	2	-	-	-	-	-	3	2	1	-	-
MENIHEK FORMATION	226	35	9	4	6	6	-	-	13	5	20	1	1
	72	32	7	6	8	4	-	-	14	4	22	2	1
TAMARACK RIVER FORMATION Member A	196	26	7	29	-	8	5	5	9	2	4	1	4
	196a	17	6	35	-	12	9	7	4	1	6	1	2
	343	34	21	10	-	5	6	-	9	3	10	1	1
	181	30	7	23	-	6	1	3	15	1	13	1	-
	340	15	4	38	-	15	2	3	9	1	9	-	4
Member B	310	38	6	2	-	9	-	7	22	1	10	3	-
	346	42	11	2	-	-	2	-	22	4	13	2	2
Member C	240	42	17	2	-	5	-	1	13	2	11	3	4
	351	49	12	-	-	-	-	6	12	2	8	5	6
	317	44	12	-	-	-	-	1	23	2	12	3	3
	349	46	6	-	-	2	-	1	30	3	5	-	7
	330	44	15	3	-	-	-	-	16	2	18	-	2
	350	55	10	-	-	-	-	2	18	5	7	2	1
SIMS FORMATION	255	57	9	6	-	5	-	3	8	3	8	-	1
Member A	31	34	26	21	-	8	5	-	1	2	2	-	1
	32	68	15	4	-	8	-	-	-	-	5	-	-
	347	47	10	3	-	4	29	-	-	-	7	-	-
	59	63	17	3	-	3	-	2	5	3	4	-	-
	007	74	3	3	-	-	-	-	7	3	8	-	2
	29	73	8	4	-	-	-	2	7	1	5	-	-
Member B	256	71	2	-	-	-	-	-	2	3	21	1	-
	75	76	5	-	-	-	-	-	7	3	6	-	3
	111	61	11	3	-	-	-	-	10	3	7	1	4
	231	55	11	2	-	-	-	-	9	3	15	2	3
	355	59	7	-	-	-	-	-	1	6	25	1	1
	79	73	7	-	-	-	-	-	2	5	12	-	1
	77	72	5	-	-	-	-	-	2	3	15	2	1
	78	63	5	-	-	-	-	-	1	4	26	-	1
	352	76	6	-	-	-	-	-	5	5	7	-	1
	008	77	4	-	-	1	-	-	5	2	10	-	1
	40	80	5	1	-	-	-	-	1	1	11	-	2
	156	63	5	-	-	-	-	-	11	2	16	-	3
	213	76	5	-	-	-	-	-	5	2	14	-	-
Transition B-C	76	88	2	-	-	-	-	-	1	1	8	-	-
	80	85	6	-	-	-	-	-	2	-	6	-	1
	103	90	6	-	-	-	-	-	-	-	3	-	1
	75	89	4	-	-	-	-	-	-	-	3	1	3
	20	82	4	1	-	-	-	-	3	2	8	-	-
Member C	94	98	1	-	-	-	-	-	-	-	1	-	-
	80	95	3	-	-	-	-	-	-	-	2	-	-
	88	95	2	-	-	-	-	-	-	-	3	-	-
	242	94	2	-	-	-	-	-	1	1	2	-	-
	218	96	1	-	-	-	-	-	1	-	2	-	-
	252	95	1	-	-	-	-	-	-	-	4	-	-
	55	97	2	-	-	-	-	-	-	-	1	-	-
	95	96	2	-	-	-	-	-	1	-	1	-	-
	74	93	3	-	-	-	-	-	-	-	4	-	-
	85	94	1	-	-	-	-	-	-	1	4	-	-
	229	98	1	-	-	-	-	-	-	-	-	-	1

Q = quartz
Qp = chert
IV = volcanic fragment
Ip = plutonic fragment
Sd = sandstone fragment
C = calcareous fragment
Sl = siltstone fragment
P = plagioclase
M = microcline
O = orthoclase
Mi = mica
H = heavy mineral

Sandstone petrography for various rock units. Modal compositional analyses are based on 200 point counts of sand sized grains per thin-section. See Appendix C for location.

APPENDIX B.

	Shabogamo Intrusive Suite								
	Bottom			MacLean Sill					Top
#	249	248	124	247	246	114	129	245	116
SiO_2	46.6	46.8	47.8	49.0	53.1	53.3	54.4	55.0	69.5
TiO_2	1.80	1.26	1.91	1.72	2.25	1.79	1.47	1.59	1.25
Al_2O_3	15.40	16.10	17.35	17.40	14.55	15.85	16.35	14.45	10.85
Fe_2O_3	1.81	1.42	2.54	2.08	1.25	1.49	1.94	.83	1.74
FeO	11.61	10.46	10.21	9.62	9.47	9.39	8.33	8.50	4.51
MnO	.19	.16	.16	.16	.17	.16	.15	.13	.08
MgO	10.74	13.15	7.31	7.64	4.13	5.91	5.44	4.09	1.95
CaO	8.15	8.41	8.78	8.10	6.75	6.61	6.74	5.88	3.52
Na_2O	2.55	2.37	2.91	3.16	3.47	2.91	2.58	3.20	2.08
K_2O	.67	.52	.53	.98	1.60	1.40	1.65	1.75	2.72
P_2O_5	.33	0.22	.23	0.72	.57	.33	.21	.34	.20
LOI	1.00	.03	.44	.37	2.23	1.11	.94	2.56	1.49
TOTAL	99.14	101.25	100.37	100.60	99.56	100.75	100.20	98.30	99.89

	Shabogamo Intrusive Suite						Nimish Subgroup	
	Evening Outlier				Muriel			
#	161	162	163	164	112	47	339	A.
SiO_2	47.1	47.9	44.1	46.9	55.2	53.3	50.8	50.1
TiO_2	1.99	2.46	1.91	2.10	2.24	2.98	1.23	2.17
Al_2O_3	16.7	12.9	11.8	13.4	13.25	13.75	17.0	14.62
Fe_2O_3	1.76	2.51	3.47	2.75	2.18	1.81	3.55	5.2
FeO	9.86	12.05	14.10	11.47	9.93	10.14	4.45	7.21
MnO	.15	.21	.22	.22	.19	.17	.094	.18
MgO	7.08	4.47	6.86	3.67	2.85	3.44	4.67	2.19
CaO	8.38	7.89	7.33	8.76	4.76	5.79	5.85	3.86
Na_2O	2.87	2.68	2.58	3.38	3.51	3.11	2.11	2.83
K_2O	1.99	2.44	1.91	2.10	2.83	2.91	3.78	5.59
P_2O_5	.60	1.08	1.14	2.21	.92	1.00	.33	.67
LOI	1.51	1.05	1.18	1.07	1.42	1.50	3.73	3.36
TOTAL	100.38	99.35	99.07	99.47	99.28	99.90	99.58	97.81

	Tamarack River Formation				Sims Formation				
Unit	9B	9B	9C	9C	10a	10b	10b-c	10c	10c
Sample	300	337	317	349	255	8	76	157	1
SiO_2	68.0	54.8	68.3	71.2	86.8	82.9	96.0	97.0	96.7
TiO_2	.46	.48	.32	.25	.16	.20	-	.04	-
Al_2O_3	13.8	11.9	11.0	10.7	6.33	7.53	1.54	1.21	1.85
Fe_2O_3	4.14	2.93	2.49	2.82	.53	1.88	.10	.05	.11
FeO	1.60	1.64	1.66	.23	.34	.47	*	*	*
MnO	.024	.16	.071	.083	.008	.009	.003	.004	.003
MgO	2.49	5.24	2.80	1.96	.36	.42	.04	-	.09
CaO	.24	6.89	3.56	2.95	.02	.09	.04	.02	.19
Na_2O	.04	1.81	1.54	1.70	.05	.04	.007	.016	.012
K_2O	5.50	3.05	2.89	3.29	3.77	3.49	.46	.42	.52
P_2O_5	0.20	.13	0.12	.08	.04	.01	.07	.04	.01
LOI	3.69	10.89	3.70	4.48	1.20	1.54	.38	.35	.60
TOTAL	100.18	99.74	100.65	99.74	99.61	98.58	98.84	99.15	100.09

Chemical analyses for the Shabogamo Intrusive Suite, Nimish Formation, Tamarack River Formation and Sims Formation. Analyses were performed at Memorial University using the method outlined by Evans (1979). See Appendix C for location.

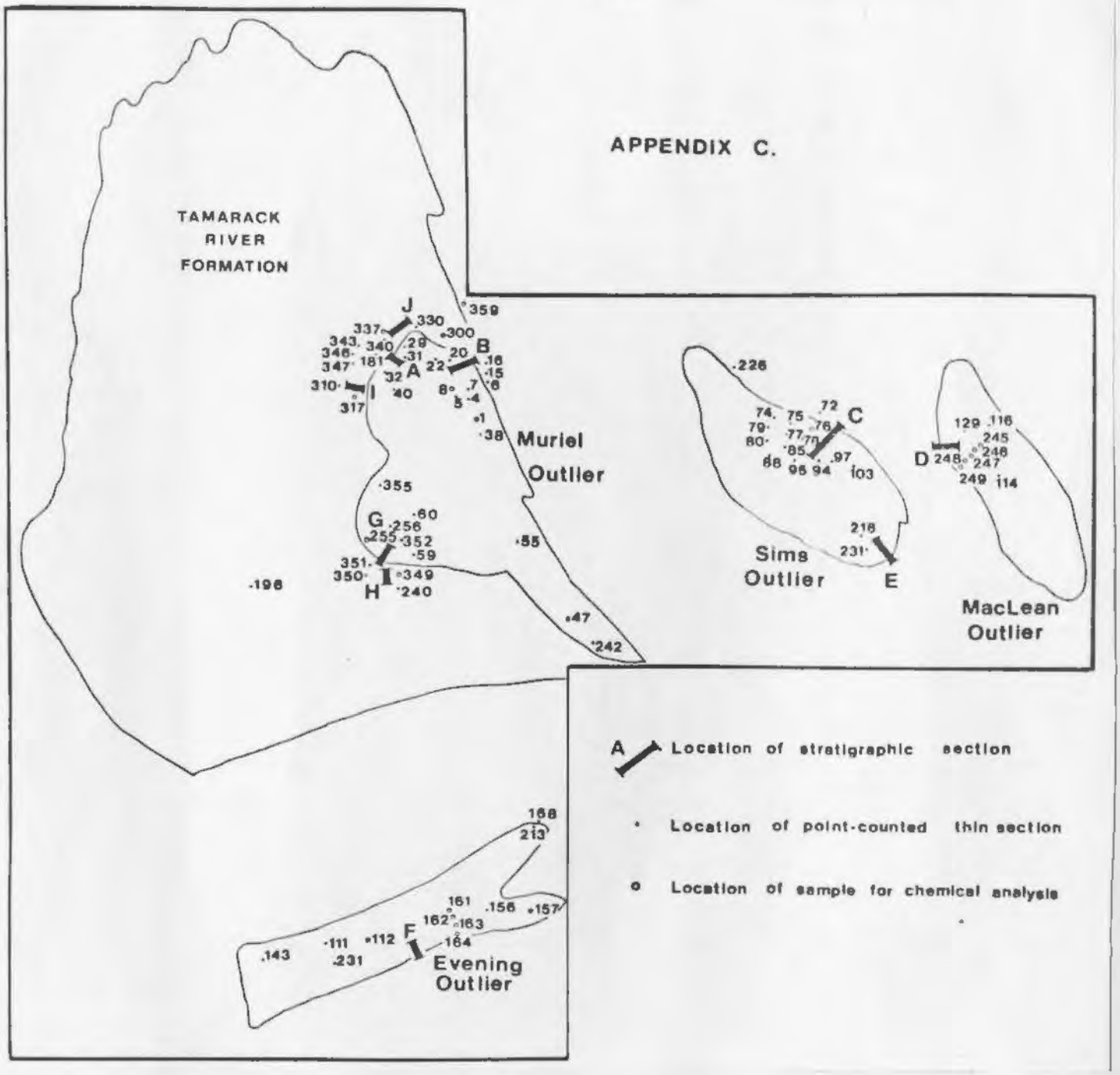

Sketch map of the Sims and Tamarack River Formations showing the location of samples used in the petrographic and geochemical studies. For the geology of the area refer to Figure 2.1 (p. 8).

APPENDIX D

SHABOGAMO INTRUSIVE SUITE

INTRODUCTION

An extensive group of mafic bodies belonging to the Shabogamo Intrusive Suite intruded the Aphebian and Paleohelikian rocks of the southern Labrador Trough (Fig. D.1) during the Elsonian magmatic event (c. 1.4 Ga) (Brooks et al., 1981). The suite is composed of leucocratic to mesocratic gabbro, norite, and diabase with subordinate amounts of diorite, granodiorite, and ultramafic rocks (Fahrig, 1967; Ware and Wardle, 1979; Noel and Rivers, 1980; Rivers, 1980a).

Most of the intrusions are located in the Grenville Province (Fig. D.1) and have been tectonically tilted and locally recrystallized to amphibolite or chlorite-actinolite-biotite schist (Fahrig, 1967; Ware and Wardle, 1979; Noel and Rivers, 1980). Only the northern most intrusions which lie in the Churchill Province (Fig. D.2) are undeformed and unmetamorphosed (Ware and Wardle, 1979). Major-oxide geochemistry (Appendix B) of the northern parts of the suite suggests that, in this area, the suite is subalkaline (Fig. D.3) and tholeiitic (Fig. D.4), according to the classification of Irving and Baragar (1971).

MACLEAN SILL

MacLean Sill is an undeformed sill, at least 180 m thick, which intrudes the Sims Formation of MacLean outlier (Fig. D.2). The sill is flat lying based on the presence of vertical columnar jointing and

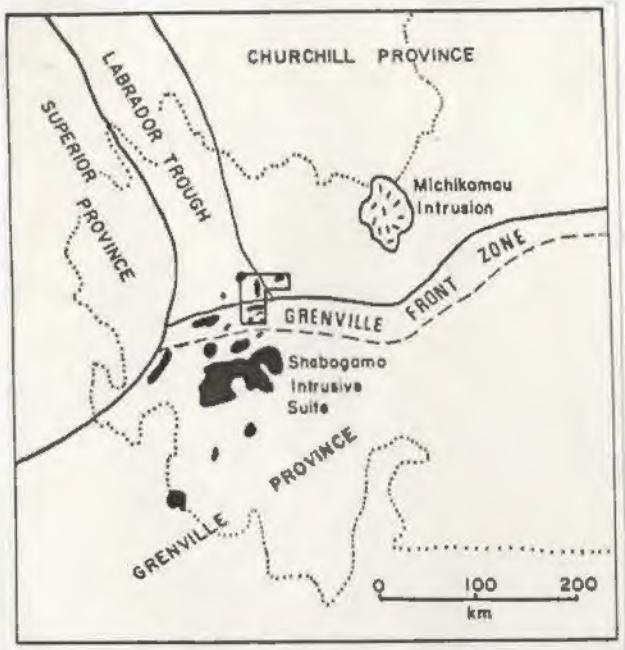

Fig. D.1: Geological subdivisions of western Labrador with the major outcrops of the Shabogamo Intrusive Suite shown in black. Area of Figure D.2 is outlined.

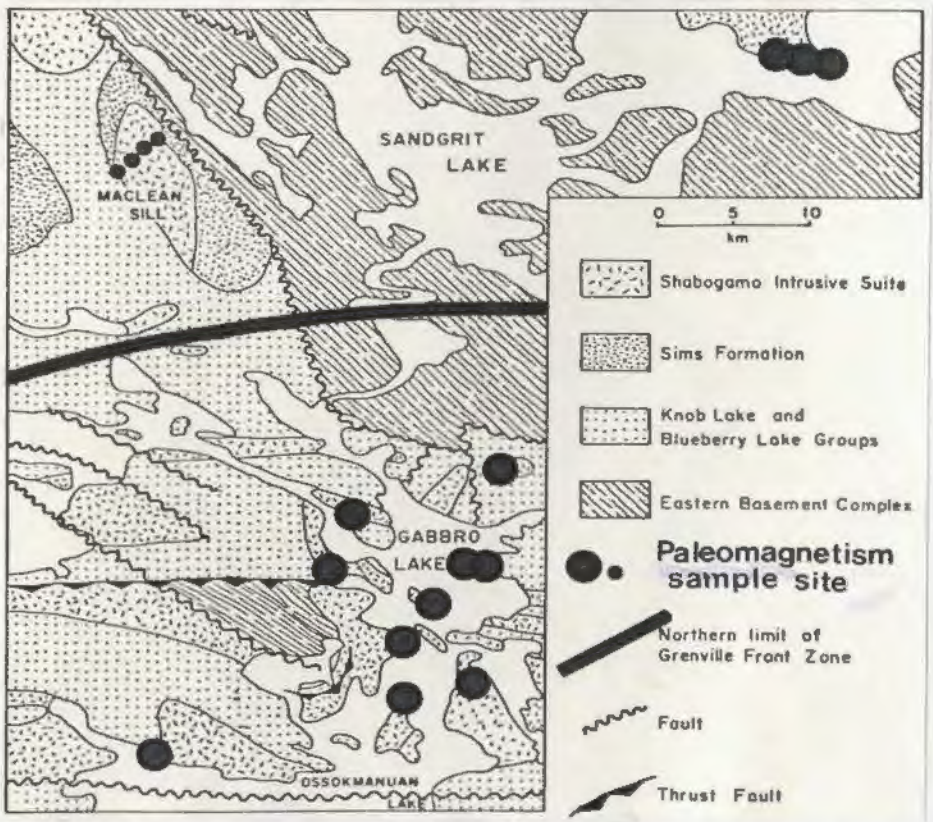

Fig. D.2: Generalized geologic map of the northeastern part of the Shabogamo Intrusive Suite, adapted from Wardle (1979), Ware and Wardle (1979) and Noel and Rivers (1980). Paleomagnetic sample sites for this study are shown as small dots, and sample stations of Fahrig et. al., 1974 as large dots.

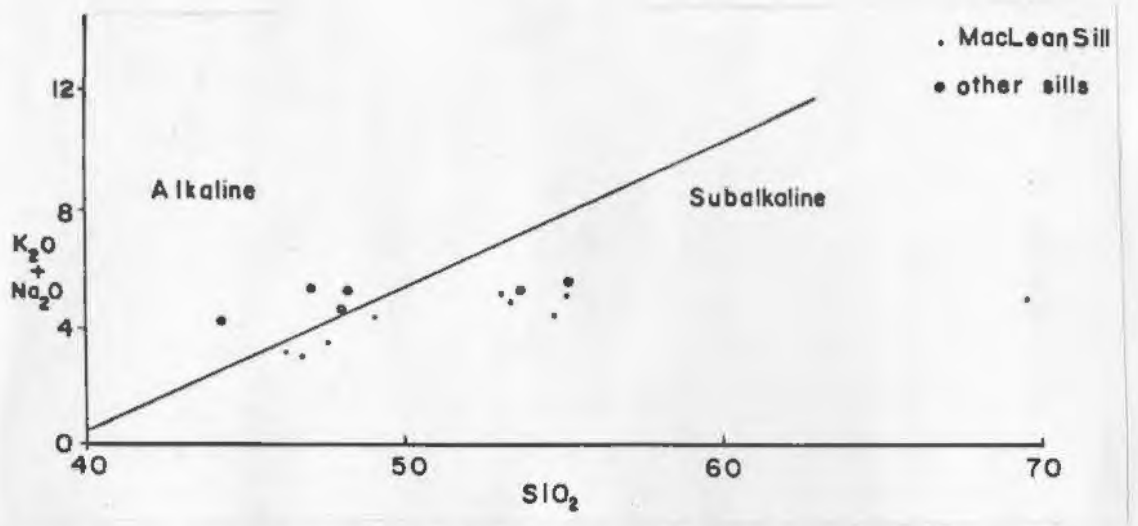

Fig. D.3: Total alkalies versus silica diagram for the MacLean Sill and other northern sills of the Shabogamo Intrusive Suite. Boundary line between alkaline and subalkaline is according to Irving and Baragar (1971).

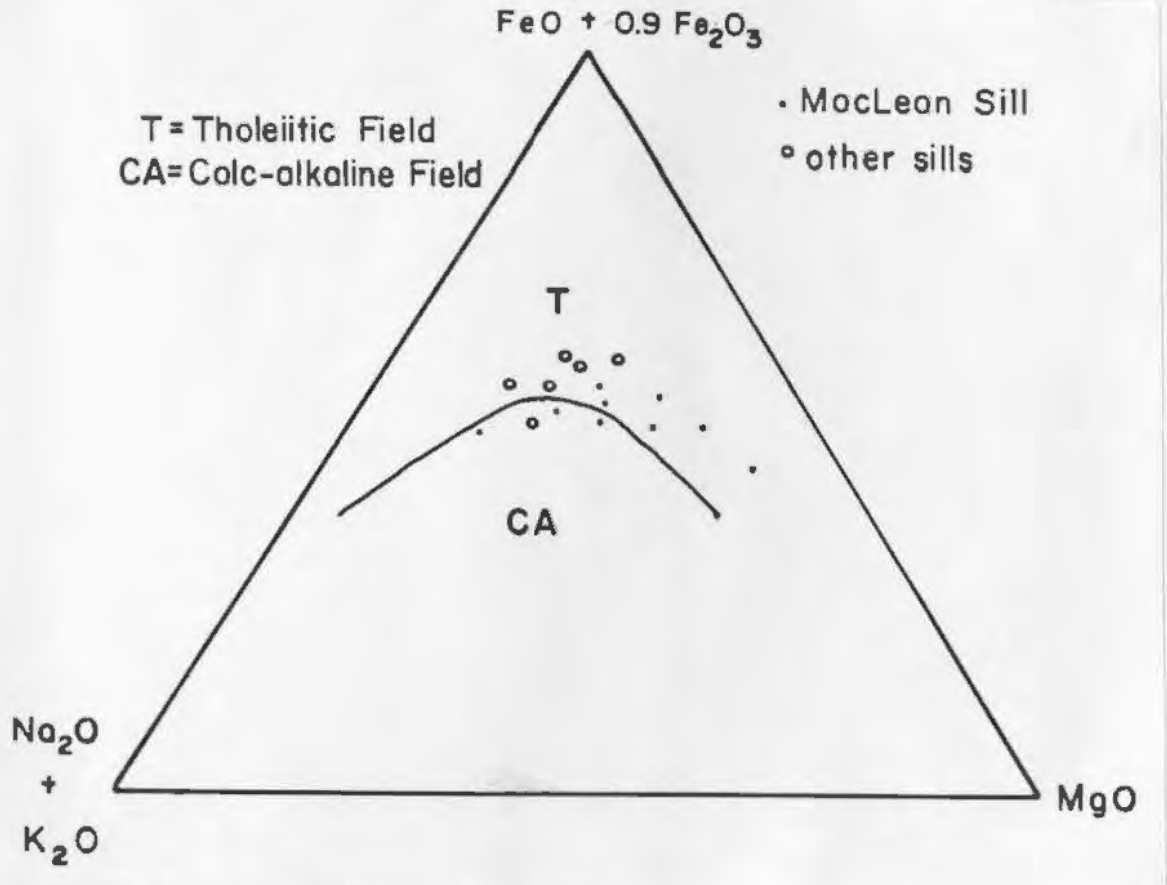

Fig. D.4: An AFM diagram for the MacLean Sill and other northern sills of the Shabogamo Intrusive Suite. Tholeiitic and calc-alkaline fields are according to Irving and Baragar (1971).

horizontal primary igneous layering. The upper and lower contacts are not exposed, but the highest exposures contain abundant xenoliths of Sims Formation quartzarenite, up to 3 m in diameter, and the occasional xenolith of granite-gneiss from the Eastern Basement Complex. The outer margins of the xenoliths are deeply embayed. Internally, the xenoliths possess equant recrystallization textures.

Mineralogically, the sill is divided into a lower zone, 145 m thick, of medium- to coarse-grained ophitic to subophitic olivine-diabase and an upper zone, 35 m thick, of fine- to coarse-grained granophyric diorite or granodiorite (Fig. D.5). The lower zone is composed of fresh to slightly-serpentinized olivine, plagioclase, augite, and ilmenite with accessory biotite and sphene (Fig. D.5). In contrast, the upper zone consists of granophyre, saussuritized plagioclase, altered pyroxene, amphibole, biotite, chlorite, ilmenite and quartzarenite xenoliths, with accessory epidote and apatite (Fig. D.5). The granophyre consists of fine-grained intergrowths of quartz, orthoclase and plagioclase with cuneiform, wormy, bulbous, parallel, blocky and radiating forms. This mineralogical subdivision is reflected by a distinct chemical variation (Fig. D.5). As the amount of olivine decreases the MgO values fall and with the increase in granophyre content the silica values increase. Other oxides, notably total iron and the alkalis (Na_2O & K_2O) show only slight variation through the sill (Fig. D.5).

The bulk of the granophyric diabase found at the top of the MacLean Sill is interpreted to have been derived by assimilation of Sims Formation quartzarenite into the mafic magma. Such a mechanism could explain the great relative thickness of granophyre and the lack of

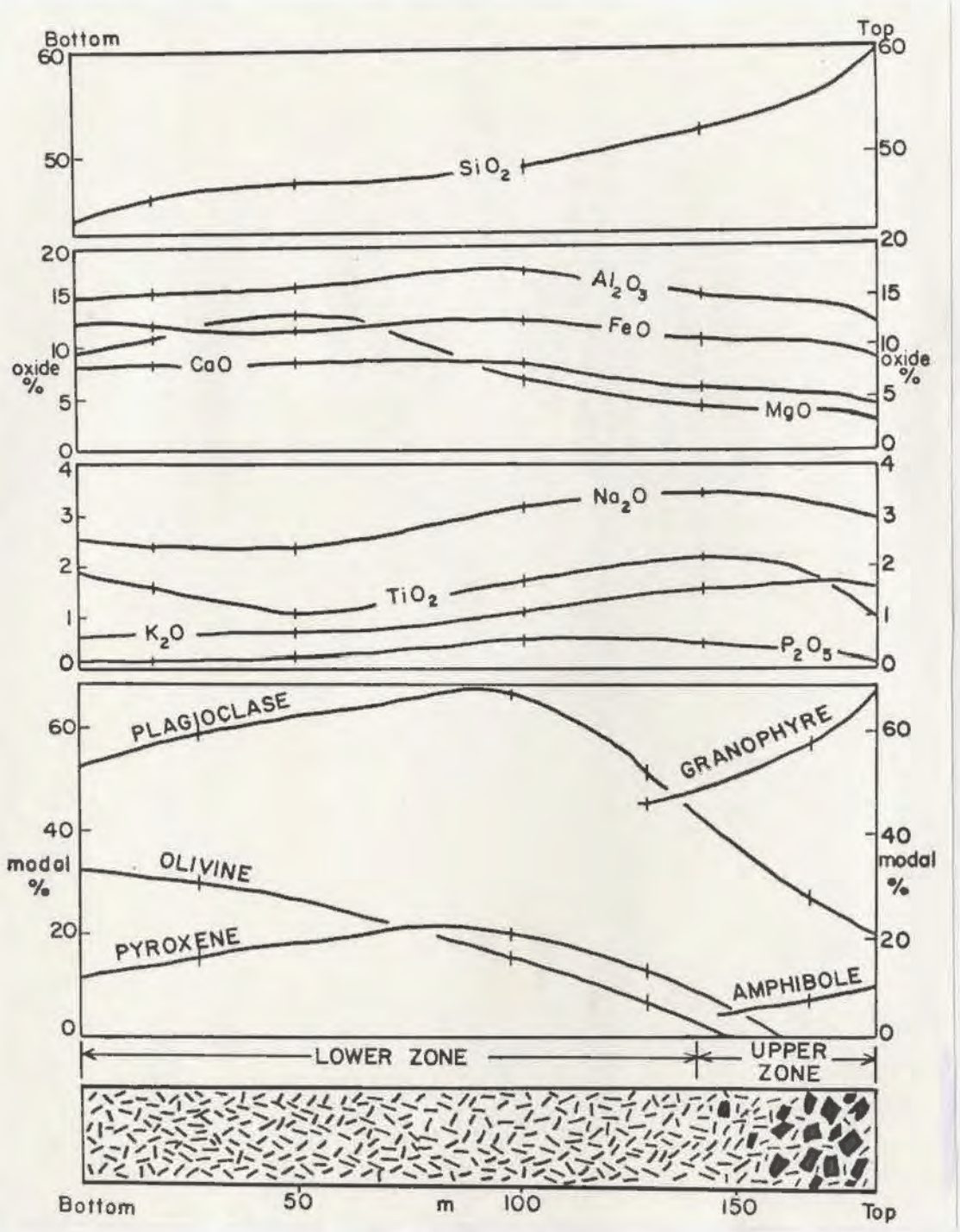

Fig. D.5: Variation of oxide % and modal mineralogy with height in the MacLean Sill. Oxide % samples are numbered 245 to 249 (Appendix B). Modal mineralogy is based on 200 point counts of samples from each of the four paleomagnetic sites. Total iron (FeO + Fe_2O_3) is plotted as FeO.

chemical trends within the sill characteristic of differentiation of a tholeiitic magma, such as progressive enrichment in alkalis and iron content (Carmichael et al., 1974). A similar explanation was proposed by Pouliot (1968) to account for the large volume of granophyre found at the top of the Muskox Intrusion (Northwest Territories) where it intrudes quartzarenite of the Hornby Bay Group. As an alternative interpretation, it is possible that the differentiated material has been transported laterally, and cooled elsewhere, within the sill.

PALEOMAGNETISM

Recent systematic mapping of western Labrador by Ware and Wardle (1979), Wardle (1979) and Noel and Rivers (1980) demonstrates that the bulk of sample locations of Fahrig et al., (1974), in the original study of the paleomagnetism of the Shabogamo Intrusive Suite, lie within the Grenville Front Zone (Fig. D.2), and probably have been tectonically displaced. Fahrig et al., (1974) did not recognize the extent of this deformation and failed to apply any tectonic tilt correlations to their data. This paleomagnetic study is based on samples collected from the MacLean Sill, which is located well north of the Grenville Front Zone (Fig. D.2) and is flat-lying.

Procedure and Results

Five blocks, oriented by sun compass, were collected from each of four sampling sites located at different stratigraphic levels within the MacLean Sill (Fig. D.2). The magnetic remanences of the 20 specimens were measured on a Schonstedt SSM-1 magnetometer. Alternating field

(af) demagnetizations were performed with a three-axis undirectional tumbling of the specimen. The average intensity and direction of the natural remanent magnetization (NRM) for each site are presented in Table D.1 along with Fisher (1953) statistics. 'R' represents the vector sum of the unit vector along each sample's magnetization direction, 'K' is an estimate of precision (the greater the value, the better the precision) and 'α 95' the half angle of the cone of 95% confidence.

The average intensity of NRM for the four sites is 9.52×10^{-3} emu/cm^3 with a standard deviation of 6.60×10^{-3} emu/cm^3, both of which are normal for mafic igneous rocks (Tarling, 1971). The NRM directions are dispersed, with directions at three sites plunging downward (positive inclination) to the east and one site plunging upward (negative inclination) to the east (Fig. D.6A,B).

After alternating field demagnetization, dispersion among the remanence directions for the various sites was significantly reduced. Specimens were all demagnetized at 100 Oe intervals between 0 and 1200 Oe. Some were additionally subjected to fields up to 1800 Oe. The specimens have high coercivities and reached a stable end-point with a minimum amount of dispersion, at 1200 Oe. The results are plotted in Fig. D.6A,B and show the af-demagnetization paths for each of the four sites. Remanent directions for sites 1, 2, and 3 move from an eastward declination with a positive inclination to an eastward declination with a negative inclination along a great circle. Site 4 directions move very little during demagnetization, the NRM already being of eastward declination with negative inclination (Fig. D.6A,B).

Table D.1

Shabogamo Intrusive Suite

	Natural remanent magnetism							Treated					
L	N	M	D	I	R	K	α95	af Oe	D	I	R	K	α95
1	5	1.60×10^{-2}	76.6	11.1	4.955	89.9	8.1	1,200	71.9	-22.1	4.990	405.3	3.81
2	5	1.23×10^{-2}	115.8	37.7	4.830	23.6	16.1	1,200	82.6	-15.7	4.944	71.6	9.1
3	5	9.52×10^{-3}	94.1	45.0	4.890	36.3	12.9	1,200	74.0	-24.2	4.976	165.0	6.0
4	5	2.49×10^{-4}	90.4	19.9	4.958	88.9	8.2	1,200	90.1	-27.2	4.973	145.6	6.3

L = site number, N= total number of oriented cores, M = intensity of NRM, D, I = directions, R = resultant vector, K = estimate of precision, α95 = cone of confidence, af Oe = optiumium alterating cleaning field.

Table D.2

Summary of Results

Rock Unit	Area	B	N	Dm	Im	Oe	Dm	Im	R	K	α95	Pole	dm	dp
Shabogamo Intrusive Suite a	MacLean sill	4	20	93.0	19.4	1200	79.6	-22.5	3.888	79.8	10.35	39.7^{o}E, 3.4^{o}S	11.0	5.8
" b	Southern sites	10	58	102.7	50.2	350-800	104.4	35.4	9.135	10.4	15.7	1.9^{o} E, 7.5^{o}N	16.8	9.3
" b	Northern sites	3	12	74.1	49.2	100-250	76.3	9.4	2.879	17.0	31.4	33.7^{o} E, 11.9^{o}N	32.0	16.0
Michikamau Intrusion c		12	54			100-1000	259.5	11		43	6.5	142.5^{o}W, 1.5^{o}S	7	3.5

a = this study, b = Fahrig et. al.(1974), c = Murthy et. al. (1968) & Emslie et. al.(1976), B = number of collecting localities, N = total number of oriented cores, Dm, Im are mean directions, R = resultant vector, K = estimate of precision, α95 = cone of confidence, dm and dp are polar errors.

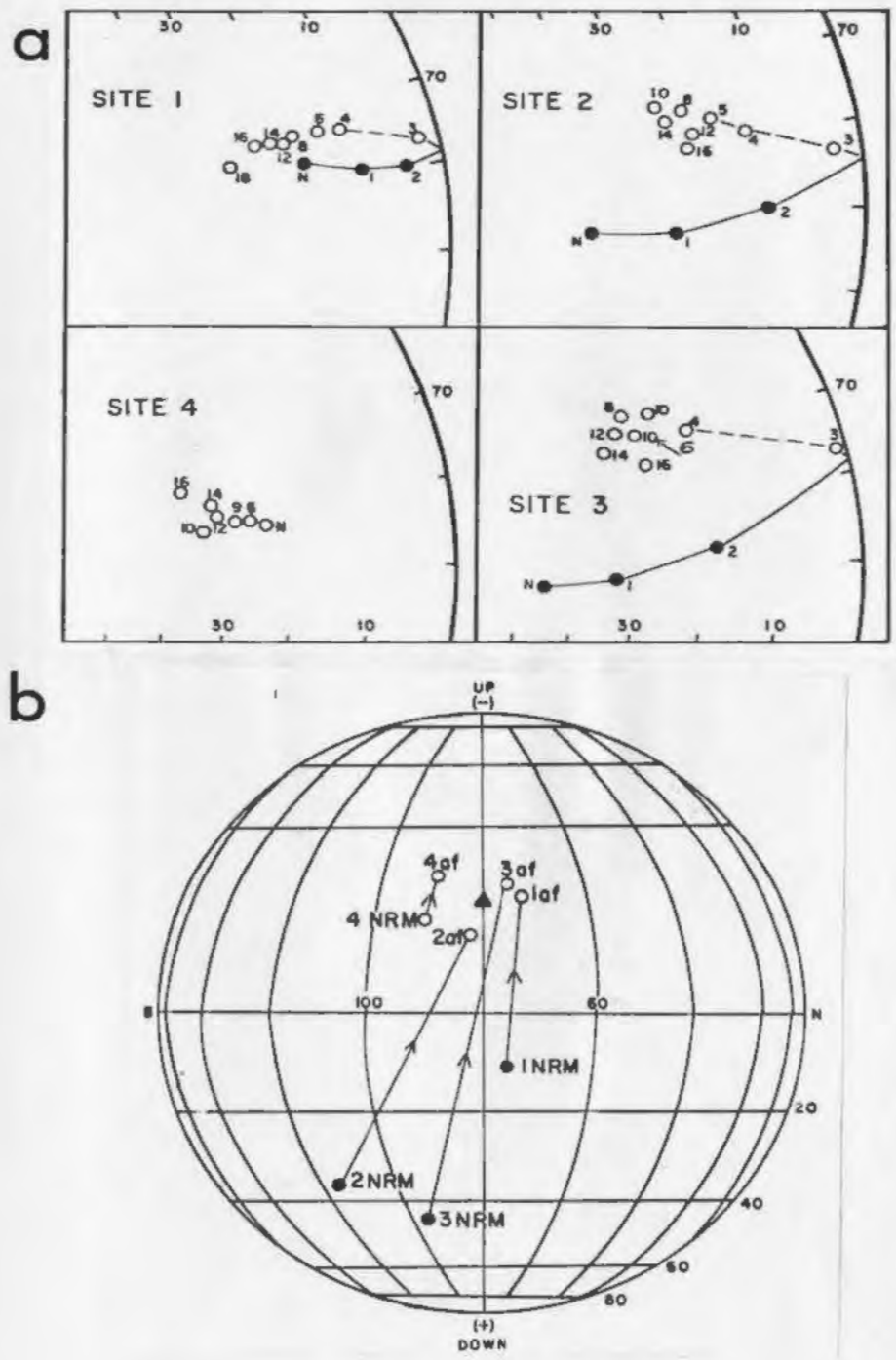

Fig. D.6A: Stereonets showing the magnetization directions of representative samples from each of the four sites. Solid circles, downward (+ve) inclinations, open circles upward (-ve) inclinations.

Fig. D.6B: A spherical projection of the average path taken between NRM and af cleaned directions. Solid triangle indicates average of the cleaned directions for all sites.

It is convenient to divide the sites into two groups based on their relative resistance to af demagnetization. Sites 1 and 4, located near the margins of the sill, have, on average, remanence intensities of 89, 68.5, and 29% of NRM intensities after 300, 800, and 1200 Oe demagnetizations respectively. Site 2 and 3 located within the interior of the sill are more easily demagnetized, having, on average, remanence intensities of 81.5, 31.5, and 6.5% of NRM intensities after 50, 300, and 1200 Oe demagnetizations. This difference in resistance to demagnetization, or degree of coercivity, between the marginal and interior sites is most apparent when the relative intensities of two representative samples for the two groups are plotted against Oe for af demagnetization (Fig. D.7A) and against temperature for thermal demagnetization (Fig. D-7B). Both types of demagnetizations show that the marginal sites have higher coercivities for a given level of demagnetization than the interior sites.

These differences in relative coercivity between marginal and interior sites have had no detrimental effect on the remanence directions obtained from af demagnetization. Directions from both the marginal and interior sites after af demagnetization converge to a common region with low dispersion values (Fig. D.7B). However, thermal demagnetization of marginal and interior sites failed to isolate a common remanent direction. The remanences obtained by thermal demagnetization, of the marginal sites are much the same as the directions from af demagnetization but those of the interior sites are scattered (Fig. D.7C).

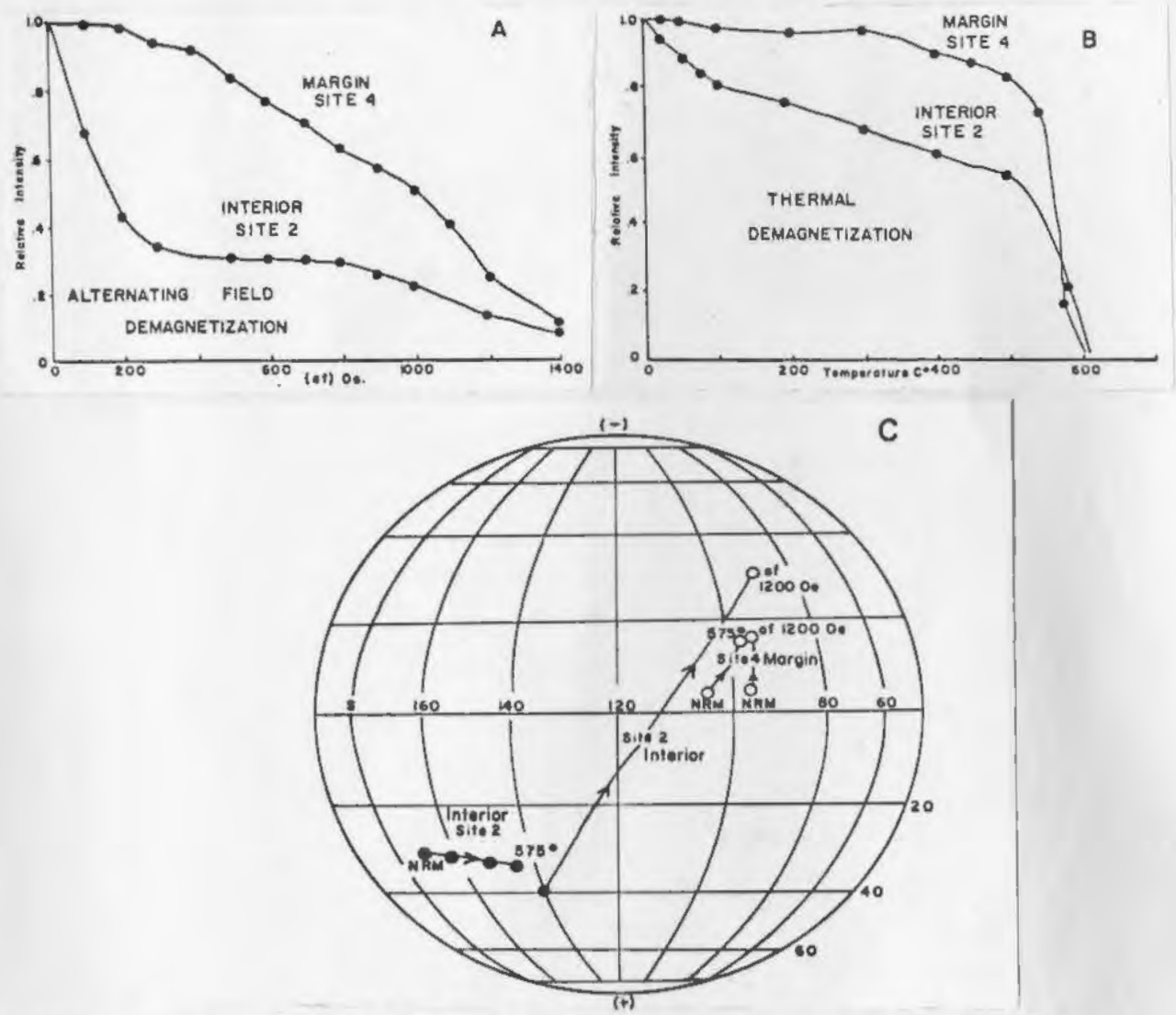

Fig. D.7A: Decay curve of intensity during af demagnetization for a representative speciman from an interior site (#2) and a marginal site (#4).

Fig. D.7B: Decay curve of intensity during thermal demagnetization from an interior site (#2) and a marginal site (#4).

Fig. D.7C: Magnetization directions accompanying the representative interior and marginal sites during af (open circles) and thermal (solid circles) cleaning. Plotted on a spherical projection.

Magnetic Mineralogy

The opaque minerals in the diabase are almost exclusively ilmenite with a minor amount of magnetite, both of which range in size from 0.5 to 2mm. The range of blocking temperatures, 550 to 600°C, determined during thermal demagnetization (Fig. d.7B) indicates that magnetite is the principal carrier of the thermoremanence (Irving, 1964). However, the individual magnetite grains in the diabase are too large to retain the high coercivities measured by af demagnetization (Irving, 1964). This suggests that submicroscopic exsolution lamellae of magnetite within the ilmenite carry the magnetic remanence.

Conclusions

The mean direction of all 20 specimens after 1200 Oe demagnetization was used to calculate a virtual paleopole located at 39.7°E, 3.4°S, with dp = 5.8° and dm = 11.0° (Table D.2). "Dp" is the semi-axis of the ellipse of 95% confidence along the great circle through the site and "dm" is the other semi-axis. This result is interpreted to be a virtual paleopole because it is not known whether the MacLean Sill cooled for a sufficiently long time to average out secular variation. At the present time, secular variation of the pole has a periodicity of 10^3 years (Irving, 1964). Such a time interval is greater than the 900 years estimated by the cooling model of Jaegar (1968) to be necessary for the cooling from 1200°C to 300°C for a 180m thick diabase sill such as the MacLean Sill.

Discussion

The virtual paleopole position for the MacLean Sill sites is significantly different from the paleopole positions (Table D.2) reported by Fahrig et al. (1974). Both Fahrig et al. (1974) and this study show that the rocks of the suite generally have remanences with high coercivities (Table D.2) and that during demagnetization stable endpoints were shifted to the same directions with respect to NRM directions. However, paleopole positions obtained by Fahrig et al. (1974) have low precision parameters and large error ovals (Table D.2). Their results can be subdivided into two groups: northern sites, 30 km west of MacLean Sill, and southern sites 40 km south of MacLean Sill (Fig. D.2).

The paleopole for the southern sites is 30° away from the pole of the MacLean Sill sites (Fig. D.8). This difference in pole positions can be explained by either an anticlockwise rotation of about 30° of this portion of the Grenville Province with respect to the MacLean Sill and the rest of the Churchill Province (Fahrig et al. 1974) or the southern sites have undergone, on average, a 30° tilt to the southeast (Fig. D.9). The latter suggestion seems most likely if one considers the degree of Grenvillian deformation now recognized in the area. The southern sites of Fahrig et al. (1974) lie in the Grenville Front Zone, an area interpreted by Noel and Rivers (1980) to have undergone three phases of Grenvillian deformation. The first phase produced large-scale southeast-dipping recumbent folds and associated thrust faults (Fig. D.2). The second and third phases produced easterly-trending folds and northwesterly-trending folds, respectively. Although it is probable

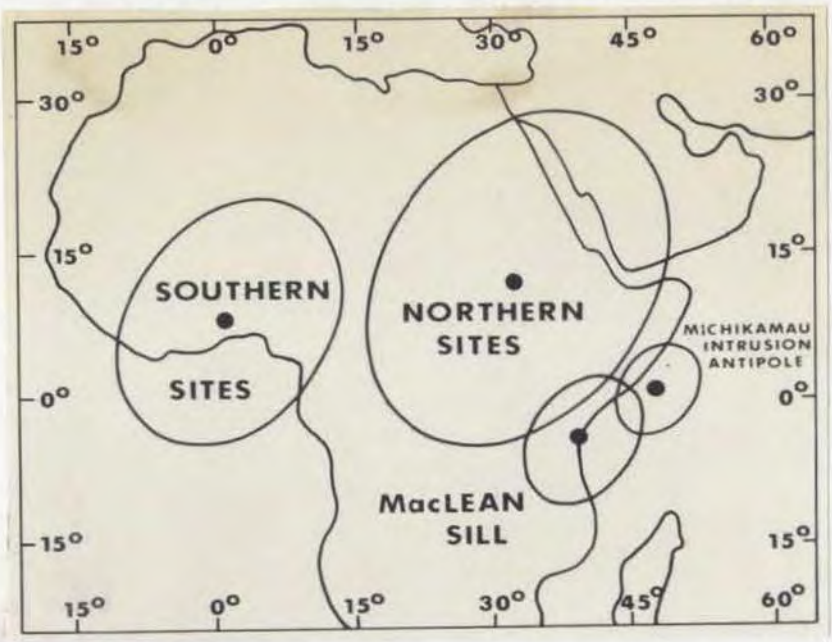

Fig. D.8: A map of Africa, with paleopoles of Shabogamo Intrusive Suite from MacLean Sill (this study) and the northern and southern sites of Fahrig et. al. (1974). Also plotted is the antipole of the Michikamau Intrusion. Ovals represent 95% confidence limits.

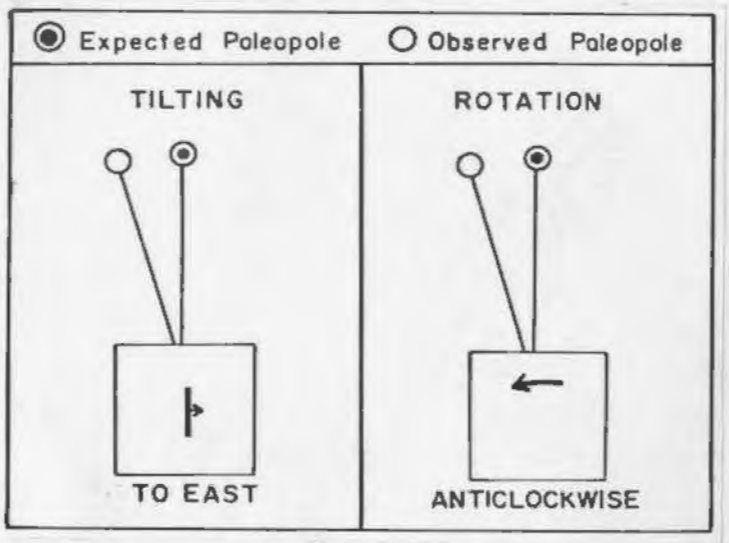

Fig. D.9: Two possible explanations for a westward displacement between an observed paleopole (southern sites Fahrig et. al., 1974) and expected paleopole (MacLean Sill, this study). Taken from Irving (1979).

that the larger bodies of the intrusive suite resisted much of this deformation, it is likely that some intrusions are at least gently to moderately dipping. Therefore, the difference in paleopole positions is probably a reflection of the average amount of tilting that the southern sites underwent during the Grenvillian Orogeny.

The northern sites of Fahrig et al. (1974) lie well north of the Grenville Front Zone (Fig. D.2) and their paleopole position overlaps at the 95% confidence level with the MacLean Sill paleopole, but possesses large error limits (Fig. D.8). The cause of this poor precision is not known but it should be noted that the northern sites reached a stable end point during af demagnetization at a lower field (250 Oe) than the field employed for the MacLean Sill sites (1200 Oe) (Table D.2). Because the northern sites are less resistant to af demagnetization than the Maclean Sill sites, it is possible that the northern sites may have failed to completely preserve their magnetic remanences. Further af demagnetization by Fahrig et al. (1974) of samples from the northern sites may have generated a paleopole closer to the MacLean Sill paleopole position and with improved precision.

The Shabogamo Intrusive Suite paleopole position from the MacLean Sill statistically overlaps at 95% confidence level (Fig. D.8) the antipole position reported for a neighbouring Elsonian intrusion, the Michikamau Intrusion (Murthy et al. 1968; Emslie et al. 1976). The Michikamau Intrusion is a large anorthosite to leucotroctolite massif located about 100 km northeast of MacLean Sill (Fig. D.1). The age of crystallization for the Michikamau Intrusion is estimated at 1.46 Ga based on U-Pb zircon dating (Krogh and Davies, 1973). K-Ar dates on the intrusion fall into 1.40 ± .50 Ga) range (Wanless et al., 1965). In

comparison, dating of the Shabogamo Intrusive Suite has yielded a whole rock Rb/Sr age of 1.44± .05 Ga, a whole rock Sm/Nd age of 1.37± .05 Ga (Brooks et al., 1981) and $^{40}Ar/^{39}Ar$ incremental release date of 1.35± .02 Ga on biotite (Dallmeyer, 1980). These ages indicate that within the limitations of the various dating techniques the Michikamau Intrusion and Shabogamo Intrusive Suite are broadly comtemporaneous.

The paleopole position for the Michikamau Intrusion is considered to be a well-established tie point for the plotting of the apparent polar-wandering path for the Canadian Shield at 1.4 Ga (Berger and York, 1980). The reliability of the 1.4 Ga paleopole position for this portion of the Canadian Shield is enhanced by having similar pole positions for two neighbouring Elsonian intrusions.

Summary

The 1.4 Ga Shabogamo Intrusive Suite straddles the Grenville Front in western Labrador and is part of the widespread Elsonian magmatic event. Paleomagnetic samples collected from a flat-lying sill located north of the Grenville Front yield a virtual paleopole position at 3.97°E, 3.4°S with dp = 5.8° and dm = 11.0°. This paleopole overlaps statistically with the neighbouring Elsonian pluton, the Michikamau Intrusion, which is also dated at 1.4 Ga.

The previous paleomagnetic work done on this suite used samples collected from sills south of the Grenville Front, within the Grenville Front Tectonic Zone. The paleopole positions obtained from this previous study and the present study differ by about 30°. It is suggested that this discrepancy is a reflection of the average amount of tectonic deformation that the sills of the Grenville Front Tectonic Zone have undergone during the Grenville Orogeny.

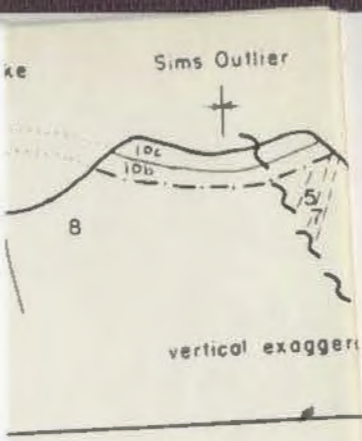
Sims Outlier
10c
10b
5
8
vertical exaggera

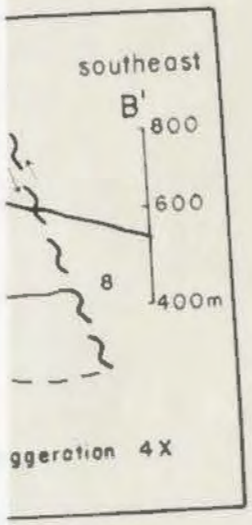
southeast
B'
800
600
400m
8
ggeration 4X